# EXPERIMENTAL EVALUATION OF THE EFFECT OF COAL COMBUSTION PRODUCTS ON CONSTRUCTABILITY, DAMAGE AND AGING RESISTANCE OF ASPHALT MASTICS

by

Emil G. Bautista

A Dissertation Submitted in

Partial Fulfillment of the

Requirements for the Degree of

Doctor of Philosophy

in Engineering

at

The University of Wisconsin-Milwaukee

May 2015

ABSTRACT

EXPERIMENTAL EVALUATION OF THE EFFECT OF COAL COMBUSTION PRODUCTS ON CONSTRUCTABILITY, DAMAGE AND AGING RESISTANCE OF ASPHALT MASTICS

By

Emil G. Bautista

The University of Wisconsin-Milwaukee, 2015
Under the Supervision of Professor Konstantin Sobolev

Developing a cost-efficient and long-term road infrastructure requires innovative approaches that are both green and environmentally sustainable. Today, building a sustainable, long-lasting, and efficient road infrastructure with little or no repairs is a challenging task and highly innovative technological breakthroughs are urgently needed. For many years fly ash has been effectively used as a partial replacement of portland cement in the production of different types of concrete, as well as in embankments and soil stabilization. On the other hand, the use of Coal Combustion Products (CCPs), including fly ash, as a mineral filler in asphalt pavements has been very limited. Only few researchers have reported on the benefits of CCPs in asphalt concrete. In this way, potential performance benefits that CCPs can offer to asphalt concrete are under-investigated.

Increasing the durability of asphalt pavement with CCPs additives is a promising technology that can significantly reduce the escalating costs related to rehabilitating and reconstructing of asphalt concrete pavements while offering a green and sustainable solution. In this study, asphalt binders from different sources and levels of modifications were blended with different types of CCPs particulate and natural filler to make mastics of different composition. This study investigates the beneficial effects of CCPs potential

on rheological and performance related parameters of asphalt binders. Experiments were conducted at the mastics level to determine the effects of CCPs on stiffness, constructability, rutting, fatigue damage, thermal resistance and aging of asphalt binders utilizing the Superpave® methodology. As expected, increase in stiffness of the asphalt binders with CCPs was observed. The addition of up to 15% CCPs (by volume) produces no significant change in the rheological properties as measured by the shear complex modulus (G*). At higher dosages, such as 25% and 40%, the changes in stiffness appear to be significant. Statistical evaluation of the performance of mastics rheological and physical and chemical properties of CCPs demonstrated a good correlation with Rigden Voids, as well as content of CaO, $SO_3$ and $Al_2O_3$. The research results proved that the particulate materials (CCPs and fillers), at all concentrations, improve the high temperature rutting resistance of mastics. Intermediate temperature fatigue damage results demonstrated significant dependency on CCP, binder and polymer modification types. In general, Class F fly ash is very beneficial material improving rutting, elastic recovery, and aging of mastics. At the same time, these mastics maintain the performance for workability and low temperature resistance without detrimental effects. Class C fly ash improved workability, and low temperature resistance without detrimental effects on the other performance indicators. At lower concentrations Spray Dryer Absorber (SDA) materials have demonstrated potential of extending the asphalt binder, but in general, due to variability of SDA materials test, results are not consistent; it is difficult to predict the influence of these CCP due to sensitivity to the type of binder and dosage. Therefore, further investigation is needed to understand the potential synergy between this type of CCPs and polymer modified binders.

## DEDICATION

I dedicate this work to all people that throughout the years have guided and supported me. Especially to my family and my girlfriend for their unconditional support.

# TABLE OF CONTENTS

# LIST OF FIGURES

## LIST OF TABLES

# LIST OF ABBREVIATIONS

| | |
|---|---|
| CCP | Coal Combustion Products |
| SDA | Spray Drying Agent |
| ASTM | American Society for Testing Materials |
| AASHTO | American Society of State Highway and Transportation Officials |
| DSR | Dynamic Shear Rheometer |
| G* | Complex Shear Modulus |
| $G^*_r$ | Relative Complex Shear Modulus |
| $\delta$ | Phase Angle |
| $\delta_r$ | Relative Phase Angle |
| G*/Sin $\delta$ | Superpave® Rutting Factor |
| G*Sin $\delta$ | Superpave® Fatigue Factor |
| MSCR | Multiple Stress Creep Recovery test |
| RTFO | Rolling Thin Film Oven |
| PAV | Pressure Aging Vessel |
| BBR | Bending Beam Rheometer |
| SGC | Superpave® Gyratory Compactor |
| VMA | Voids in Mineral Aggregates |
| VFA | Voids Filled with Asphalt |
| CDI | Construction Densification Index |
| TDI | Traffic Densification Index |
| IDT | Indirect Tensile Test |
| SEM | Scanning Electron Microscope |

## ACKOWLEDGMENTS

I would like to thank to my advisors Dr. Konstantin Sobolev and Dr. Ahmed Faheem for their support and guidance to help complete this thesis. I would like to thank Dr. Habib Tabatabai, Dr. Rani El-Hajjar and Dr. Ilya Avdeev for agreeing to be part of my committee.

I would also like to thank EPRI and the others sponsors of the research project that made possible this work. Special thanks to Ken Ladwig and Art Covi. Also thanks to Dr. Carl Johnson from Stark Pavement Corp. and Carlton Travis and Gail Hoard from Payne & Dolan for their help to conduct part of the experimental plan of this thesis.

In addition, I would like to thank all the students and lab colleagues that help me out throughout this process; Rajan Saha, Justin Flickinger, Clayton Cloutier, Scott Muzenski, Reza Moini, Rani Pradoto, Ismael Flores, Jesus Castro, Jason Atchinson, Nathaniel Havener, Katie LeDoux , Craig Vindedahl, Christopher Ball, Gaven Kobes and Marina Kozhukhova. It has been very gratifying to meet and work with all you.

I also want to express gratitude to Dr. Ronald Perez for his unconditional support.

# CHAPTER 1.

# SCOPE OF WORK

## 1.1 INTRODUCTION

Asphalt cement was first used in Sumeria (Mesopotamia), around 6,000 B.C., in the shipbuilding industry and years later its application continued in various parts of the world for building and paving blocks, caulking for ships, and numerous waterproofing applications. The first asphalt pavement in the United States was laid in 1876 on Pennsylvania Avenue in Washington, D.C. (Roberts et al., 1996). Almost 150 years have passed since the first asphalt pavement application and the demand on pavement infrastructure in terms of traffic loadings, service life and vehicle miles travelled has been rapidly increasing. Recent transportation statistics indicate that from 1993 to 2002, truck traffic has increased by more than 33% while lane miles have increased by only 2%. The total vehicle miles travelled in the United States is expected to increase by 50% in the next 20 years and, more importantly, freight movement is expected to double by 2025. While the number of road miles only increased by 5.2% from 1980 to 2008, the number of vehicles on the road increased by 94.7% over the same period—this is a clear indication of the importance of building high-quality roads to maintain the strategic importance of highways to the U.S. economy and national security. In addition to increased traffic demands, the escalating crude oil prices and increasing costs of energy in general are expected to increase the asphalt production costs. This opens up the need for better quality roads giving the opportunity to civil engineers and materials researchers to investigate novel materials that will meet the specifications for modern high-performance transportation infrastructure.

Asphalt or flexible pavements are designed as layered systems in which better materials are placed on the top where the intensity of the stress is high and inferior materials are located at the bottom where the stress intensity is low (Huang, 2004). The top layer of flexible pavements is composed of Hot Mix Asphalt (HMA) which is made of asphalt binder, aggregates and air voids. By mass, the asphalt cement (binder) is approximately 5% and the aggregates correspond to the remaining 95%.

Asphalt cement or binder is a complex mixture of petroleum hydrocarbons with various chemical structures composed of hydrogen, carbon and heteroatoms, such as, oxygen, sulfur, nitrogen, vanadium and nickel. At low temperatures asphalt cement can be very elastic and brittle, at high temperatures it can be very fluid (viscous) and at intermediate temperatures asphalt cement is considered a viscoelastic material as it exhibits both elastic and viscous properties. Because of these variations in behavior, at different temperatures, asphalt cement is considered a thermoplastic material.

Modification of asphalt cement with polymers or particulate materials (i.e., fillers) helps to increase the performances and meet enhanced specifications. Asphalt cement modification has been practiced for over 5 decades, but have received more attention in the past couple of decades after the development of the Superpave® specification by the Strategic Highway Research Program (SHRP) researchers (Roberts et al. 1996).

The modification of asphalt cement aids to enhance the overall performance of a binder by widening the range between the binder’s high- and low- temperature grades and also targets a specific improvement in a binder's performance in response to a particular severe service condition, such as a pavement carrying very high traffic volumes or a high percentage of slow-moving, heavy vehicles (Bahia et al. 2001).

Aggregates can be classified as coarse aggregates and fine aggregates. According to the American Association of State Highway and Transportation Officials (AASHTO) the No. 10 sieve size (2.00 mm) separates the coarse and fine aggregates (AASHTO M 145). Gravel, boulders and cobbles are considered coarse aggregates since they are retained on the No. 10 sieve (2.00 mm) and above. Sand and minerals fillers are considered as fine aggregates since they pass the No. 10 sieve (2.00 mm). Mineral fillers are defined as the fraction of the fine aggregates that passes the No. 200 sieve (0.075 mm). The blend of asphalt and particulate fillers is referred to as "mastic." Although usually fillers represent less than 8% of Hot Mix Asphalt (HMA) by mass, the interactions of fillers with asphalt binder, and coarse and fine aggregates, clearly affect HMA field performance. These effects have been known since the beginning of this century, and numerous studies have focused on quantifying the effect of fillers on HMA performance (Lee and Rigden, 1945; Warden et al, 1959; Ishai and Craus, 1977; Ishai and Craus, 1980; Kandhal, 1981; Anderson and Tarris, 1982; Bolk et al., 1982; Sarsam, 1984; Anderson, 1987; Mogawer, 1996; Ishai and Craus, 1996; Taybebali et al., 1998; Silva et al., 2005). Some researchers have evaluated mastics, while others have tested HMA to identify the filler characteristics that affect HMA performance.

Since the early 1900's Richardson noted that the use of mineral fillers in asphalt increases the stiffness of the asphalt-filler mix (Richardson, 1905). Coal Combustion Products (CCPs) in asphalt binder can be considered as fillers in a viscoelastic matrix.

Einstein in 1911 observed that the loading of fillers into a matrix increases the stiffness of the composite in a linear manner, with a rate of increase called the Einstein coefficient (Einstein, 1911). However, this linear increase can only be observed at diluted filler concentrations, which varies between 10% to 40% by volume depending on the filler and the matrix (Shenoy 1999, Lakes 2002). The increase in stiffness is theorized such that, when the inter-particle distance is large compared with the mean particle size, the particle movement is slow that its kinetic energy can be neglected and there is no resulting slip relative to the particle surface. Thus, filler particles are practically hindering the matrix flow, thereby increasing its stiffness.

Despite many investigations reporting on the beneficial use of fly ash in asphalt, there is a lack of systematic and comprehensive study on the effects of different types of modern fly ash (including Clean Coal Ash) based on Superpave® mix design and performance testing methodology (AASHTO, 2007). Superpave® is the newest asphalt mix design method which provides the guidance on the selection and proportioning of asphalt cement and aggregates for HMA. This methodology also includes the requirements for mineral fillers to be effectively incorporated into the mix, but the general believe is that the interaction between the asphalt cement and mineral fillers is not very important and a simple mass ratio is implemented for quality control during the production of HMA. The amount of filler that can be included according to specifications is limited to a ratio in the range of 0.6 - 1.2 by mass of the filler to the binder, which in terms of volume, for asphalt-filler mix corresponds to 20-40% content.

## 1.2 RESEARCH APPROACH

Construction materials researchers have extensively investigated the use of by-products such as fly ash to improve the material properties (Ramme and Tharaniyil 2004, Sobolev and Naik 2005). Fly ash has been used extensively in portland cement concrete; however, there are few limited applications in which fly ash has been tested in asphalt pavements (Ali et al. 1996; Churchill et al. 1999; Asi et al. 2005; Tapkin, 2008; Faheem and Bahia, 2010; Sobolev et al. 2013).

Sobolev et al. (2013) reported that the introduction of fly ash into asphalt mixtures (ASHphalt) improves the performance at levels compared to those achieved through polymer modification. This is attributed to the unique spherical, beneficial size distribution and chemical properties of fly ash. The use of fly ash in bitumen based materials is attractive as it improves the performance and reduces costs and environmental impacts. Advantages of fly ash in asphalt include improved mixing, placing and compaction, stability, resistance to water damage, rutting resistance, flexibility, and resistance to freeze-thaw damage (Tapkin, 2008).

Despite these reported benefits, the application of fly ash in asphalt technology has not been completely utilized. Fly ash in HMA has not been adopted on a commercial scale and Class C material has received the most of the research focus. Therefore, this technology remains an open question as no definite consensus has been reached on how to use fly ash in asphalt with controlled performance. Class F and off spec fly ash, such as Spray Dryer Absorber (SDA) materials, have not been thoroughly explored for use in asphalt mixtures which gives a great potential for the research and future use.

A 2010 study sponsored by the National Cooperative Highway Research Program (NCHRP 9-45) concluded that the performance of “natural” fillers produced from rock-crushing operations is significantly different from “manufactured” fillers produced as by-products to industrial operations such as CCPs. The study recommended the investigation of the manufactured fillers independently and individually to model and quantify its effects on asphalt performance (Bahia et al, 2011).

This study evaluates the potential benefits related to CCP application in flexible pavements in terms of performance at the mastic level. Experiments were conducted at the mastic and mixture levels, and concept was refined by a field construction helping to quantify the benefits of using fly ash in asphalt pavements. The reported research provides essential data to the paving industry, contractors, and state agencies that are currently considering different types of CCPs in their asphalt mix designs. This study also helps to increase the awareness of the sustainable potential of CCPs at academic, industrial, and governmental levels.

## 1.3 PROBLEM STATEMENT

The United States has more than 2 million miles of paved roads and highways, and 90 to 94% of those are surfaced with asphalt concrete (Figure 1.1). Based on the National Asphalt Pavement Association (NAPA), there are approximately 4,000 asphalt plants in the U.S.—at least one in every congressional district. Each year, these asphalt plants in the U.S. produce 500 to 550 million tons of asphalt pavement material worth in excess of $30 billion (NAPA, 2015).

Increased traffic demands and factors such as the escalating price in crude oil plus rising energy costs, all contribute to increased production costs of asphalt concrete. Spending these dollars on a sustainable, resilient and efficient road infrastructure with longer service life and little or no repairs is a challenging task; however, increasing the durability of pavements can significantly reduce the cost of rehabilitating and reconstructing asphalt concrete pavements. The beneficial use of CCPs in asphalt can potentially make a substantial contribution to this demanding mission.

**Figure 1.1 Asphalt concrete has a high content of coarse aggregates which interlock to form a stone skeleton filled with a mastic of bitumen and filler; it is compacted onsite to target 8% air void content to ensure the adequate performance under traffic and environmental conditions**

With continual repair of an aging U.S. transportation infrastructure and increasing transportation volumes on the U.S. highways, there is an urgent need for high-performance paving materials incorporating substantial quantities of industrial by-products (e.g., waste glass, fly ash) with improved performance and service life which meet the sustainability objectives.

Developing a cost-efficient and long-term road infrastructure requires innovative approaches that are both green and environmentally sustainable. Today, building a sustainable, long-lasting, and efficient road infrastructure with little or no repairs is a challenging task and highly innovative technological breakthroughs are urgently needed. The asphalt industry is currently spending millions of dollars on polymer modifications of the asphalt binder in order to meet the improved performance requirements. Modified asphalt cements are likely to represent as much as 15% of the total annual tonnage of asphalt binder used in the United States (Bahia et al. 2001).

Unfortunately, this method ultimately increases the cost of the raw materials and overall production. On a survey targeting users and suppliers of modified asphalt cement under NCHRP Project 9-10 the majority of state agencies express their intention to increase the use of modified asphalt cement in the future.

Increasing asphalt pavement durability with CCPs additives is such technology that can significantly reduce the escalating costs of rehabilitating and reconstructing asphalt concrete pavements while offering a green and sustainable solution.

Figure 1.2 shows that the use of fly ash has increased through the years until 2006, but beyond this year the utilization takes a downward trend and currently less than 50% of produced fly ash is used (ACAA, 2012). This figure raises the alarm that new markets and innovative uses of CCPs are needed to enhance the utilization of a waste material that otherwise will be stored in landfills, which, according to statistics, corresponds to two thirds of the fly ash production nationwide.


**Figure 1.2 Production and Utilization of Fly Ash (American Coal Ash Association, 2012)**

## 1.4 HYPOTHESIS

The Main Hypothesis

The use of Coal Combustion Products (CCP), such as fly ash and Spray Dryer Absorber (SDA) materials, can improve the performance of asphalt binders to levels exceeding that of conventional fillers used in asphalt technology. Thereby, the use of CCP additives is an innovative approach to reduce the cost of rehabilitating and reconstructing asphalt concrete pavements while offering a green and sustainable solution for new construction.

Sub hypothesis

- CCP additive is a cost-efficient alternative to natural components and can meet the long-term road infrastructure demands.

- CCP addition can improve the mechanical stability of asphalt pavements.
- CCPs can increase the longevity of pavement infrastructure by improving the resistance to thermal cracking and the ability to relieve internal thermal stress build-up during the winter months.
- The conventional mix design procedures and pavements construction technologies are applicable for asphalt with CCPs.
- CCPs can to effectively extend the asphalt binder used in the mix, thereby reducing the amount of asphalt binder needed for required performance.
- The performance of CCP materials (such as fly ash and SDA) depends in the type, composition and physical properties.

## 1.5 OBJECTIVES

- To describe CCPs characteristics based on physical properties and chemical composition.
- To evaluate the potential benefits of CCPs application in flexible pavements in terms of performance at the mastic level.
- To investigate the effect of CCPs addition on rheological behavior of mastics at conventional mixing and performance temperatures.
- To evaluate the effect of different types of CCPs on workability, rutting resistance, recovery, aging resistance and low temperature resistance.
- To describe the distress performance of asphalt mastics depending on type, dosage, composition, and variability of CCPs.
- To evaluate the benefits of using CCPs in asphalt mixtures in terms of commonly accepted performance criteria (such as Superpave®) used by the asphalt industry.

## 1.6 RESEARCH METHODOLOGY

To meet the objectives of this study, the following tasks were planned:

**Task 1: Conducting the detailed literature review.** Find and report on published research efforts on asphalt mastics and particulate composites and use of CCPs on asphalt.

**Task 2: Collect different types of Coal Combustion Products, such as, fly ash Class C and F, and Spray Dryer Absorber (SDA) and natural fillers materials**. Following the evaluation of type, chemical composition (especially, CaO and carbon contents), physical properties (particle size, surface area, fineness, specific gravity) and the type of sorbents used for air emissions controls, collect the representative specimens of CCPs from appropriate sources for testing.

**Task 3: Evaluate the chemical and physical properties of collected CCPs and fillers.** Obtain materials that represent CCPs classes and sources with wide range of properties. Select natural filler as the control for comparison with the CCPs.

**Task 4: Conduct laboratory testing on asphalt mastics with CCPs and control fillers.** Blend collected CCPs/fillers with asphalt binders from different sources at different levels of modifications representing the range of asphalt binders used in the U.S. Produce and test the mastics at multiple concentrations of CCP, to evaluate the influence of the fillers based on the following properties:

1- Increase of stiffness (influence on rheological parameters, such as, complex modulus (G) and phase angle ($\delta$))

2- Constructability (viscosity)

3- Short term oxidative aging related distresses including rutting resistance (Superpave® $G^*/\sin\delta$, non-recoverable compliance (Jnr) and %Recovery).

4- Long term oxidative aging related distresses. These distresses can be used to assess the benefits of CCPs in retaining the asphalt's desirable viscoelastic properties after the exposure to long-term aging simulation versus the effects of with natural fillers and polymer modification; this will serve to assess the feasibility of CCPs as an aging retarder. Long-term aging-related distresses include test for the following properties:

   - Fatigue performance (Superpave® $G^*\sin\delta$)
   - Aging Index (PAV aged G* and Unaged G*)
   - Low temperature performance (Creep Stiffness ($S_t$) and m-value)

5- Extending Asphalt Binder. This involves testing the fundamental viscoelastic properties of the mastic as CCP or filler concentration increases. Based on the preliminary testing and data from literature, it is predicted that the viscoelastic properties remain unchanged at lower filler concentrations. Testing can identify the critical dosage of CCP which has negative effects on the essential properties of the asphalt binders and mastics.

**Task 5: Develop correlations between CCPs characteristics and mastic performance.**

**Task 6: Validate CCP incorporation at the mix level in the laboratory and the field.**

# CHAPTER 2.

# LITERATURE REVIEW

## 2.1 ASPHALT BINDER

### 2.1.1 Chemistry

Crude petroleum is a complex mixture of hydrocarbons that occurs as a part of a transformation process of dead prehistoric organisms buried beneath the sedimentary rocks. This transformation process occurs when these organisms are subjected to varied pressures and temperatures over a very long time that is estimated to be over the millions of years (Roberts et al., 1996). Asphalt cement is obtained by a distillation process of crude petroleum so the chemical properties vary from one crude source to another since the nature and composition of hydrocarbons varies.

The principal elements that form the asphalt cement are carbon, hydrogen, sulfur, nitrogen and heavy metals such as vanadium and nickel.

When asphalt cement is mixed with a non-polar, normal alkane solvent such as propane, pentane, hexane, or heptane the non-soluble part is known as asphaltenes and the soluble part is known as resins and oils. The resins and oils are also called maltenes or petrolenes.

Asphaltenes are commonly considered to be the most polar and highest molecular weight fraction of asphalt which is of great importance because, due to their higher polarity, these comprise the compounds capable of interacting and associating.

Asphaltenes are of great influence in the determination of the mechanical and rheological properties of asphalts due to the viscosity-building properties (Boduszynski, 1980). The increase of asphaltene content produces asphalt cement that is harder, more viscous, with lower penetration and higher softening point (Read et al., 2003).

The resins have the function of acting as a medium that disperse the asphaltenes throughout the system to provide a uniform and stable liquid. In general, these are behaving as semi-solid or solid materials. The oils are soluble in most solvents and on oxidation these provide asphaltenes and resins molecules from the blend. In general, oils are colorless or white liquids (Roberts et al., 1996).

Based on the asphaltene content, asphalt cement can be classified as sol and gel asphalts. Sol asphalts have low concentration of asphaltenes and represent a system in which the resins keep the asphaltenes highly dispersed in the oily phase. Sol asphalts show Newtonian flow behavior. On the other hand, gel asphalts have large concentrations of asphaltenes and represent a system in which the resins are not very successful in dispersing the asphaltenes. Gel asphalts show non-Newtonian flow behavior.

The rheological properties, aging characteristics, and performance of HMA mixtures are affected by the degree to which asphalt behaves as a sol or a gel (Roberts et al., 1996).

### 2.1.2 Age Hardening

Age hardening is a phenomenon that occurs in asphalt binders due to exposure to oxygen, ultraviolet radiation and changes in temperatures causing the asphalt binder to become stiffer and less ductile (Read et al., 2003). The longer the asphalt binder is exposed to these external agents the more it hardens.

The first significant hardening of asphalt binders takes places at the pugmill or drum mixer where heated aggregate is mixed with hot asphalt cement (Roberts et al., 1996). During this short period of mixing asphalt cement can experience substantial variations in its rheological properties such as a decrease in penetration and an increase in viscosity due to the exposure of very thin asphalt films to air at temperatures which range from 135 to 163°C (275 to 325°F).

After the asphalt binder is mixed  with aggregates and delivered to the job site and compacted, age hardening can take place at an accelerated rate when the air void content is higher than the originally designed. A higher air void content provides easy entry for air, water and light. Thicker asphalt cement films around the aggregate particles harden at a slower rate compared to thin films (Roberts et al., 1996).

Six factors known to contribute to age hardening of asphalt cement during mixing and service were reported in the literature (Kandhal, 1973; Vallerga, 1957):

1. Oxidation,
2. Volatilization,
3. Polymerization,
4. Thixotropy, also known as steric hardening,
5. Synerisis, and
6. Separation

Changes in asphalt cement properties, like penetration at 25°C (77°F) and viscosity 60°C (140°F), and also changes in pavement properties, like percent air voids in the pavements, have been known to affect pavement performance with time, and have been found to follow a hyperbolic model (Brown, 1957; Lee, 1973; Kandhal, 1975).

Based on this theory, the changes in physical properties follow a hyperbolic function with time and approach a definite limit as time increases (Roberts et al., 1996). The following equation expresses the age hardening of asphalt in the field:

$$\frac{T}{\Delta Y} = a + bT \qquad \text{Eq. 2.1}$$

Where:

$\Delta Y$ = change in test property with time T or the difference between the zero-life value and the value at any significant time,
T = time,
a = constant, the intercept of Eq. 2.1 line on the ordinate,
b = slope of the Eq. 2.1 line,
1/b = the ultimate change of the property at infinite time.

The degree of age hardening can be quantified in terms of penetration or viscosity. The percent retained penetration (Eq. 2.2) and the aging index (Eq. 2.3) have been used to assess relative aging of asphalt cements of different grades and different sources.

$$\%\text{Retained Penetration} = \frac{\text{Penetration of aged asphalt}}{\text{Penetraton of original asphalt}} * 100 \qquad \text{Eq. 2.2}$$

$$\text{Aging Index} = \frac{\text{Viscosity of aged asphalt}}{\text{Viscosity of original asphalt}} \qquad \text{Eq. 2.3}$$

### 2.1.3 Modification

Modern demand on pavement infrastructure in terms of traffic loadings and service life rapidly increases which dictates the need for better quality roads. For years, asphalt cement has been used as binding materials providing smooth surface on top of the pavement structure for vehicles to move from one place to another.

Asphalt cement is the residue obtained after the crude petroleum is extracted from the underground deposits and refined. Over the years researchers have studied how to characterize the asphalt cement and have developed materials specifications that satisfy the requirements for good quality roads. The modification of asphalt cements with polymers or particulate composites are used to increase the materials performance and exceed the specifications. Asphalt cement modification was practiced for over five decades, and recently, have received more attention especially, after the development of the Superpave® specifications by the Strategic Highway Research Program, SHRP (Roberts et al., 1996).

Modified asphalt cements are likely to represent as much as 15% of the total annual tonnage of asphalt binder used in the United States (Bahia et al., 2001). On a survey targeting users and suppliers of modified asphalt cement under NCHRP Project 9-10 the majority of state agencies express their intention to increase the use of modified asphalt cement in the future.

The modification of asphalt cement aids to enhance the overall performance of a binder by widening the range between the binder’s high- and low- temperature grades and also targets a specific improvement in a binder’s performance in response to a particular severe service condition, such as in pavements carrying very high traffic volume or with a high percentage of slow-moving, heavy vehicles (Bahia et al., 2001)

Asphalt cement modifiers can be classified in three different ways: (1) by the mechanism by which the modifier alters the asphalt properties, (2) by the composition and physical nature of the modifiers and (3) by targeting an asphalt property that needs improvement (Bahia et al., 2001).

Based on the composition asphalt modifiers can be classified as polymers (elastomeric and plastomeric), fillers, fibers, hydrocarbons, antistripping agents, oxidants, antioxidants, crumb rubber and extenders (Bahia et al., 2001).

In the case of this study, mineral fillers were utilized to modify the asphalt cement. Asphalt cements are simple thermo-rheological materials that can be characterized by using linear viscoelasticity principles and simple geometry within which stress and strain fields are simple to calculate. When asphalt cement is modified with mineral fillers, this material becomes a complex system that shows dependency on sample geometry making its characterization more challenging (Bahia et al., 2001).

Under the NCHRP Project 9-10 certain characteristics of modified asphalt cement were recognized to require a special attention (Bahia et al., 2001). These characteristics are:

1. Storage stability,
2. Shear-rate dependency of viscosity,
3. Strain dependency of rheological response,
4. Effect of mechanical working, and
5. Loading-rate dependency and time-temperature equivalency.

If this modifier-specific characteristics are disregarded, the contribution of modifiers to pavement performance may be under or overestimated (Bahia et al., 1997).

## 2.2 COAL COMBUSTION PRODUCTS (CCPs)

Fly ash is a fine-grained, powdery particulate material of spherical shape produced from burning pulverized coal in  the electric power generating plants (Figure 2.1), also known as a coal combustion product (CCP). These fine-grained spherical glassy particles are collected from the exhaust gases by the electrostatic precipitators or bag filters. During the combustion of coal, mineral impurities like clay, feldspar, quartz, and shale fuse in the gas flow and float out of the combustion chamber along with exhaust gases. As the fused material rises, it cools and solidifies into the powder material known as fly ash. Fly ash accounts for 75-85% of the total coal ash, and the remainder is collected as bottom ash or boiler slag (Siddique, 2011).

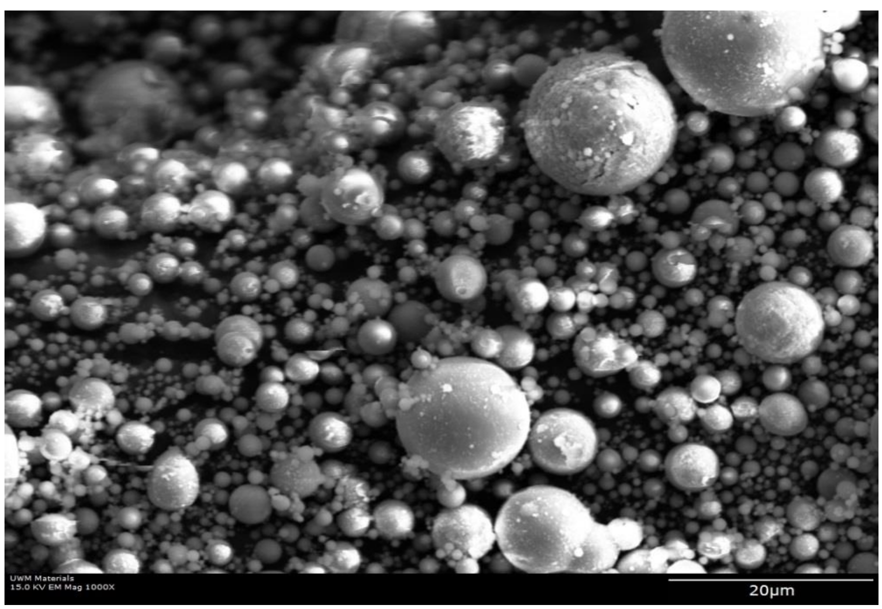


**Figure 2.1 Scanning Electron Microscope of Fly Ash (1000x Magnification)**

Fly ash from different power plants and even from the same power plant are likely to be different depending on several factors. These factors are: the type and mineralogical composition of the coal, degree of coal pulverization, type of furnace and oxidation conditions, and the way in which fly ash is collected, handled and stored before use (Sidique, 2011).

### 2.2.1 Environmental Benefits

The utilization of fly ash has many important environmental benefits since this lead to the reduction of coal by-products that must be disposed in landfills. Fly ash can also be used as partial substitution of other natural resources and materials which translates into a reduction of the used of virgin natural resources.

Other important benefits of utilization of fly ash are in the reduction in energy and emitted greenhouse gases (and other adverse air emissions) attained with the replacement of manufactured material (e.g., cement) with fly ash. Fly ash is also known to improve the service life of concrete roads and structures by enhancing the durability of concrete.

### 2.2.2 Use of Coal Combustion Products

In 2006, the American Coal Ash Association (ACAA) reported that 65.7 million metric tons (72.4 million tons) of coal fly ash were produced of which less than 1% (52,608 tons) was used as mineral filler in asphalt. Figure 2.2 summarizes the common applications of fly ash in engineering.

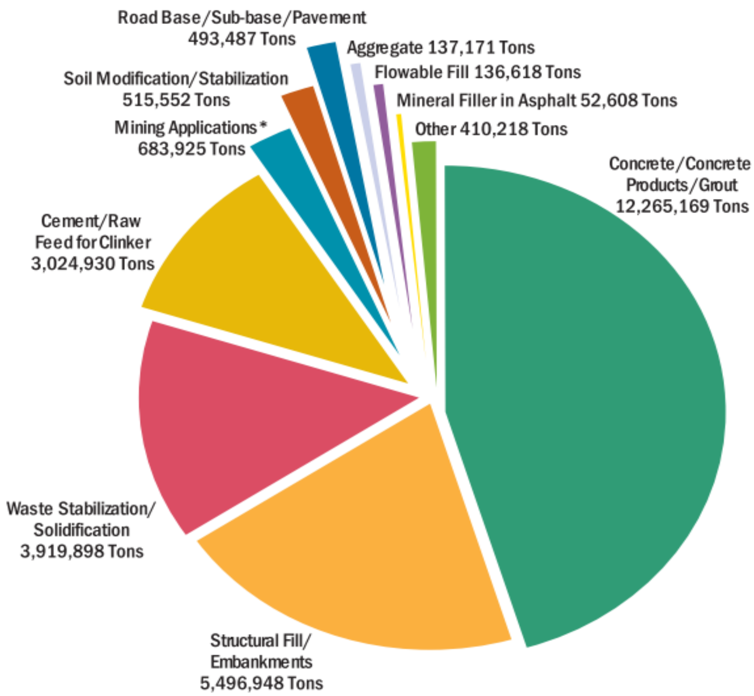


**Figure 2.2 Common Applications of Fly Ash (after the American Coal Ash Association 2006)**

Mineral fillers are defined by the ASTM as finely divided mineral matter such as rock dust, slag dust, hydrated lime, hydraulic cement, fly ash, loess, or other suitable mineral matter. Since the early 1900's, mineral fillers were used as fillers in asphalt and numerous studies have identified the benefits of this materials (Richardson, 1905).

## 2.3 ASPHALT MASTIC COMPOSITE

When solid particles are distributed in a continuous matrix of different composition it can be classified as a dispersion. Different types of dispersed systems (Table 2.1) can be defined depending on the nature of the disperse phase and medium (Tadros, 2010).

**Table 2.1 Types of disperse systems (after Tadros 2010)**

| Disperse Phase | Disperse Medium | Type |
|---|---|---|
| Solid | Liquid | Suspension |
| Liquid | Liquid | Emulsion |
| Liquid | Solid | Gel |
| Liquid | Gas | Aerosol |
| Gas | Liquid | Foam |
| Solid | Solid | Composite |

Asphalt mastics are particulate composite materials where the asphalt binder, the continuous phase or matrix, is mixed with mineral fillers particles. These fillers particles are the dispersed phase within the matrix. Composite materials are made from two or more materials with significantly different physical or chemical properties, that when combined, produced a material inheriting the best characteristics of the individual components. In a complex multiphase system, such as asphalt mastics, it is necessary to control the rheological properties during preparation and to maintain the long-term physical stability during the application (Tadros, 2010). Rheology is the science that deals with the deformation and flow of matter and can explain the behavior of viscoelastic materials.

The particle size distribution of the internal phase is of great importance for optimal design of particulate composites. Depending on the dimensions of the particles, the system can be identified as colloidal or outside of the colloidal range. In colloidal systems the particles are within 1 nm to 1000 nm (1 µm) range. On the other hand, with particles larger than 1 µm the system is outside of the colloidal range. As previously stated, fly ash size range is between 10 and 100 µm, which makes the fly ash asphalt mastic a system that falls outside the colloidal range.

In both of these cases the property of the system is determined by the nature of the interface which separates the internal phase from the medium in which it is dispersed. The structure of the interfacial region determines the properties of the system and, especially, the tendency of the particles to agglomerate in units or to remain dispersed as individual particles (Tadros, 2010).

Rigden (1947) studied different filler characteristics which can be directly related to the characteristics of filler-binder mixtures, at low and high filler concentrations. By measuring the bulk volume of compacted dry samples and considering the asphalt required to fill the voids in the dry compact as “fixed” asphalt while the asphalt in excess of such volume is considered as “free” asphalt. In his research, Ridgen called this concept “the fractional voids concept” and found that the value of the fractional volume voids in compacted dry filler, obtained by the developed test method and later modified by Anderson (1987), is related to the filler-binder flow properties (viscosity) for a wide range of stress and temperatures (from 0°C to 45°C). Rigden used the coni-cylindrical viscometer and the constant load tensile test to study the viscosity of filler-binder systems at low and high concentrations, respectively and noticed that as the concentration of filler is increased the viscosity increases rapidly until it reaches a maximum value in which measurement of viscosity becomes difficult. This maximum value occurs at a concentration of filler corresponding to the binder content giving the maximal resistance to deformation also known as the optimum binder content. The Rigden Voids test was used for a number of fillers and correlate to an optimal binder content; the relationship was found to be independent of the type of filler. This leads to the most important finding, that the degree of packing of filler in a filler-binder system largely determines the flow properties of the system and that the chemical differences between various fillers are of lesser significance (Rigden, 1947).

The importance of the fractional volume voids is that it depends on other filler physical properties like particle size distribution, shape and surface texture. Other filler characteristics such as fineness, percentage passing No. 100 sieve, percentage passing 10 micron sieve, bulk density in benzene, specific surface, shape factor or surface roughness investigated by Rigden had no unique relationship with the behavior of filler-binder systems

Tunnicliff (1960) investigated the importance of size distribution, shape and surface texture results on the stiffening of asphalt mastics. It was postulated that mineral fillers of the same size distribution, shape and surface texture but of different mineralogy or surface chemistry can result in various stiffening effects. Therefore, the effect of mineral fillers on mastics and HMA could be very different due to asphalt-filler interaction characterized by a gradient of stiffening. The gradient of stiffening is greatest at the surface and decreases with distance from the particle (Figure 2.3).

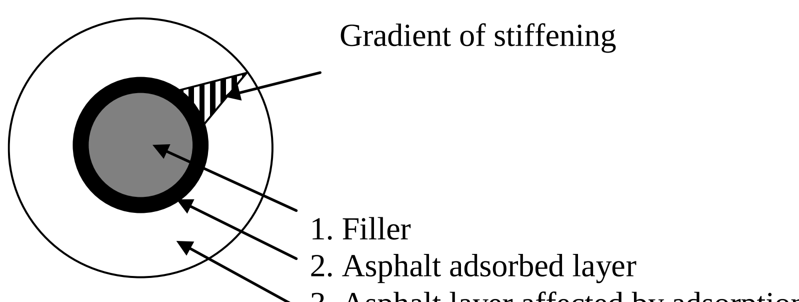


**Figure 2.3 The hypothesis of asphalt-filler interaction (Tunnicliff 1960)**

Based on Tunnicliff (1960) theory and considering the fractional voids concept introduced by Rigden (1947), Faheem (2009) proposed a conceptual model of the interaction of the fillers with surrounding asphalt matrix that considers the asphalt mastics as particulate composite material. Figure 2.4 presents the increase of stiffness of the mastic due to the addition of mineral fillers.

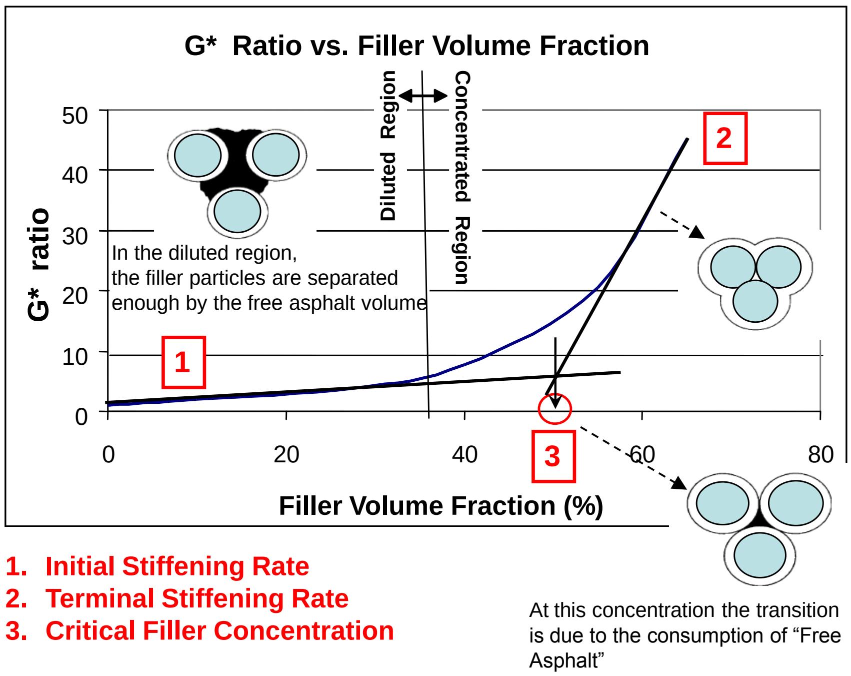


**Figure 2.4 Conceptual model parameters of the increase of stiffness in terms of filler influence (Faheem 2009)**

Two different regions can be clearly identified for mastics with the proposed model. On the left side of the plot the increase of the stiffness is linear up to a certain filler volume concentration. This region is called the diluted region. Within this region the stiffness is highly dependent of the free asphalt content that separates the filler particles. Faheem (2009) called the stiffening rate within the diluted region as Initial Stiffening Rate.

On the other hand, the right side of the plot is identified as the “concentrated region”, where the rate of increase becomes nonlinear and rapidly reaches and asymptotic linear trend. Faheem (2009) states that as the volume of free asphalt starts to diminish toward the end of the diluted region, the stiffness of the mastic starts to increase rapidly and called this increase of stiffening rate the Terminal Stiffening Rate. Faheem (2009) also identified the Critical Filler Concentration as the transition between the diluted and concentrated regions.

### 2.3.1 Effect of incorporation of fillers on stiffness of asphalt mastic

The influence of fillers in asphalt binders has been in the center of attention of researchers for many years starting from the early 1900’s. Researchers found that the incorporation of filler particles, irrespective of their properties, to asphalt binder increases the stiffness of the composite.

Richardson (1905) demonstrated that the effect of fillers on stiffening asphalts varies depending on the geometric characteristics and the interaction with the asphalts. It was theorized that the behavior of mineral aggregate surfaces and film thickness are the basis for the construction of a perfect asphalt mixture. It was postulated that the more viscous the bitumen and the larger amount of filler, the thicker the film thickness is, translating to greater cementing power.

Einstein (1911) observed that the loading of fillers to a matrix increases the stiffness of the composite in a linear manner, with a rate of increase called the Einstein coefficient. However, this linear increase can only be observed within diluted filler volumes, which varies between 10% to 40% depending on the filler and the matrix

(Shenoy, 1999; Lakes, 2002). The increase in stiffness is theorized such that, when the inter-particle distance is large compared with the mean particle size, such as in diluted system, the particle relative movement is negligible that the associated kinetic energy can be neglected and so is no slip relative to the particle surface. Thus, the filler particles are hindering the matrix flow, thereby increasing the stiffness of mastics.

Winniford (1961) used a sliding plate microviscometer to measure the effect of a variety of mineral fillers, such as quartz, calcium carbonate and bentonite clay, on asphalt rheology. He studied the influence of filler concentration on the viscosity of asphalt-filler systems and found that the filler effect  was less pronounced in higher grade asphalts, which suggests that the viscosity-increasing mechanism involves the movement of asphaltenes and filler particles. The effect of particle size, shape, surface characteristics and surface chemistry of mineral fillers on the rheology of asphalt was investigated. It was reported that: (1) finer filler particles increased the viscosity at a higher rate vs. coarser particles, (2) the effect of shape was relatively small; however, the full effect of particle shape can be more pronounced at a higher shear rate, that exceeded the testing capacity if of the equipment used  for his research, (3) asphalt mixed with mineral surfaces with a thin nonpolar layer resulted in higher than normal viscosity, and (4) basic filler (e.g., calcium carbonate) produced high relatively viscosity when mixed with asphalt with high asphaltenes contents; however, acidic filler (bentonite) produced relatively high viscosity when mixed with asphalt with low asphaltenes contents.

Winniford also noticed that asphalts deviated from Newtonian response as the filler concentration was increased; also, the temperature susceptibility was lower than that of unfilled asphalts in temperatures ranging from 77°F up to 130°F (25 up to 54°C), and that thixotropic hardening was influenced by the presence of fillers. This type of hardening is more pronounced in relatively fluid systems and is reduced by increasing viscosity of the media (Winniford, 1961).

Kallas and Puzinaukas (1961) studied the effects of mineral fillers on the properties of sheet and dense graded asphalt mixtures. Eleven mineral fillers and one asphalt cement of 85-100 penetration grade were used in this study. The fillers were of a wide variety of mineralogical compositions, particle sizes and shapes. Among these fillers, a fly ash with a specific gravity of 2.538 was used. Kallas and Puzinaukas used a Marshal compactor to determine the densities, stability and flow values and also measured water and temperature susceptibility of asphalt mixtures. A sliding plate microviscometer was used to measure the viscosity of filler-asphalt mixtures and adsorption of asphalt from low concentration benzene solution was used to determine the relative affinities of a given filler to asphalt.

The authors found that the amount of asphalt required to produce maximal density, and minimal aggregate voids content vary widely for some fillers, with kaolin clay and limestone dust being the most effective in replacing asphalt in the mixture. Fly ash had intermediate effects in replacing asphalt in the mixture. All mineral fillers increase the Marshall stabilities of sheet asphalt mixtures and dense graded asphalt mixtures, the only exception was asbestos filler used in dense graded asphalt mixtures. With respect to water susceptibility, authors found that the fly ash used in this study had no water susceptibility and noted that, generally, fillers containing hygrocospic moisture have higher water susceptibility. With the help of sliding plate viscometer it was found that the addition of fillers induces non-Newtonian flow in asphalt-filler mixtures, but the relation between this behavior and filler concentration varies widely according to type of filler.

Heukelom and Wiga (1971) investigated the effects of the particle-particle interaction on the dispersion and differentiated two extreme cases. These two extreme cases are known as the flocculated state, in which the agglomeration of particles can occur and the fully peptized state, in which the continuous phase separates all particles from one another. When the particles are in flocculated state are not completely peptized, the particles can occupy larger volumes increasing the effective volume concentration and resulting in a higher viscosity. A unique relationship was developed to express the rheological characteristics of dispersions in terms of volume concentration and rate of shear. The goal was to derive a generalized equation that could be valid for various dispersions assuming that the stiffness of the mastic at a filler volume concentration equal to the maximal packing approaches infinity (Eq. 2.4).

$$\frac{1}{\sqrt{\eta_r}} = 1 - (1+k)(1+m)C_v \quad \text{Eq. 2.4}$$

where,

$\eta_r$ = relative viscosity
k = shear rate factor
m = peptization and shape factor
$C_v$ = volume concentration of the fillers

This unique relationship uses two factors, one that takes into account the shape and state of peptization (1+m) and another that takes into account the rate of shear (1+k).

Anderson and Goetz (1973) studied the mechanical behavior and reinforcement of asphalt-filler mixtures. Authors investigated the stress-strain response of mastics and the potential for the interaction between two mineral fillers and two asphalt binders. The mineral fillers used where quartz and calcite, representing the range of materials between acidic and basic. These two mineral fillers were divided in three different ranges of sizes under the No. 200 sieve to study the interaction with different particle size of the fillers. Two asphalt binders of this study were of AC-20 viscosity grade but, with different viscosities at 77°F (25°C) which indicates that one represents a Newtonian fluid and the other a non-Newtonian fluid. Mineral fillers were added at a concentration of 40% by volume.

Anderson and Goetz applied sinusoidal and quasi-static shear stress to asphalt and asphalt-filler samples at three different temperatures and measured the resulting strains to characterize the dynamic and creep behavior and determined that asphalt-filler mixtures can be characterized as thermos-rheological simple linear viscoelastic materials. By comparing quasic-static, sinusoidal and viscosity results authors evaluated the potential for the reinforcement with mineral fillers. They noticed that the viscosity of the Non-Newtonian asphalt binder increased with decreasing the particle size, concluding that mastic behavior is dependent on particle size. On the other hand, the viscosity of Newtonian asphalt binder was independent of particle size. This indicates that the reinforcement potential of the mineral fillers is more pronounced for the non-Newtonian mixtures which led to the conclusion that the reinforcement is due to physico-chemical interaction.

Dukatz and Anderson (1980) conducted the creep and resilient modulus tests at different temperatures to determine the effect of type and quantity of mineral fillers on the mechanical properties of filler-asphalt mixtures and asphaltic concrete paving mixtures. Eight mineral fillers were mixed with two different asphalt of AC-20 viscosity grade at filler-asphalt ratio of 0.5 and 1. Asphalt concrete samples were compacted with a kneading compactor and testing for air voids, Marshall stability and density was performed.

From the creep measurements performed with the cone and plate viscometer using reference unfilled and filled asphalt samples authors found that the mineral filler or asphalt type have no significant effect on the time-temperature shift function of samples prepared at asphalt-filler ratios below 1. This was a clear indication of no significant differences and effect on temperature susceptibility of tested samples.

Using a diametral modulus device authors found a very significant effect of fillers on the creep compliance (long-term non-recoverable response) of asphalt concrete mixtures. On the other hand, authors found no apparent effect due to asphalt or mineral type on the resilient modulus or short-term elastic response. Authors noticed that the excessive amounts of mineral fillers can make mixtures difficult to compact and also noticed that the increase in the percentage of mineral filler reduced the volume of air voids by an amount equivalent to the volume of added mineral filler. However, authors found no definite trends on Marshall stability and density of asphalt concrete mixtures.

Anderson et al. (1983) studied the influence of baghouse fines on asphalt mixtures design. Authors determined the properties of seven baghouse dust specimens from typical plants operations and studied the effect of these fillers on the response of asphalt concrete mixtures. The penetration, viscosity at 275 and 140°F (135 and 60°C), and softening point of the asphalt-dust mixtures prepared with seven fillers at five filler-asphalt ratios were measured. The penetration results indicated a decrease in the penetration with increase of filler content. On the other hand, viscosity and softening point increase with increase in filler content. These results are a clear indication of the stiffening potential of fillers in asphalt  mastics. The penetration, the viscosity and softening point were independent of filler size which means that fineness alone is not sufficient indicators for stiffening potential.

The Marshall stability, flow and air voids of asphalt mixtures made with different baghouse dust were investigated. Increase of dust filler content, type of mineral filler and filler-asphalt ratio did not affect significantly the Marshall stability response. This confirmed the poor relationship of the Marshall stability and stiffness. On the other hand, flow and air voids values were sensitive to concentration of the baghouse dust.

Anderson et al. (1992) used the Dynamic Shear Rheometer (DSR) and Bending Beam Rheometer (BBR) tests to study the rheological behavior and failure response of mastics with two mineral fillers, quartz and calcite, added to four asphalt cements. Authors concluded that the addition of minerals has neither effect on the temperature shift factors nor the rheological response, but changed the frequency dependency by shifting the relaxation times to longer times thereby stiffening the asphalt. I was noticed that for the mastics studied, the presence of mineral filler did not significantly affect the rate or level of oxidative or physical hardening and the strain and energy-to-failure characteristics of asphalt cement at low temperatures.

Ray Brown et al. (1996) conducted work to characterize Stone Matrix Asphalt (SMA) fine mortars using the Superpave® binder protocol tests. Authors characterized the fine mortar fraction using the Superpave® system to determine the effects of the mortar components on the overall mortar performance.

The materials used in this research were one virgin asphalt cement, three modified asphalt cements, two mineral fillers and three fiber types used as stabilizing additives. The asphalts were modified with Styrene-Butadiene-Styrene (SBS), Styrene-Butadiene-Rubber (SBR) and with polyolefin.  The mineral fillers used were fine limestone dust and baghouse fines produced from limestone and natural sand mixture at a Hot Mix Asphalt (HMA) plant.

At high temperatures (64°C), the baghouse fines produced mortars with higher DSR stiffness than the limestone dust. This is contrary to what was expected since the limestone dust was finer material than the baghouse fines. The SBS modified binder based fine mortars had a higher DSR stiffness than the mortars with SBR and polyolefin modifiers. The stiffness results at intermediate (service) temperatures (25°C) after the material was aged demonstrated no difference between limestone dust and baghouse fines. On the other hand, the SBS modified fine mortars were less stiff when compared to the fine mortars prepared with virgin, SBR modified and polyolefin modified asphalts. At low temperatures (-12°C), the baghouse fines tend to increase the fine mortar stiffness at a higher degree than the limestone dust.

Authors concluded that the most of the stiffening effect comes from the mineral filler, but that the filler size is not the only parameter in specifying fillers. The parent material and the filler particle angularity most be considered as important factors for the design of an effective mix.

Mogawer and Stuart (1996) studied the properties of asphalt mastics and mixtures to distinguish between the mineral fillers and also to determine the relationship between free binder content and properties of mastics and mixtures. The free binder content is determined by subtracting the total volume of binder used in a mixture from the fixed binder volume calculated from the Anderson modified Rigden voids test. In this study eight different types of mineral fillers, including one fly ash with a very high specific gravity (3.180), an asphalt binder graded as AC-20 and cellulose fibers (stabilizing additive) were used to prepare mastics. These mastics were tested using the Bending Beam Rheometer (BBR), Ring and Ball apparatus and Dynamic Shear Rheometer (DSR). The BBR, the Ring and Ball apparatus and the DSR were unable to identify the effects of mineral fillers on performance, but the BBR and the Ring and Ball had a good correlation with the free binder content (with a $R^2$ = 0.95 and 0.92, respectively). On the other hand, the DSR test had a poor correlations with the free binder content (with a $R^2$ = 0.49). Also a poor correlation was established between the DSR and the Ring and Ball apparatus results ($R^2$ = 0.05). From these results authors concluded that the tests used were not successful to distinguish between the fillers with good and bad performance, but good correlations were found between the BBR and Ring and Ball test results and the free binder content .

Shashidhar and Romero (1998) proposed  a fundamental approach to understand the influence of fillers and asphalt properties on the stiffening potential of fillers in asphalt. Relationships between the maximum packing factor ($\varphi_m$), the generalized

Einstein coefficient ($K_E$) and known properties of the fillers, such as, average particle size, gradation, particle shape and mastic properties, such as, asphalt-filler interface, presence of agglomerates and degree of dispersion was investigated. A Dynamic Shear Rheometer (DSR) was used to determine the complex shear ratio ($G^*_r$) at intermediate temperatures (7 to 45°C) and high temperatures (45 to 82°C) using an 8mm and 25mm parallel plate geometries, respectively.

Authors found that the stiffening effect of particles with sizes bellow 10 μm is higher than that for particles with sizes above 10 μm which means that finer particles stiffened asphalt more than coarser particles. It was noticed that the same fillers behave differently in different asphalts which is a sign of the asphalt-filler interaction on stiffening. The fillers with low maximal packing factor were poorly dispersed in asphalts and agglomerates increased the stiffness of the mastic increasing the Einstein coefficient.

Authors concluded that the proposed approach can predict accurately the stiffening potential taking into account the agglomeration, degree of dispersion and asphalt-filler interface.

Faheem and Bahia (2008) studied the effect of mineral fillers on damage resistance of asphalt mastics to permanent strain accumulation and fatigue. Two asphalt binders, PG58-28 and PG70-22, and two fillers of different mineralogy, limestone (basic) and granite (acidic) were mixed at 25% and 50% concentration by volume and tested using the DSR. The permanent strain was measured from creep and recovery test. The rutting resistance of asphalt mastics was investigated at 52°C, 58°C and 64°C. The fatigue test was conducted under repeated shear cyclic loading at 28°C and the complex shear modulus (G*) and phase angle ($\delta$) were measured as a function of number of loading cycles. Fatigue resistance was characterized by the amount of loading cycles required for a 50% reduction of the complex shear modulus (G*). The Superpave® fatigue factor, G*sin $\delta$, was also measured. Results proved that mineral fillers significantly increase the complex shear modulus and fatigue life of asphalt mastics as compared reference asphalt binders. The addition of fillers enhances the mastic resistance to rutting, in terms of total terminal strain and non-recoverable compliance. These effects were found not to be highly dependent of filler mineralogy. The fatigue life of mastics was significantly larger than that of the asphalt binder, with the limestone filler (basic) having more positive effects than the granite filler (acidic). This observation can be related to the mineralogical properties of the filler. Faheem and Bahia (2008) also found that G*sin$\delta$ results increased consistently with the addition of fillers. It was reported that the G*sin$\delta$ appears not to be sensitive to filler type.

Faheem (2009) measured G* ratio for fly ash and granite blends at different filler content. The increase in the G* ratio with the addition of fillers is illustrated by Figure 2.5. The initial rate of stiffness increase is comparable between the fillers. For the granite filler, around 35% by volume, the rate of stiffening starts to increased rapidly until 50% by volume where no more filler could be added without introducing air voids. On the other hand, fly ash transition to such ultimate dosage was more gradual.

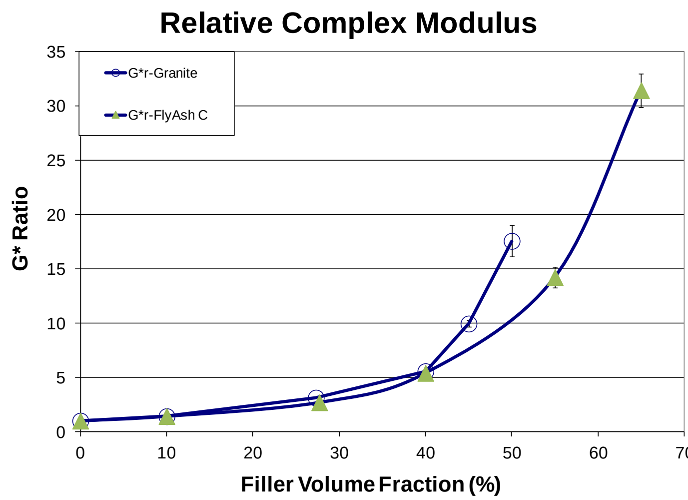


**Figure 2.5 The effect of filler concentration on G* ratio (Faheem 2009)**

Faheem (2009) also investigated the mastics integrity using the DSR Tack test. The maximum integrity of the mastic with granite is achieved at 27% volume concentration, while in the fly ash mastics this parameter is achieved at 45% (Figure 2.6). In general, at concentrations more than 10% by volume, the mastics with fly ash outperform that of the mastics with the granite filler, indicating that fly ash enhances the bonding strength and improves the tack factor vs. the standard fillers used in the paving industry. It is important to note that similar performance was observed for different mastics based on binders from a different crude source.

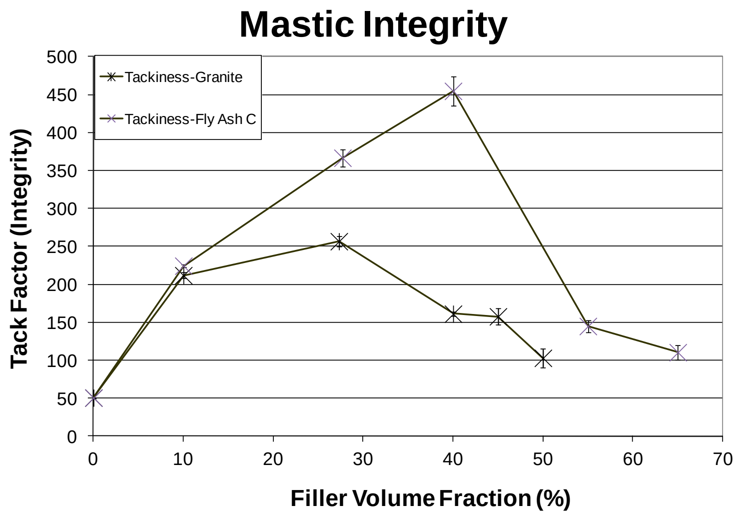


**Figure 2.6 Tack Factor (mastic integrity) at different filler concentrations (Faheem 2009)**

The superior tackiness of the fly ash based mastics was demonstrated with respect to the rheological performance of the mastics. Faheem et, al. conducted a preliminary study on the impact of fly ash on asphalt binder aging. Many pavement failures were linked to the oxidative aging of binders, and observed failures include the thermal cracking, fatigue cracking, and surface raveling.

### 2.3.2 Influence of fillers on aging resistance of asphalt mastics

Miró et al. (2005) studied the effect of fillers on the aging of bitumen blends with fillers added by volume. The researchers added two types of fillers, hydrated lime and calcium carbonate to an 80 to 100 penetration bitumen and prepared a mixture with granite aggregates. Asphalt mixtures were compacted into Marshall molds and tested after aging in an oven at 80°C for 0, 2, 4 and 7 days using the Barcelona Traccion Directa (BTD) test at 20°C and at deformation rate of 1 mm/min. After BTD test the bitumen was extracted from the specimens by the centrifuging method to assess the effect of the filler on the aging of bitumen. Miró et al. (2005) analyzed the penetration, softening point and dynamic viscosity (at 135°C) of the recovered bitumen and observed that the addition of hydrated lime filler produces a slight decrease in the penetration and a slight increase in the softening point and dynamic viscosity. According to the researchers these results indicate that the addition of filler improves the aging resistance of bitumens.

Miró et al. (2005) also analyzed the critical load, the maximum deformation and the specific fracture energy of aged mixtures using the BTD. The increase in the load and the decrease in the deformation were correlated with aging. However, these properties were not affected by the addition of investigated fillers. Still, the potential protective effect of hydrated lime in asphalt expected. Authors concluded that the specific energy of fracture, calculated from the BTD test, allows to establish a criterion for selecting the ideal content of filler to minimize the aging of the bitumen.

Huang and Zheng (2007) studied the effect of filler surface on the rheological properties with respect to long-term aging. Two different types of fillers, limestone and granite, and two asphalt binders from different sources classified as PG58-28 and PG58-10 under the Superpave® binder testing protocol were used in the reported study. Asphalt-filler mixes were prepared by mixing 20% of filler (by the weight of asphalt) and aged in the Pressure Aging Vessel (PAV) at 60°C for 100, 400, 800 and 2000 hours. A frequency sweep was conducted on the aged materials on a Dynamic Shear Rheometer at 25°C and 60°C using 8 and 25 mm plate testing geometries.

The researchers reported that the properties of the asphalt binder are dependent on the duration of aging, a phenomenon that can be considered, in term of rheological properties, similar to temperature dependency. As a result, at a given frequency the aging time increases the complex modulus increases and the phase angle decreases at a given frequency (Figure 2.7).

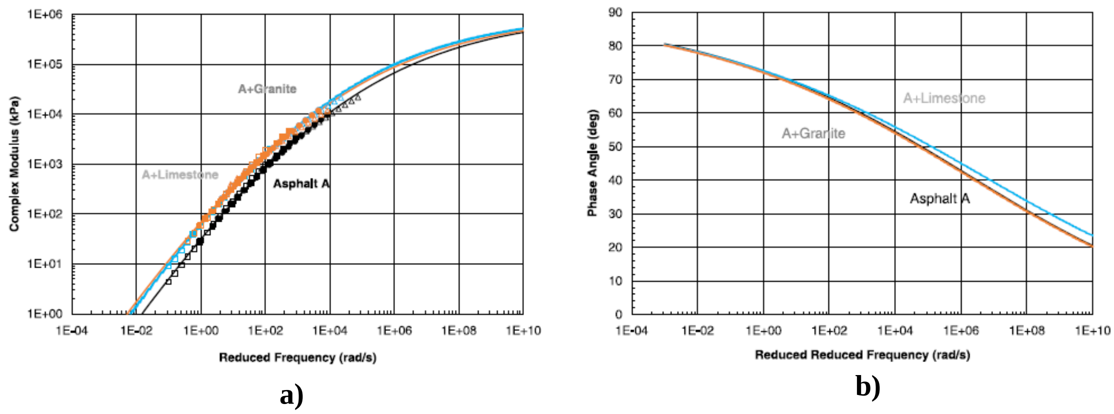


**Figure 2.7 Aging master curves for (a) Complex Modulus and (b) Phase Angle (Huang and Zheng 2007)**

Wu and Airey (2011) investigated the influence of two fillers of different mineralogy, limestone (basic) and gritstone (acidic), on the aging properties of mastics and their recovered binders. The DSR and Fourier Transform Infrared Spectroscopy (FTIR) test were used to investigate the transformations in asphalt mastics and binders at different stages aging in the Thin Film Oven Test (TFOT).

Authors found that the acidic and basic fillers affect the bitumen aging in different ways due to their mineral structures and interaction with the binder: the basic limestone filler had stronger adsorption capability than the acidic gritstone filler.  It was concluded that the aging properties of mastics are mineral dependent and so the mineral fillers can influence aging through catalyzing oxidation of bitumen components by absorbing oily components and adsorbing polar fractions.

### 2.3.3 The use of fly ash in asphalt mixtures

The idea of using fly ash as a mineral filler in asphalt mixtures is not a new concept. Carpenter (1952) determined that a Class F fly ash had an excellent effect on the retained compressive strength of asphalt concrete specimens immersed in water. Warden et al. (1952) determined that fly ash was a suitable filler in terms of mixing, placing, and compaction; the resulting asphalts had demonstrated stability, resistance to water damage, and flexibility.

Zimmer (1970) analyzed the effect of carbon content in fly ash and determined that specimens prepared with fly ash had a higher retained strength after immersing in water. Sankaran and Rao (1973) compared fly ash with other fillers such as kaolin clay and crushed dust and determined that fly ash at 2 % filler content provided the best stability among the other fillers. Henning (1974) investigated the effect of a Class C fly ash on asphalt mixture properties and concluded that the addition of 4 % fly ash resulted in the highest stability, flow, and increased compactability, as indicated by lower air void content. Improved stability of develop HMA with fly ash after immersion in water was also noted.

Galloway (1980) studied the addition of lignite fly ash and indicated that fly ash retards the rate of age hardening of asphalt cement. Furthermore, Rosner et al. (1982) used two fly ash types (Class C and Class F) as a mineral filler and an anti-stripping agent for asphalt concrete mixtures. The asphalt concrete samples were tested against moisture damage by determining the indirect tensile strength of dry and moisture-conditioned specimens following AASHTO T-165. The conditioned specimens were immersed in warm water bath 140°F (60°C) for one day. The retained strength was compared with the dry specimens. Rosner et al. determined the retained strength of the samples increased as additional fly ash was used in the mixtures. In most of the cases, the retained strength of fly ash mixtures weas considerably higher than than obtained by mixtures with other filler materials.

Suheibani (1986) evaluated fly ash as an asphalt extender, which is a material that is capable of extending the binder in asphalt (on volumetric and mechanical levels). Suheibani analyzed the effect of particle size of fly ash on the viscosity of the asphalt. The effect of fly ash on density measurements, voids, and the mechanical properties of asphalt was also examined. Indirect tensile strength of asphalt (using cylindrical specimens), creep, and resilient modulus testing proved that the addition of Class F fly ash can provide superior fatigue life, rutting resistance, and improved tensile strength.

In addition, Tons et al. (1983) investigated the use of Class F fly ash as a bitumen extender. Bitumen was replaced by various percentages of different fly ash types and tests were conducted on asphalt specimens to determine the resistance to moisture damage, thermal cracking, rutting, fatigue life, and asphalt hardening. Noticeable improvements were observed with reduced asphalt hardening, improved moisture and freeze-thaw damage resistance, rutting resistance, increased fatigue life, higher density and higher tensile strength (Tons et al. 1983).

Based on a workability index tested at various temperatures, Cabrera and Zoorob (1994) also established that fly ash based hot-mixed asphalt can be mixed at a temperature as low as 120ºC compared with 160ºC used for conventional control mix.

Fly ash mixes were compacted at temperatures as low as 85°C -110°C without any detrimental effects on engineering and performance properties. It is important to note that the conventional mix required a compaction temperature range of 132ºC to 135ºC. Authors reported considerable energy savings through placement of fly ash asphalt mixtures at lower temperatures compared with conventional mixes.

The effect of filler replacement with fly ash, lime, and portland cement on the performance of asphalt concrete was investigated by Tapkin (2008). He reported an increase in the Marshall stability values and a decrease of flow values for fly ash specimens (vs. control specimens with calcareous filler). It was concluded that filler replacement with fly ash provides a considerable economy of bitumen in asphalt mixtures designed for the equivalent stability. Due to the stiffening of the bitumen in the asphalt-aggregate mixture the fatigue life of fly ash asphalt specimens was found to be considerably higher than that of the other fillers used in the study.

Sobolev et al. (2013) investigated the properties of Rolling Thin Film Oven (RTFO) aged mastics with Class C and Class F fly ash. Two binders with different performance grades (PG58-28 and PG70-22) were used to determine the percent change in G* after RTFO aging. These binders were blended with the fillers at two concentrations (5% and 60% by weight).

Figure 2.8 shows that at 5% concentration of Class C fly ash G* the percent change value for PG70-22 is lower than that of the plain binder, indicating that there can be a binder-filler synergy that can result in the aging protection effect of the fly ash. For the mix with 5% Class F fly ash, the G* percent change values slightly decreased for

PG58-28 and increased for PG70-22. At higher fly ash concentrations (60%), the change in G* for both Class C and Class F fly ash was minor in the case of PG70-22 binder, but was much higher for the PG58-28 binder, demonstrating that up to 60% of fly ash can be effectively used in higher grade binders such as PG70-22 without considerable effect on long-term performance (e.g., stiffening).

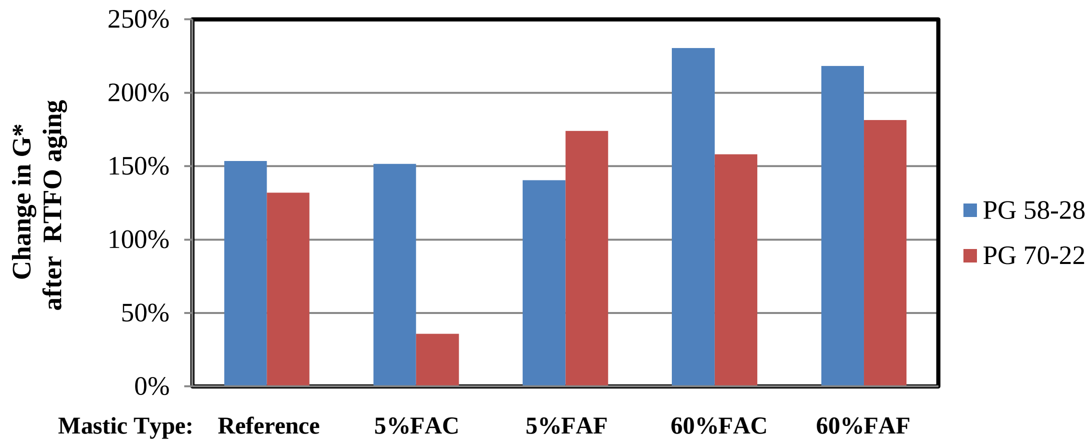


**Figure 2.8 Change in G* after RTFO aging for mastics with fly ash (Sobolev et. al 2013)**

In order to evaluate the performance of aged mastics at low temperatures, Sobolev et al. (2013) used the BBR (Bending Beam Rheometer) test to quantify the change in stiffness and measure the relaxing coefficient of a mastic/binder at PG (Performance Grade) specified low temperature. Figure 2.9 (a) shows the calculated $S_r$ values confirming the trend observed for the $G_r$*. At low fly ash concentrations, the addition of fly ash reduces the measured low temperature stiffness, except for mixtures with 5% of fly ash Class C blended with PG58-28 binder where no change in the stiffness was observed. Class F fly ash had the most reduction in low temperature stiffness, with a 25% decrease in stiffness for PG70-22 binder. This indicates that the low temperature stiffening effect due to oxidative aging is reduced by the addition of fly ash used at lower concentrations. Figure 2.9 (b) shows the relative m-values which represent the ability of tested specimens to relax the thermal stresses.  An increase in the m-value indicates an improved ability to relax thermal stresses. The results of the m-value demonstrated the superiority of Class F fly ash at lower addition rates to improve the thermal relaxation of the mastics. The addition of 5% of Class F fly ash provided the most improvement for both binders. At the same concentration, Class C fly ash provided some increase in the m-value (2%) for PG70-22, with no change in the m-value for PG58-28. The results prove that even at a 60% addition, Class F fly ash provided nominally better thermal relaxation compared with the reference binders.

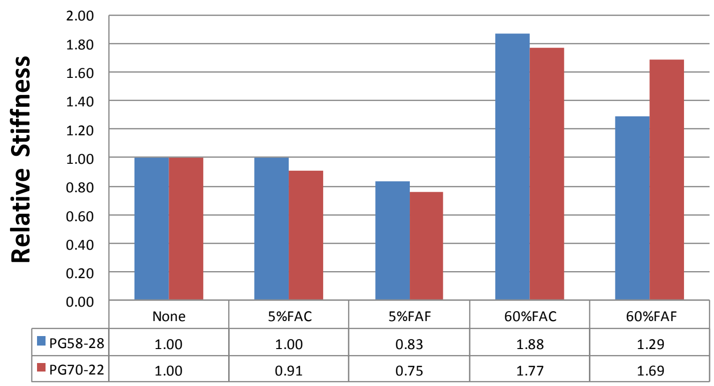


**a)**

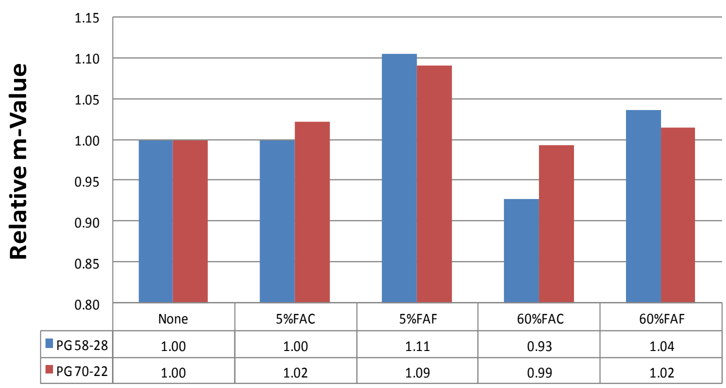


**b)**

**Figure 2.9 Relative low temperature stiffness (a) and relative m-value (b) of aged mastics with fly ash (Sobolev et. al 2013)**

Sobolev et al. (2013) also conducted a limited study on the effect of Class C fly ash on the performance of HMA mixtures. In this experiment, a standard Wisconsin Mix was evaluated to determine the constructability of mixes with fly ash and the initial feasibility of fly ash addition. The standard HMA mixtures with 1-3% of fly ash (by weight of bitumen content) were compacted and tested. Another mixture was designed to replace 10% of the asphalt binder with fly ash. The objective was to evaluate the ability of fly ash to extend the asphalt binder and thus save on the overall cost of the pavements, since the asphalt binder is the most expensive component of the mixture. Figure 2.10 shows the percentage of air voids in the mix per number of compaction gyrations. The compactability was evaluated by calculating the number of gyrations to reach 8% air voids in the mix. The results demonstrated minimal change in the mixture compaction for HMA mixtures with fly ash, or even for mixtures with fly ash replacing 10% of the asphalt binder. This is a very promising result, because it indicates that fly ash can be used in asphalt saving a substantial amount of asphalt by extending the binder without compromising the air void structure.

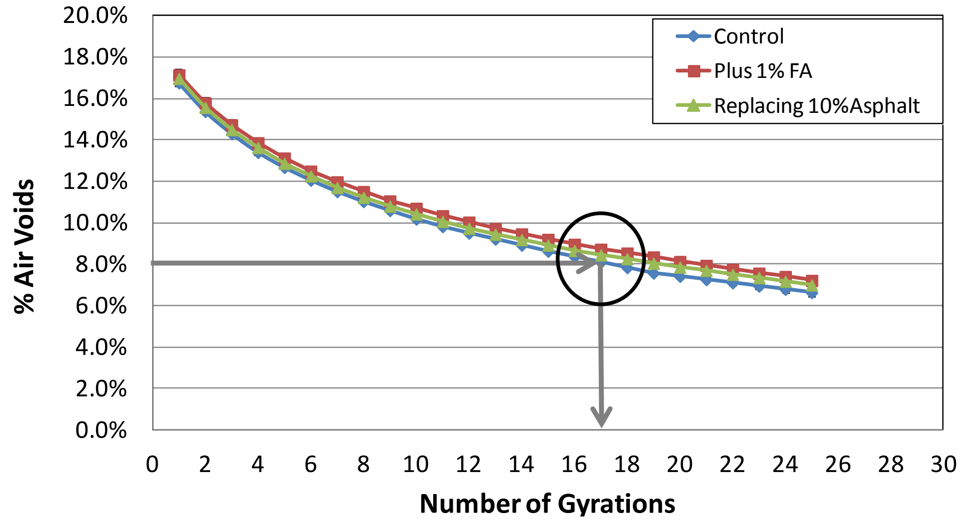


**Figure 2.10 Compactability of HMA/ASHphalt samples (Sobolev et. al 2013)**

# CHAPTER 3.

# MATERIALS AND TESTING METHODS

## 3.1 SUPERPAVE® ASPHALT BINDER TESTING PROTOCOL

Asphalt is defined by the American Society for Testing Materials (ASTM) as a dark brown to black cementitous material in which the predominant constituents are bitumen's which occur in nature or are obtained in petroleum processing (ASTM D242).

Asphalt is a viscoelastic material of particular interest to engineers since it is a strong cement, readily adhesive, highly waterproof, durable, and a hundred percent recyclable material. As a viscoelastic material, asphalt cement has both, elastic and viscous characteristics.

In viscoelastic materials the relationship between the stress (σ) and strain (ε) is time dependent (Lakes 2009). The science that studies viscoelastic materials (including the deformation and flow) in is called rheology.

Four types of asphalt binders of different grades, sources and level of modifications were used in this research,  mixed with different CCPs and characterized using the Superpave® testing protocols. Superpave® specifications classify asphalt cement in performance grades that are tied to environmental conditions. This enables to develop an asphalt cement grading system based on climate that can be applied to all unmodified asphalts and many modified binders. In other words, the evaluated physical characteristics of asphalt, cement are the same for all grades of asphalts but the temperature at which those characteristics are evaluated is determined by the climatic conditions specific to paving location (Roberts et al. 1996).

Under this system asphalt binders are characterized according to their performance as PG HT-LT. The PG stands for performance grade, HT represents an average 7 day maximum pavement temperature and -LT represents minimum pavement temperature for which the binder is appropriate. The binders used in this research were unmodified PG58-28, PG64-28 and acid modified and polymer modified PG64-28M and PG70-28. This means that these asphalt binders are suitable for maximum pavement temperature of 58, 64 and 70 °C and minimum pavement temperatures of -28 °C.

The Superpave® system was developed by the Strategic Highway Research Program (SHRP) for specifying paving asphalt based on its performance characteristics. This system was developed with the intention of addressing four types of pavement distresses: permanent deformation, fatigue cracking, low temperature cracking and moisture damage. In addition to pavement distresses, Superpave® takes into account the oxidation (aging) process experienced by asphalt cement during the Hot Mix Asphalt (HMA) production and service life of the pavement. Both of these oxidation processes are simulated in the lab using the Rolling Thin Film Oven (RTFO) and Pressure Aging Vessel (PAV).

The Dynamic Shear Rheometer (DSR), Rotational Viscometer (RV) and Bending Beam Rheometer (BBR) were used to determine non-performance related and performance related parameters. Mastics with CCPs and natural filler were prepared with asphalt binders of different grades, sources and modification levels, tested at three to five prescribed concentrations between 5% and 40% (by volume). The acid and polymer modified (PM) of reference PG58-28 binder was used to obtain the intermediate grade binder, PG64-28M and the high grade binder PG70-28.

Non-performance related rheological parameters, such as Complex Modulus (G*) and Phase Angle (δ), were measured to evaluate the interaction between the different asphalt binders and CCP materials at high temperature and at wide range of concentrations. Superpave® performance specification (AASHTO M320) tests such as constructability, rutting, fatigue and thermal resistance were conducted on unaged, RTFO and PAV aged mastics. These tests were conducted to determine the mastic rheological and performance properties to understand the level of CCP-matrix interaction and provide the feedback for HMA mixture design.

The viscosity of unaged asphalt mastics was measured with a Brookfield RV as an estimate of the constructability or workability. Superpave® G*/sinδ, non-recoverable compliance (Jnr), %Recovery at high service temperature were measured on the DSR as an estimate of rutting behavior. Also, Superpave® G*sinδ at intermediate service temperature were measured with the DSR as an estimate of fatigue behavior. For aging resistance of mastics incorporating CCPs the PAV aged G* and unaged G* were compared. Finally, thermal resistance was determined using the BBR at low service pavement temperature to measure the creep stiffness (St) and m-value.

**Table 3.1 Test matrix for the rheological study of mastics**

| Mastic Property | Response Variable | Test Method | Aging | Asphalt | CCPs/ Fillers | Conc. | Temp. |
|---|---|---|---|---|---|---|---|
| **Complex Modulus and Phase Angle** | G* and δ | DSR<br>25 mm PP | Unaged | PG58-28<br>PG64-28<br>PG70-28 | 9 | 5 | PG |
| **Constructability** | Viscosity | Rotational Viscometer | Unaged | PG58-28<br>PG64-28M<br>PG70-28 | 9 | 5 | 135°C |
| **Rutting Resistance** | Accumulated strain<br>Non recoverable compliance | DSR/ MSCR<br>25 mm PP | RTFO Aged | PG58-28<br>PG64-28<br>PG64-28M<br>PG70-28 | 9 | 5 (2)<br>3 (2) | PG and +PG |
| **Fatigue Resistance** | G*sin d | DSR<br>8 mm PP | PAV aged and Unaged | PG58-28<br>PG64-28<br>PG70-28 | 7 | 5 (2)<br>3 (1) | Intermediate PG temp |
| **Thermal Cracking Resistance** | S and m | BBR | PAV aged | PG58-28<br>PG64-28<br>PG70-28 | 7 | 5 (2)<br>3 (1) | Low PG temp |

## 3.1.1 Aging Procedures

### 3.1.1.1 Rolling Thin Film Oven (RTFO)

The Superpave® PG binder specification calls for short term aged asphalt binder to be tested at high service temperatures to determine rut damage resistance. The Rolling Thin Film Oven (RTFO), described under AASHTO standard designation T240, simulates the aging of the asphalt binder at mixing and construction stages. Asphalt binder is exposed to elevated temperatures to simulate manufacturing and placement aging. The RTFO also provides a quantitative measure of the volatiles lost during the aging process.

The basic RTFO procedure takes unaged asphalt binder samples in cylindrical glass bottles (jar) and places these bottles in a rotating carriage within an oven. The carriage rotates within the oven while the 163°C (325°F) temperature ages the samples for 85 minutes. Samples are then stored for use in physical properties tests or the Pressure Aging Vessel (PAV).

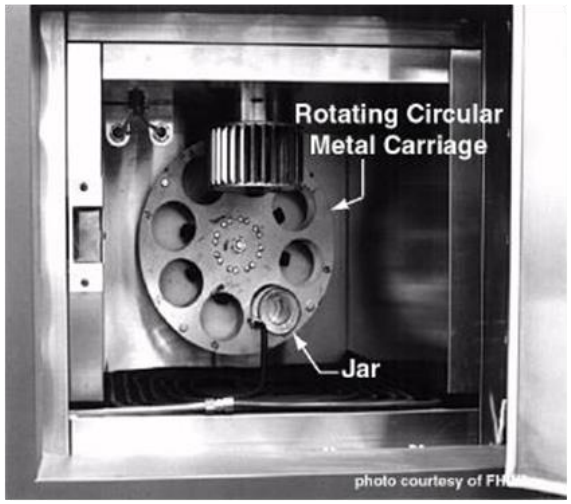


**Figure 3.1 Rolling Thin Film Oven (RTFO)**

### 3.1.1.2 Pressure Aging Vessel (PAV)

After considering short term aging the Superpave® PG binder specifications also considers long term aging of asphalt binder for physical property testing at intermediate temperature to determine fatigue damage resistance and at low temperature to determine thermal damage resistance.  According to AASHTO standard R28 RTFO aged asphalt binder is exposed to heat and pressure to simulate in-service aging over a 7 to 10 year period in the Pressure Aging Vessel (PAV) machine. The basic PAV (Figure 3.2) procedure takes RTFO aged asphalt binder samples, places them in stainless steel pans and then ages them for 20 hours in a heated vessel pressurized to 305 psi (2.10 MPa or 20.7 atmospheres). The heating temperature will depend on the climate for which the asphalt binder is going to be used. Typically it ranges from 90°C to 110°C. The final material is degassed for 30 minutes in a vacuum oven at 170°C. Samples are then stored for use in physical property tests.

**Figure 3.2 Pressure Aging Vessel (PAV)**

### 3.1.2 Dynamic Shear Rheometer (DSR)

#### 3.1.2.1 Time Sweep

One way to characterize the viscoelastic materials is by dynamic testing through the application of a sinusoidal stress (strain) load to the material. In this case, the response strain (stress) is usually sinusoidal. In this case a time lag between the stress sinusoid and the strain sinusoid is observed. This time lag is known as the phase angle ($\delta$). The Dynamic Shear Rheometer (DSR) measures a specimen's complex shear modulus ($G^*$) and phase angle ($\delta$). The $G^*$ means the sample's total resistance to deformation when repeatedly sheared, while $\delta$ is the lag between the applied shear stress and the resulting shear strain. Figure 3.3 shows this phenomenon, where $\Delta t$ is equal to the time lag.

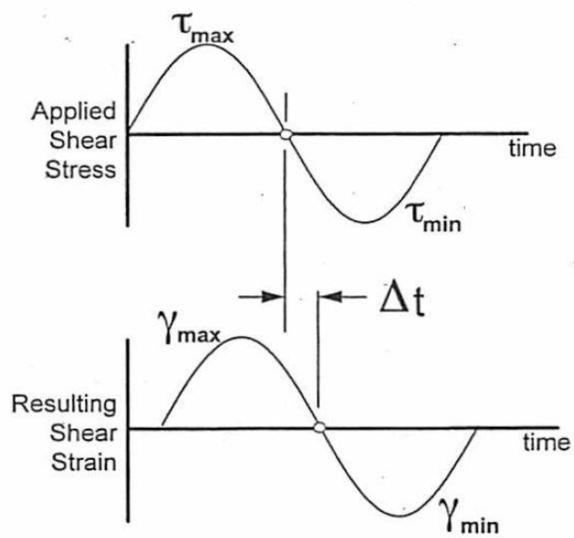


**Figure 3.3 Stress-Strain Response of Viscoelastic Materials (after the Asphalt Institute 2003)**

For elastic material the stress/strain reaction to load is immediate resulting in the $\delta$ =0°. For viscous materials, since the stress is proportional to the strain rate, the $\delta$ = 90° ($\pi$/2). For viscoelastic materials the $\delta$ is in between 0° and 90° ($\pi$/2).

The stress and strain function on Figure 3.3 can be expressed mathematically by:

$$\sigma(t) = \sigma_0 sin(\omega t + \delta) \qquad \text{Eq. 3.1}$$

$$\varepsilon(t) = \varepsilon_0 sin(\omega t) \qquad \text{Eq. 3.2}$$

where:

$\sigma_0$ = peak stress
$\varepsilon_0$ = peak strain
$\omega$ = frequency of loading, rad/s
T = period

For analysis, the stress function can be broken into two functions of the same frequency (Macosko 1994), one in phase with the strain (sin ωt) and another out of phase with the strain (cos ωt) (Eq. 3.3).

$$\sigma(t) = \sigma_0 \sin\delta \cos\omega t + \sigma_0 \cos\delta \sin\omega t \qquad \text{Eq. 3.3}$$

The in phase function (sin ωt) represents the elastic component (δ =0°) and the out of phase function represents the viscous component (δ = 90°). Since the Hooke's Law is also applicable to shear stress (τ) and shear strain (γ), Eq. 3.3 can be written as:

$$\tau(t) = \tau_0 \sin\delta \cos\omega t + \tau_0 \cos\delta \sin\omega t \qquad \text{Eq. 3.4}$$

By dividing Eq. 3.4 by the shear strain ($\gamma_0$) two dynamic moduli can be identified. One with the in-phase function called Shear Storage Modulus (G') (Eq. 3.5) and another with the out-phase function called Shear Loss Modulus (G") (Eq. 3.6).

$$G' = \frac{\tau_0 \cos\delta}{\gamma_0} \qquad \text{Eq. 3.5}$$

$$G'' = \frac{\tau_0 \sin\delta}{\gamma_0} \qquad \text{Eq. 3.6}$$

In viscoelastic materials, the Shear Storage Modulus (G') represents the elastic portion and it is a measure of the stored energy. On the other hand, the Shear Loss Modulus (G") represents the viscous portion and it is a measure of the energy dissipated as heat (Meyers and Chawla, 1999).

Using trigonometry it can be seen that:

$$\tan\delta = \frac{G''}{G'} \qquad \text{Eq. 3.7}$$

The prime and double prime notation has it origin in complex numbers (Macosko, 1994). In this way a Complex Shear Modulus (G*) can be defined as:

$$G^* = G' + iG'' \qquad \text{Eq. 3.8}$$

Where G' is the real component and G" the imaginary component of the Complex Shear Modulus (G*).

The Complex Shear Modulus (G*) represents the stiffness of material for a specific frequency of loading and its graphical representation can be seen in Figure 3.4. It is observed that the higher the time lag between the stress and strain (δ), the higher the G" is and the more viscous the material is.  Then again, the smaller the time lag between the stress and strain (δ), the higher the G' is and the more elastic the material is.

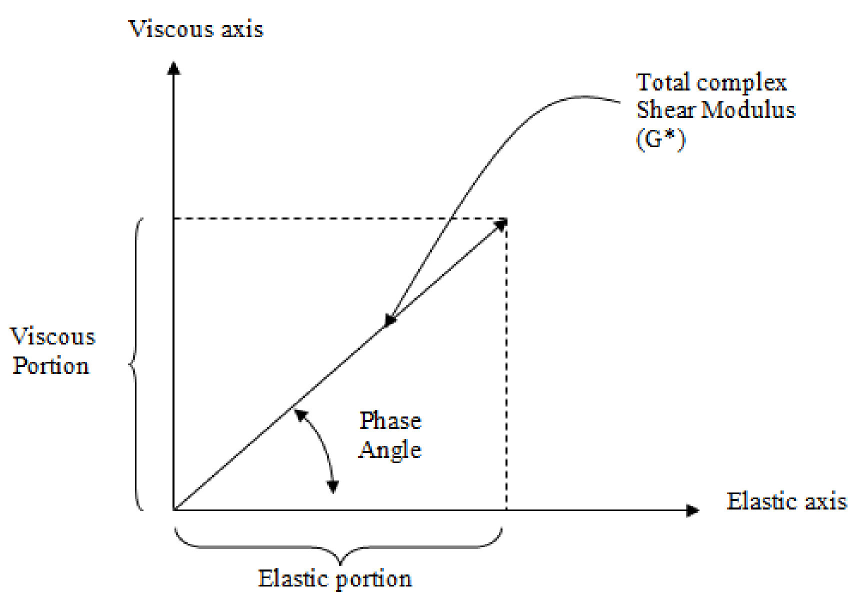


**Figure 3.4 Complex Shear Modulus Representation**

The specified DSR oscillation rate of 10 radians/second (1.59 Hz) is selected to simulate the shearing action (an average traffic speed according to the standard) corresponding to traffic speed of about 55 mph (90 km/h). The G* and δ are used as predictors of HMA rutting and fatigue cracking. In early pavement life, rutting is the main concern, while upon aging the fatigue cracking becomes the major concern.

To measure the asphalt cement rutting resistance at high pavement service temperatures the Superpave ® system uses a rutting factor, G*/sin δ. According to AASHTO M320, when unaged asphalt cement is tested under the dynamic loading at the maximum pavement service temperature, this factor must be equal or greater than 1.00 kPa. On the other hand, when Rolling Thin Film Oven (RTFO) aged asphalt binder is tested under the dynamic loading at the maximum pavement service temperature this factor must be equal or greater than 2.20 kPa.

According to AASHTO T315, under a controlled strain test the target strain level for unaged materials should be 12%. This target strain level is defined by the Superpave® as strain level where the asphalt binder is still within the linear viscoelastic region. Under this phase of the research all the tests were conducted on asphalt mastics, so the strain level was reduced to 5% for unaged asphalt binder.

To measure the asphalt cement fatigue cracking resistance at intermediate pavement service temperatures the Superpave® system uses a fatigue factor, G*sin δ. When asphalt cement aged in the RTFO and Pressure Aging Vessel (PAV) is tested under the dynamic loading at the intermediate pavement service temperature the fatigue factor has a maximum limit of 5,000 kPa. According to Superpave®, the intermediate testing temperature depends on the asphalt binder used and it is determined by adding the high and low PG temperatures, dividing it by two and adding 4°C. Similar to unaged materials, for this research, the target strain level for PAV aged materials was reduced to 0.6% so the material is tested in the linear viscoelastic region. The target strain value for PAV aged asphalt binder according to AASHTO T325 is 1%. These strain levels were selected based on limited experiments to assure the linear viscoelastic response

#### 3.1.2.2 Multiple Stress Creep and Recovery (MSCR)

The Multiple Stress Creep and Recovery (MSCR) test, using the Dynamic Shear Rheometer, is a recent development to the Superpave® Performance Graded (PG) asphalt binder specification. This test is conducted according to the AASSHTO standard T350 at a high pavement service temperature and is related to pavement rutting damage resistance. This test method is comparable to elastic recovery, toughness and tenacity, and force ductility of the asphalt binders. This test was primarily developed to characterize the polymer modified binders.

The G*/sinδ test conducted by DSR is not sufficient to characterize the rutting resistance of polymer modified binders; therefore it is usually coupled with this test to characterize the deformation resistance and recovery influenced by the polymer modification (D'Angelo, 2009). In this test method a load of 0.1 kPa is applied initially for 1 sec (conditioning load) and released (recovered) for 9 sec, and then this process continues for a total of 10 cycles. Afterwards, a load of 3.2 kPa is applied for 1 sec and recovered for 9 sec for another 10 cycles (Figure 3.5). In this research, an additional load of 10 kPa was used to complement the standard 0.1 kPa and 3.2 kPa sequence. This test is run on RTFO aged samples at high PG grade temperature. The MSCR test was conducted on unmodified asphalt binders PG58-28 and PG64-28 and on acid and polymer modified asphalt binder PG64-28M and PG70-28 blended with the eight CCPs and the reference limestone fillers.

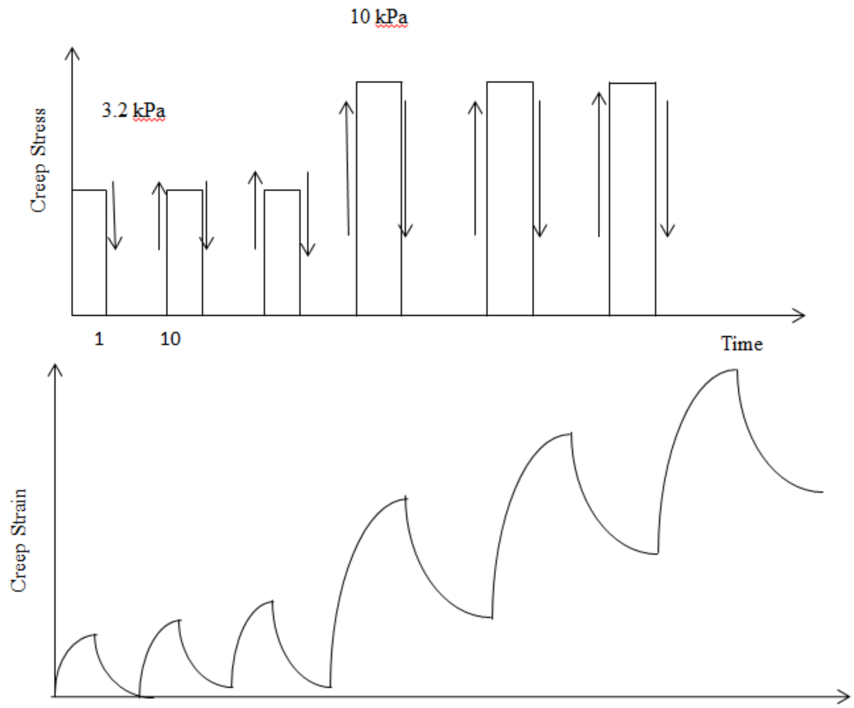


**Figure 3.5 Multiple stress creep and recovery test principle according to AASHTO T350 standard**

The calculation method for non-recoverable creep compliance (inverse of complex modulus), Jnr is demonstrated by Figure 3.6. The percent recovery is calculated from the resulting strain values by using MS Excel as demonstrated by Figure 3.7. Research demonstrated that Jnr is highly correlated with pavement rutting (D'Angelo 2009). As the asphalt binder becomes stiffer, the Jnr becomes lower and % Recovery goes higher.

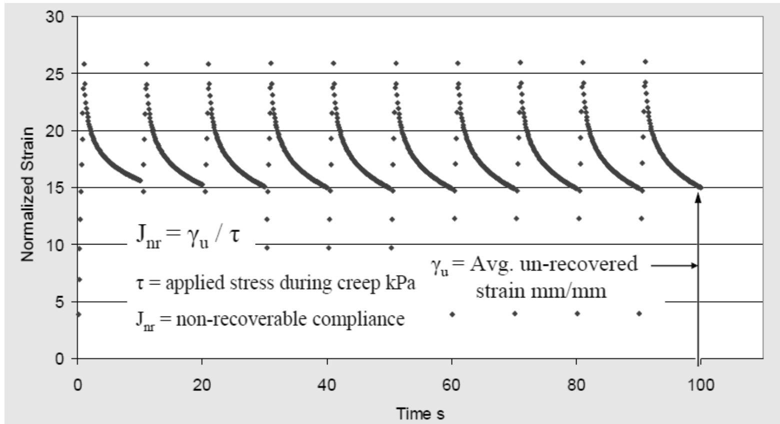


**Figure 3.6 The determination of $J_{nr}$ (after D'Angelo, 2009)**

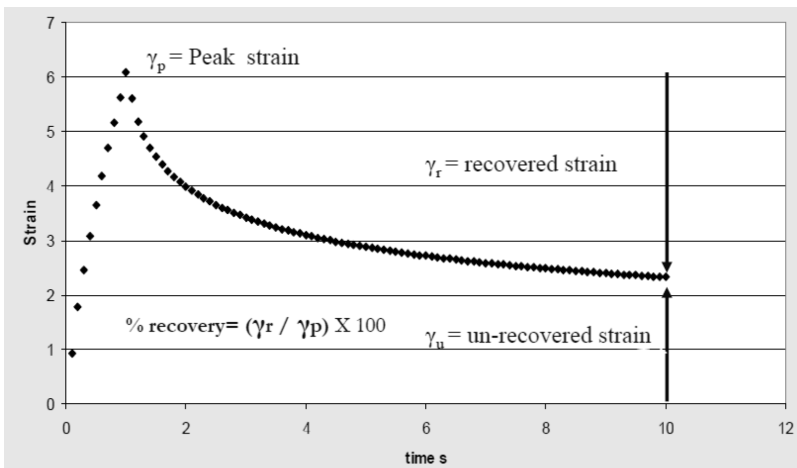


**Figure 3.7 The determination of percent recovery (after D'Angelo, 2009)**

### 3.1.3 Brookfield Rotational Viscometer (RV)

The Rotational Viscometer (Figure 3.8) is used under the Superpave® testing protocol to measure the asphalt viscosity at high construction temperatures (above 100°C). Since at such high temperatures the behavior of the most asphalt binders is totally viscous, a viscosity measurement is sufficient to represent the workability of the asphalt.

According to ASTM D4402, during this test the torque on a rotating spindle in a thermostatically controlled sample holder with asphalt is measured to determine the relative resistance to rotation. The torque and speed are used to estimate the viscosity of the asphalt in pascal seconds (Pa.s), milipascal seconds (mPa.s) or centipoises (cP). As with other viscoelastic material, the asphalt cements behavior is affected by temperature and load. The temperature at which asphalt is heated has an influence on its flow characteristics. The higher the temperature the more flowable (less viscous) the material will be. During the production process of Hot Mix Asphalt (HMA) it is important to determine the right temperature at which asphalt binder needs to be heated for sufficient flowability required for a proper mixing with aggregates and to assure that the end product can be pumped, handled and compacted.

The Superpave® binder specifications set the viscosity limit for unfilled asphalts at a maximum of 3 Pa.s at 135°C. For the Rotational Viscometer (RV) test the viscosity at 135°C is reported as the average of three readings. Viscosity of mastics was measured at 135°C using a #27 spindle. The test started with 30 minutes of conditioning of the specimen at the testing temperature. During the last 10 minutes of equilibrium the spindle started to rotate at 20 rpm for 900 seconds. The viscosity measurements were taken every 300 seconds of testing, recording the average of the apparent viscosity to evaluate the effect of CCPs and reference filler on mastics workability. Work conducted on mastics made with natural fillers under the NCRHP 9-45 project sets the limit on relative viscosity to 5 (Bahia et al. 2011).

Although mastics are known to be shear dependent materials the shear rate speed was kept at 20 rpm because it is the most commonly used shear rate in binder testing in accordance with Superpave® binder protocol. Work conducted under the NCHRP 9-45 found that the relative ranking of mastics did not change as a function of shear rate (Bahia et al. 2011).


**Figure 3.8 Rotational Viscometer (RV) (Pavement Interactive, 2015)**

### 3.1.4 Bending Beam Rheometer (BBR)

To measure the asphalt cement thermal cracking resistance at low pavement service temperatures the Superpave® system measures the creep stiffness ($S_t$) and the slope of the creep stiffness (m-value). Creep is defined as a progressive deformation of a material under constant stress so when a creep experiment is conducted the stress is increased instantly from 0 to $\sigma_0$ and the strain $\varepsilon(t)$ is recorded versus time.

As shown in Figure 3.9, a typical creep response of a viscoelastic material is to demonstrated the instantaneous deformation at $t_0$ as soon as the stress is applied, then an increase in strain from $t_0$ to $t_1$ when the applied stress is continued and once the stress has been removed the material will respond with partial or total recovery (Lakes 2009).

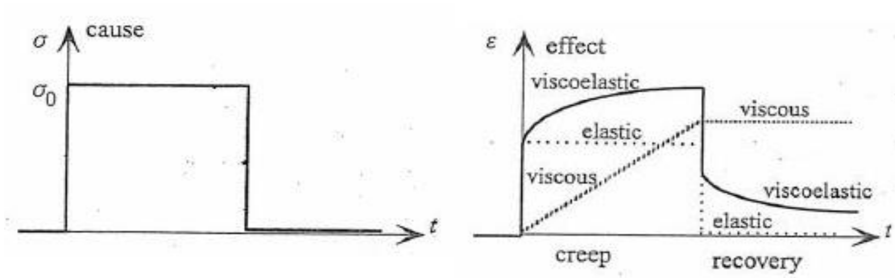


**Figure 3.9 Creep and Recovery. Stress (σ) and Strain (ε) versus time (t) (after Lakes 2009)**

The Bending Beam Rheometer (Figure 3.10) test was conducted according to the standard AASHTO T313. Low temperature cracking is generally found mostly in older, brittle pavements; therefore, the test is performed on the long-term aged material, after Pressure Aging Vessel (PAV). When asphalt cement aged in the RTFO and PAV is tested under creep loading at low pavement service temperature the creep stiffness ($S_{(t)}$) is calculated using the Bernoulli beam classic theory as a function of time, sample geometry and deflection (Eq. 3.9).

$$S\,(t) = \frac{P\,L^3}{4bh^3\delta(t)} \qquad \text{Eq. 3.9}$$

where,

S(t) = creep stiffness (MPa) at time t,
P = applied constant load, (N)
L = distance between beam supports, 102 mm,
b = beam width, 12.5 mm,
h = beam thickness, 6.25 mm, and
δ(t) = deflection (mm) at time, t.

According to Superpave®, for asphalt binders the creep stiffness $S_{(t)}$ must not exceed 300 MPa. Also the slope of the creep stiffness is calculated as an indication of the relaxation of the asphalt binder at low temperatures and it is called m-value. The m-value must be at least 0.300. The standard states that the stiffness value at 60 seconds is reported because it is correlated to 2 hours of actual traffic loading, resulting in pavement cracking. The test is conducted at the low PG temperature plus 10°C, and the time temperature superposition is applied to calculate the response at the low PG temperature; this allows for shorter testing times (Ng Puga, 2013). Therefore, for PG58-28, PG64-28 and PG70-28, the test was conducted at -18°C rather than -28°C.

**Figure 3.10 Bending Beam Rheometer**

## 3.2 SUPERPAVE® ASPHALT MIXTURE COMPACTION PROTOCOL

### 3.2.1 Superpave® Gyratory Compactor (SGC)

Superpave® mix design methodology will be used to compact asphalt mixes obtained from a pilot project. The Superpave® mixtures design procedure was develop by the Strategic Highway Research Program (SHRP) to provide guidance on the selection of aggregates and asphalt binder.

The Superpave® Gyratory Compactor (SGC), Figure 3.11, is used to compact the selected aggregates and asphalt binder to a density similar to that obtain in the field. The SGC produces HMA mixes for volumetric analysis, and it also measures the sample density throughout the compaction procedure.

**Figure 3.11 Superpave® Gyratory Compactor**

The compaction effort of the SGC is control by the vertical pressure, angle of gyration, and number of gyrations. For the Superpave® procedure, the vertical pressure is set at 600 kPa (87 psi) and the angle of gyration is set at 1.25°. The gyrations are applied at a rate of 30 revolutions per minute. The number of gyration can be varied to simulate traffic level. The SGC produces HMA specimens that are 6 inches in diameter. HMA samples compacted on the SGC and HMA loose samples are used to determine the bulk density (Gmb) and maximum theoretical density (Gmm).

The SGC is capable of recording the height of sample with each gyration throughout the test. By knowing the mass of material placed in the mold, the inside diameter of the mold, and the specimen height, the HMA specimen density can be estimated during compaction. With these measurements, a specimen's compaction characteristics plot can be develop. A compaction characteristics curve is develop by plotting the percent of maximum theoretical density (%Gmm) vs. gyrations in logarithmic scale as shown in Figure 3.12.

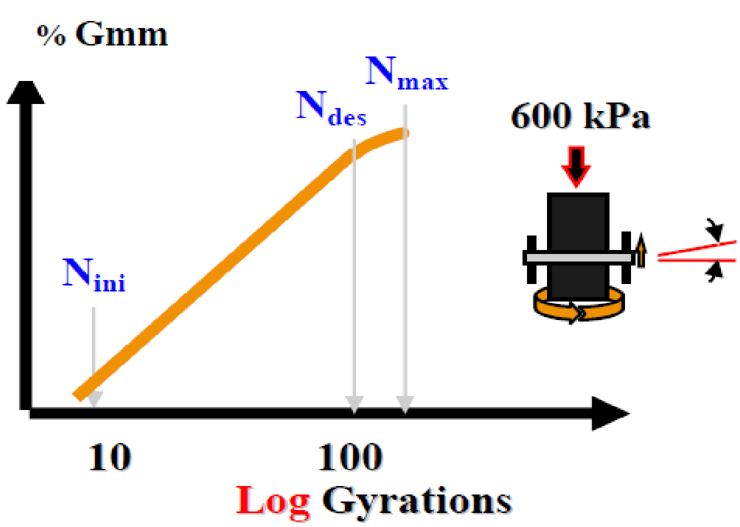


**Figure 3.12 Number of gyrations vs. percent maximum theoretical density (Faheem et al 2008)**

From this plot three important terms for the Superpave® mix design can be identified. These terms are the initial number of gyrations ($N_i$), the design number of gyrations ($N_d$) and the maximum number of gyrations ($N_m$). The importance of these terms is that they can be related to traffic levels through the Equivalent Single Axle Loads (ESALs).

$N_d$ is defined as the number of gyrations required to produce a density in the mix that is equivalent to the expected density in the field after the indicated amount of traffic. In the mix design process, the optimum asphalt content is selected as the asphalt content that provides 96%Gmm (4% air voids) when the mix is compacted at $N_d$.

Ni is a measure of mixture compactability. A mix that has 4% air voids at $N_d$ should have at least 11% air voids at $N_i$.

$N_m$ is the number of gyrations required to produce a density in the laboratory that should never be exceeded in the field. The air voids at $N_m$ are required to be at least 2%. Mixtures with less than 2% air voids are believe to be more susceptible to permanent deformation.

There are two other criteria that must be satisfied in order to meet the Superpave® mix design requirements. These two criteria's are the Voids in Mineral Aggregates (VMA) and the Voids Filled with Asphalt (VFA).

The VMA is defined as the total volume of voids within the mass of the compacted aggregate and VFA is defined as the volume of voids that is filled with asphalt. The VMA influences the performance of a mixture. A mixture with low VMA may suffer durability problems; on the other hand, a mixture with a high VMA may exhibit stability problems and could be uneconomical to produce.

The VMA and VFA are estimated by the following equations:

$$\%\mathrm{VMA} = 100 - \left(\frac{\%\mathrm{G_{mm}} @\ \mathrm{N_{des}} * \mathrm{G_{mm}} * \mathrm{P_s}}{\mathrm{G_{sb}}}\right) \qquad \text{Eq. 5.2}$$

$$\%\mathrm{VFA} = 100 - \left(\frac{\%\mathrm{VMA} - 4.0}{\%\mathrm{VMA}}\right) \qquad \text{Eq. 5.3}$$

Where:

VMA = voids in the mineral aggregate, percent of bulk volume
%Gmm @ Ndes = maximum theoretical specific gravity @ Ndes, percent
Gmm = maximum theoretical specific gravity
Gsb = bulk specific gravity of total aggregate
Ps = aggregate content, cm3/cm3, by total mass of mixture

Table 3.2 presents the volumetric design requirements according to the Superpave® mix design method. The mix design for the field pilot project is specify according to WisDOT standard 04-06 for and ESALs range of 0.3 < 1 million. ESAL is the acronym for equivalent single axle load which is a cumulative traffic load summary statistics. This concept was developed by AASHTO to establish a damage relationship for comparing effects of axles carrying different loads.

**Table 3.2 WisDOT E-1 asphalt mixture design requirements (WisDOT standards 04-06, from Table 460-2)**

| **Mixture Type** | **E-1** | | | | | | | | |
|---|---|---|---|---|---|---|---|---|---|
| **ESALs x $10^6$** | **0.3 -< 1 (20 yr. design life)** | | | | | | | | |
| **Nominal Maximum Size** | **Gyration Compaction** | | | **Air Voids, %$V_a$ (%$G_{mm}$ $N_{des}$)** | **%$G_{mm}$ $N_{ini}$** | **%$G_{mm}$ $N_{max}$** | **Dust to Binder Ratio(2) (%Passing 0.075/$P_{be}$)** | **Voids Filled with Asphalt (VFA, %)** | **%Min. VMA(3)** |
| | **$N_{ini}$** | **$N_{des}$** | **$N_{max}$** | | | | | | |
| **12.5 mm** | 7 | 60 | 75 | 4.0 (96.0%) | ≤89.0(1) | ≤98.0 | 0.6-1.2 | 70-76 | 14 |
| **19.0 mm** | | | | 4.0 (96.0%) | ≤89.0(1) | ≤98.0 | 0.6-1.2 | 65-78 | 13 |

(1)The percent maximum density at initial compaction is only a guideline

(2) For a gradation that passes bellow the boundaries of the caution zone (ref. AASHTO MP3), the dust binder ratio limits are 0.6-1.6

(3)Voids in the Mineral Aggregates (VMA)

### 3.2.2 Construction Densification (CDI) and Traffic Densification (TDI) Indexes

The SGC measures the change in height for each gyration and a plot of the density against the number of gyrations can be created. This plot is called the densification or compaction curve (Figure 3.13) and it is used to determine the Construction Densification Index (CDI) and Traffic Densification Index (TDI).

The CDI is the value under the area of the densification curve from 8 gyrations to 92% of the maximum possible density and represents the work required to compact the mixture from its density after being placed by the paver to the required density of the mix after roller compaction.

The TDI is the value under the area of the densification curve from 92% to 98% of the maximum possible density and represents the ability of the mixture to resist densification under traffic loading over its service life.

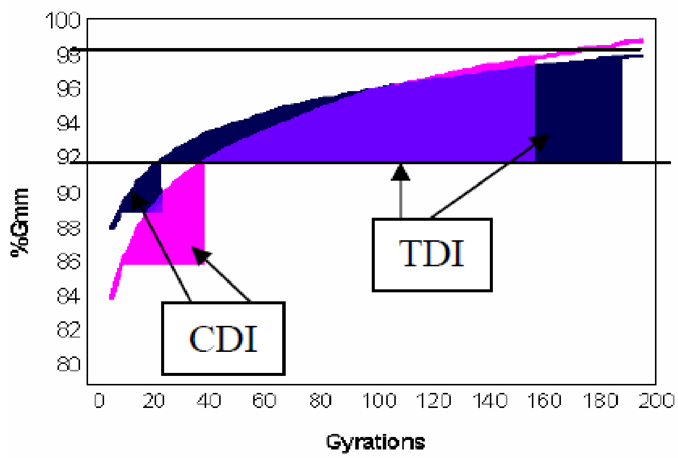


**Figure 3.13 Density Index for different mixes (Faheem et al 2008)**

After preparing HMA mixes using the SGC, this method is used to evaluate the ease of compaction of HMA by calculating the CDI. A lower value of CDI represents a mix that is more workable and easier to compact to achieve 92% Gmm.

The ability to resist traffic loads is represented by the TDI, which is an indicator of the mixture mechanical stability. A higher value of TDI represents a mix that is better able to maintain its stability and resist permanent deformation damage.

## 3.3 FIELD TESTING

### 3.3.1 Falling Weight Deflectometer (FWD)

The Falling Weigh Deflectometer (FWD) is a nondestructive testing device used to measure pavements surface deflection due to load impact. The FWD uses backcalculation routines that assume a different modulus for each layer of the pavement and then uses a specific algorithm to predict deflections in the pavements (Puppala, 2008).

The FWD applies an impulse on the pavement surface by dropping a weight mass from a specified height. The corresponding deflections are measure through a series of sensors, such as geophones. The measured deflection profiles are analyzed with different theoretical models. If the pattern and magnitude of the predicted deflections match with the measured deflections, then the assumed modulus are reported as the modulus of the pavement layers.

## 3.4 CHARACTERIZATION OF COAL COMBUSTION PRODUCTS (CCPs)

The University of Wisconsin-Milwaukee (UWM) collected different types of CCPs from power plants across the United States for a project sponsored by the Electrical Power Research Institute (EPRI). A total of 8 CCPs and one reference limestone filler from this project were tested and used in the experimental program of this research as received.

Coal Combustion Products (CCPs) are fine-grained, powdery particulate material of spherical shape, which are produced from burning pulverized coal in electric power generating plants. These fine-grained spherical glassy particles are collected from the exhaust gases by electrostatic precipitators or bag filters. During combustion of the coal, mineral impurities like clay, feldspar, quartz, and shale fuse in suspension and float out of the combustion chamber along with exhaust gases. As the fused material rises, it cools and solidifies into what is known as fly ash. One of such CCP materials is fly ash which accounts for 75-85% of the total coal ash, and the remainder is collected as bottom ash or boiler slag (Siddique 2011).

### 3.4.1 Chemical Composition

Silicon dioxide ($SiO_2$) and aluminum oxide ($Al_2O_3$) together make 45-80% of the fly ash chemical composition. Other chemical components that are present in fly ashes are: calcium oxide (CaO), iron oxide ($Fe_2O_3$), magnesium oxide (MgO), sodium oxide ($Na_2O$), potassium oxide ($K_2O$), titanium oxide ($TiO_2$), phosphours oxide ($P_2O_3$), sulfur ($SO_3$) and unburned carbon (LOI content).

According to ASTM C618 (Table 3.3) fly ash can be classified in two classes:

1) Class C, high in calcium content
2) Class F, low in calcium content

**Table 3.3 Chemical requirements (ASTM C618)**

| Chemical Composition, % | ASTM C618 Limits | |
|---|---|---|
| | Class C | Class F |
| **Silicon Oxide, $SiO_2$** | - | - |
| **Aluminum Oxide, $Al_2O_3$** | - | - |
| **Iron Oxide, $Fe_2O_3$** | - | - |
| **SAF, $SiO_2 + Al_2O_3 + Fe_2O_3$** | 50 min | 70 min |
| **Sulfur Trioxide, $SO_3$** | 5.0 max | 5.0 max |
| **Calcium Oxide, CaO** | - | - |
| **Magnesium Oxide, MgO** | - | - |
| **Potassium Oxide, K2O** | - | - |
| **Moisture Content** | 3.0 max | 3.0 max |
| **Loss of Ignition** | 6.0 max | 6.0 max |

Class C fly ashes are generally produced from lignite or sub-bituminous coal. This class of fly ash has both pozzolanic and varying degree of self-cementitious properties. On the other hand, Class F fly ashes are generally produced from burning anthracite or bituminous coal. Although this class exhibits pozzolanic properties, it rarely exhibits any self-hardening properties.

Class N is considered to be raw or calcined natural pozzolans like some ditomaceus earths, opaline chert and shale, stuffs, volcanic ashes and pumice.

#### 3.4.1.1 Loss of Ignition

The loss on ignition (LOI) test according to ASTM C311 was used to measure the organic content in CCPs. This test requires that the specimens are dried to a constant weight in an oven, in accordance with ASTM C114. The oven is then heated to 750 ± 50°C in an inert gas atmosphere to prevent the ignition. Then, once the sample is iso-thermed for a period of time, oxygen is introduced into the chamber to allow for oxidation of the organics. The LOI is reported as the amount of material loss due to ignition.

Table 3.4 summarizes the test methods used in this study to measure the chemical composition of the CCPs.

**Table 3.4 CCP chemical properties tests**

| CCPs Properties | Test Type | Equipment | Test Protocols |
|---|---|---|---|
| Chemical Characterization | Chemical Oxides | X-Ray Fluorescence | - |
| | Loss of Ignition (LOI) | TGA701 Thermogravimetric Analyzer | ASTM C311 |

### 3.4.2 Physical Properties

Fly ash consists of silt-sized particles with size ranging between 10 and 100 micron. The average grain size of silt particles according to ASTM D2487 is between 0.075 mm (No. 200 sieve) to 0.002 mm. The shape of fly ashes is generally spherical and in fresh concrete it is a major contributor to improve the fluidity and workability. The color of fly ashes can be tan to dark gray and will depend upon its chemical and mineral constituents. Fly ashes high in lime (CaO) content are generally associated to tan and light colors, fly ashes high in iron content ($Fe_2O_3$) are associated to brownish color, and fly ashes with a high amount of unburned carbon (LOI content) are associated with dark gray to black colors.

Many researchers have used the Scanning Electron Microscope (SEM) on different fly ashes to show the typical spherical shape of fly ash particles (Joshi 1970, Diamond 1985, Joshi et al. 1987, Mehta 1980). They found that some of these particles are hollow. These hollows particles are known as cenospheres or floaters and have the tendency to float on water surface since they are very light. Cenospheres are define as unique free flowing powders composed of hard shelled, hollow, minute spheres made up of silica, iron and alumina. In fly ash there is also another type of particles that can be identified called pherospheres. Pherospheres are defined as a large glassy sphere with many small spherical particles inside.

### 3.4.2.1 Specific Gravity

The specific gravity (SG) was measured with the Helium Pycnometer test in accordance with ASTM D5550. The SG is an important parameter since it is used to calculate the Rigden voids and, also, for volume to mass conversion of any material having an addition of CCP's.

### 3.4.2.2 Rigden Voids

The fractional void test, also known as the Rigden voids test was developed by Rigden (1947). This test provided a means of correlation between asphalt performance and void space. The significance of the Rigden voids test has been validated by different researchers (Ishai and Craus, 1977; Van Der Heide and Van Zantvliet, 1982; Ishai and Craus, 1996, and Faheem et al., 2012).

In this study the Rigden voids test was conducted according to the European Standard EN1097-4.

### 3.4.2.3 Particle Size Distribution (PSD)

Particle size distribution (PSD) of the Coal Combustion Products was performed in accordance with ASTM D4464 using laser light scattering. This test method is capable of measuring the equivalent spherical diameter for particle sizes in the range of 1 to 300 µm. To conduct the laser diffraction test, a sample of material is dispersed in distilled water or a compatible organic liquid (alcohol) and circulated through the path of a laser light beam. When the light beam hits a particle, it is scattered. This scattered light is then collected by a photo detector and converted to an electrical signal and analyzed with the assumption that all the particles are spherical. From this data Surface Area (SA), Fineness Modulus (FM), $D_{10}$, $D_{50}$, and $D_{90}$ were obtained.

### 3.4.2.4 Shape

Shape was observed using the TOPCON® SM-300 Scanning Electron Microscope (SEM). The SEM images of fly ash illustrate the predominant round shape of the ash of Class C and F type (Figure 3.14).

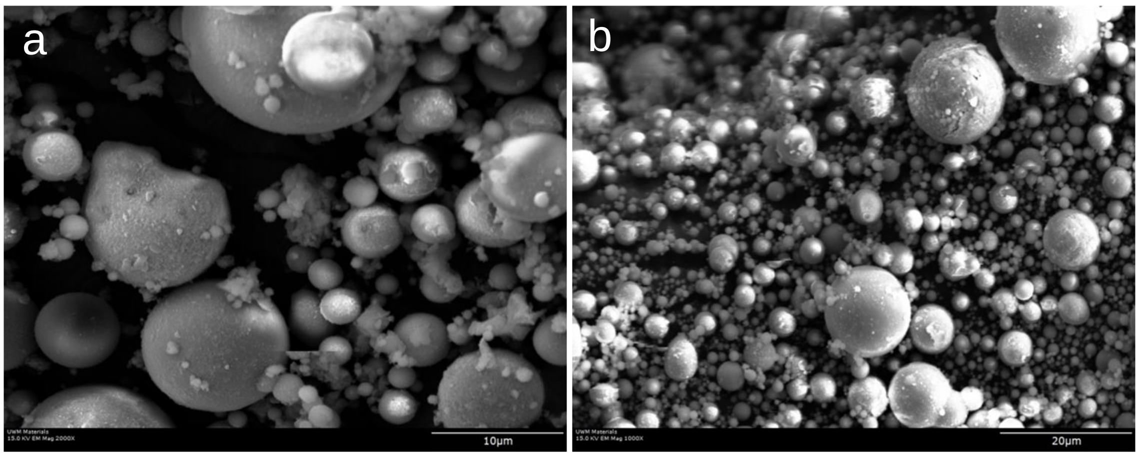


**Figure 3.14 SEM of a representative fly ash (a) Class F (b) Class C**

Table 3.5 summarizes the test methods used in this study to measure the physical properties of the CCPs.

**Table 3.5 CCP physical properties tests**

| CCPs Properties | Test Type | Equipment | Test Protocols |
|---|---|---|---|
| **Physical** | Specific Gravity | Helium Pycnometer | ASTM D5550 |
| | Fractional Voids | Rigden voids | EN1097-4 |
| | Particle Size Distribution (PSD)<br>• Surface Area<br>• Fineness Modulus (FM)<br>• $D_{10}$<br>• $D_{50}$<br>• $D_{90}$ | Laser Light Scattering | ASTM D4464 |
| | Shape | Scanning Electron Microscope (SEM) | ASTM E986 |

## 3.5 MASTIC PREPARATION

The mixing techniques for the CCPs, reference fillers and binder was optimized to avoid the incorporation of excess air into the mastic blend through the use of an adequate mixing apparatus, mixing speed, properly aligned propeller and mixing temperature controlled by the hot plate. A mechanical stirrer (Cowles Dissolver) was used at a mixing speed of 1,300 rpm and the required mass of filler was calculated based on the mass of the asphalt binder using the volume concentration and specific gravity of the material. Asphalt binder was mixed with CCPs and fillers for 30 minutes at 135 ± 5 °C. During this mixing time, a portion of CCPs and reference fillers were added at 5 minutes increments.

### 3.5.1 Proposed method to blend filler and asphalt binder

The following is the proposed procedure for blending mineral filler with asphalt step by step:

1. Preheat filler in oven at 135±5°C.
2. Heat asphalt at 135±5°C
3. Place empty quarter of a gallon paint can on top of piece of wood or plywood on scale to prevent heat from reaching the platen
4. Zero the scale.
5. Pour target mass of asphalt into the can (recommended 500-600 grams in a quarter of a gallon can)
6. Determine the mass of filler required based on the mass of asphalt according to the target filler concentration by mass.
7. Put the can of asphalt in the heat mantel and adjust temperature to 135±5°C
8. Heat asphalt in the mantel for 10 minutes
9. Insert the mechanical stirrer such that it is located at the bottom third of the can depth. (Use dispersing stirrer to prevent filler agglomeration)
10. Start mechanical stirrer at 1300 revolutions per minutes.
11. Put an aluminum foil over the can and make a hole to allow space for adding fly ash into it and make sure to prevent dust going into air.

12. Add filler in small increments while stirring, targeting mixing time of 30 minutes
13. After all the filler is added continue stirring for five minutes. This makes the total stirring time to be 30 minutes.
14. After blending, the mix will be poured into smaller ointment tins. (50-60 grams each in 8 oz ointment tins)
15. Cover ointment tins and store at room temperature for future testing.

# CHAPTER 4.

# RESULTS AND DISCUSSION

## 4.1 COAL COMBUSTION PRODUCTS (CCP) CHARACTERIZATION

Coal Combustion Products (CCPs) are the minerals that remain after coal is burned to generate electricity. In this research 8 CCPs were obtained from different coal energy plants in the United States. These 8 CCPs were divided in 3 different types: 2 Class C fly ash, 2 Class F fly ash and 4 Flue Gas Desulfurization (FGD) of the Spray Dryer Absorber (SDA) type high in CaO and $SO_3$.

In the next section these by-products are characterized by investigating their chemical composition and physical properties. The chemical oxides were determined using X-ray Fluorescence (XRF). The Specific Gravity (SG), Particle Size Distribution (PSD) and Rigden voids were used to determine the CCPs physical properties. The PSD results were used to estimate Fineness Modulus (FM), Surface Area (SA), $D_{10}$, $D_{50}$ and $D_{90}$ of the studied CCPs.

### 4.1.1 Chemical Composition

ASTM C618 is the standard that covers coal fly ash and raw or calcined natural pozzolan for use in concrete where cementitious or pozzolanic action, or both, is desired or where other properties normally attributed to fly ash or pozzolans may be desired, or where both objectives are to be achieved. ASTM C618 specifies the limits for classification of the different types of fly ash. These limits are based on the silicon dioxide ($SiO_2$) plus aluminum oxide ($Al_2O_3$) plus iron oxide ($Fe_2O_3$) contents, also known as SAF. According to ASTM C618 the SAF limits to classify fly ash as Class C and Class F are a minimum of 50.0 and 70.0, respectively. Also the sulfur trioxide content ($SO_3$) must be a maximum of 5.0%, the moisture content a maximum of 3.0% and the loss of ignition (LOI) a maximum of 6.0% for both classes.

Based on the SAF estimation it can be observed on Figures 4.1 to 4.3 that the CCPs WE05 and WE08 meet the requirements for Class C fly ash, while TA11 and LG14 meet the requirements for Class F fly ash. On the other hand, the SDA materials did not meet the requirements of ASTM C618 as it evident by lower contents of $SiO_2$, $Al_2O_3$ and $Fe_2O_3$ when compare to Class C and F fly ashes.

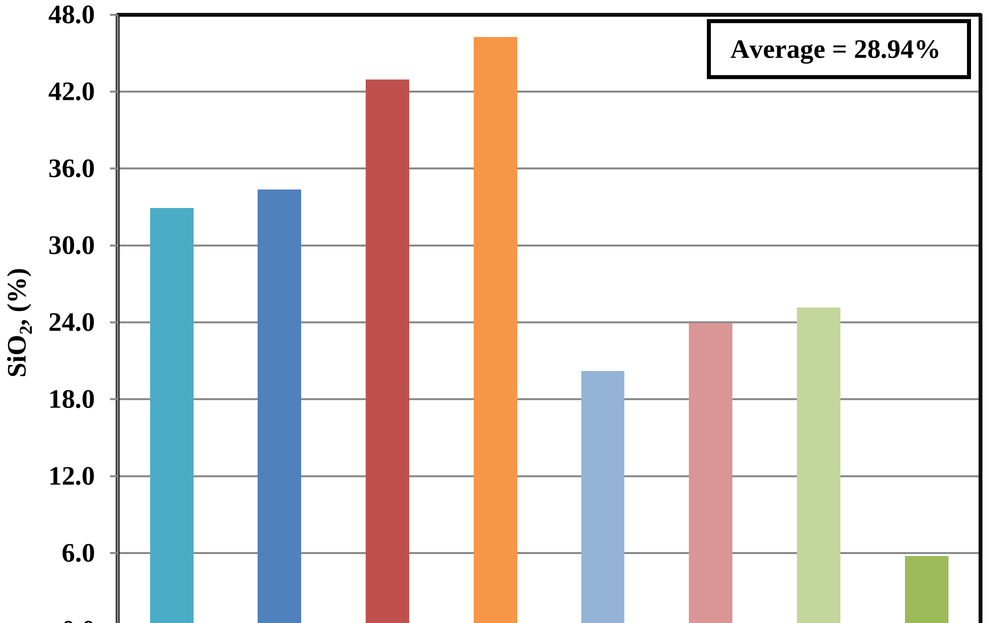


| | WE05 C | WE08 C | TA11 F | LG14 F | KC01 SDA | WP03 SDA | SF15 SDA | DL16 SDA |
|---|---|---|---|---|---|---|---|---|
| SiO2, % | 32.9 | 34.4 | 42.9 | 46.3 | 20.2 | 23.9 | 25.2 | 5.8 |

**Figure 4.1 $SiO_2$ content for investigated CCPs**

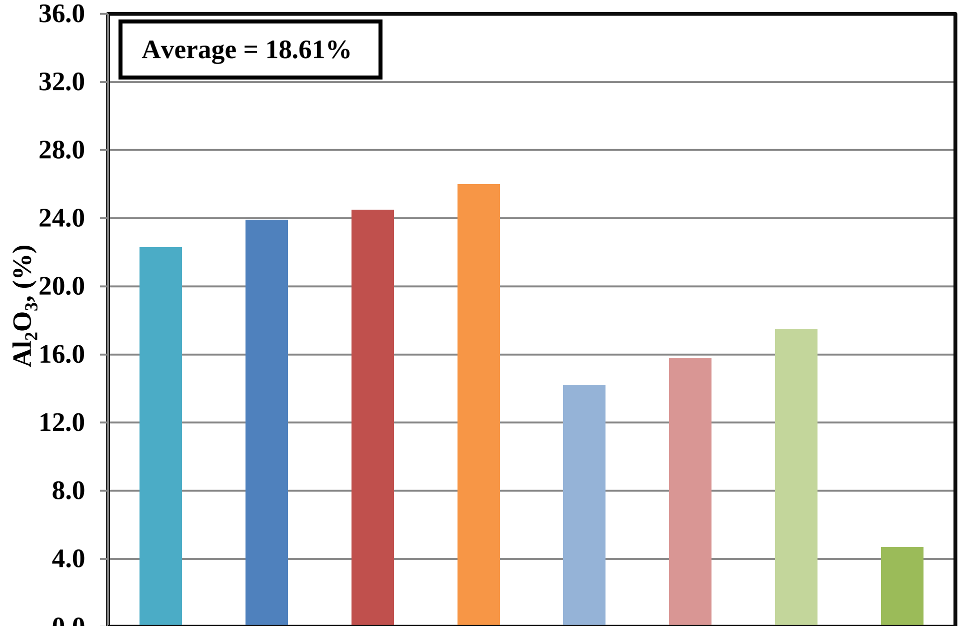


| | WE05 C | WE08 C | TA11 F | LG14 F | KC01 SDA | WP03 SDA | SF15 SDA | DL16 SDA |
|---|---|---|---|---|---|---|---|---|
| Al2O3, % | 22.3 | 23.9 | 24.5 | 26.0 | 14.2 | 15.8 | 17.5 | 4.7 |

**Figure 4.2 $Al_2O_3$ content for investigated CCPs**

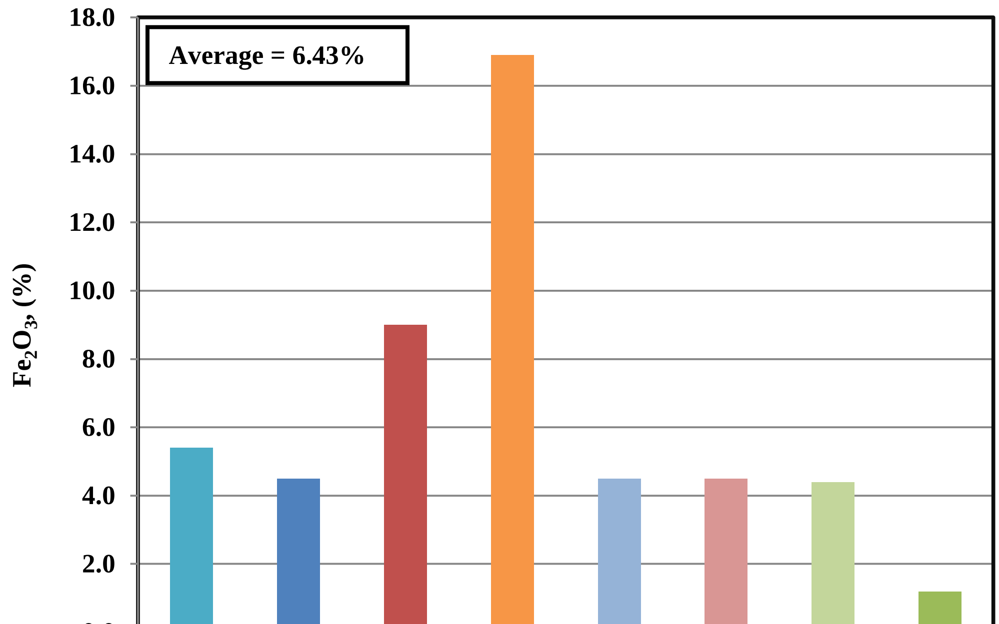


| | WE05 C | WE08 C | TA11 F | LG14 F | KC01 SDA | WP03 SDA | SF15 SDA | DL16 SDA |
|---|---|---|---|---|---|---|---|---|
| Fe2O3, % | 5.4 | 4.5 | 9.0 | 16.9 | 4.5 | 4.5 | 4.4 | 1.2 |

**Figure 4.3 $Fe_2O_3$ content for investigated CCPs**

In the literature, CaO was referred as an indicator of filler reactivity influencing the performance of asphalt binder (Ahmed et al., 2010; Wang et al., 2011). As can be seen in Figure 4.4 the CaO content shows SDA CCPs with the highest values followed by Class C and Class F. DL16 SDA shows the highest content of CaO of all reported CCPs.

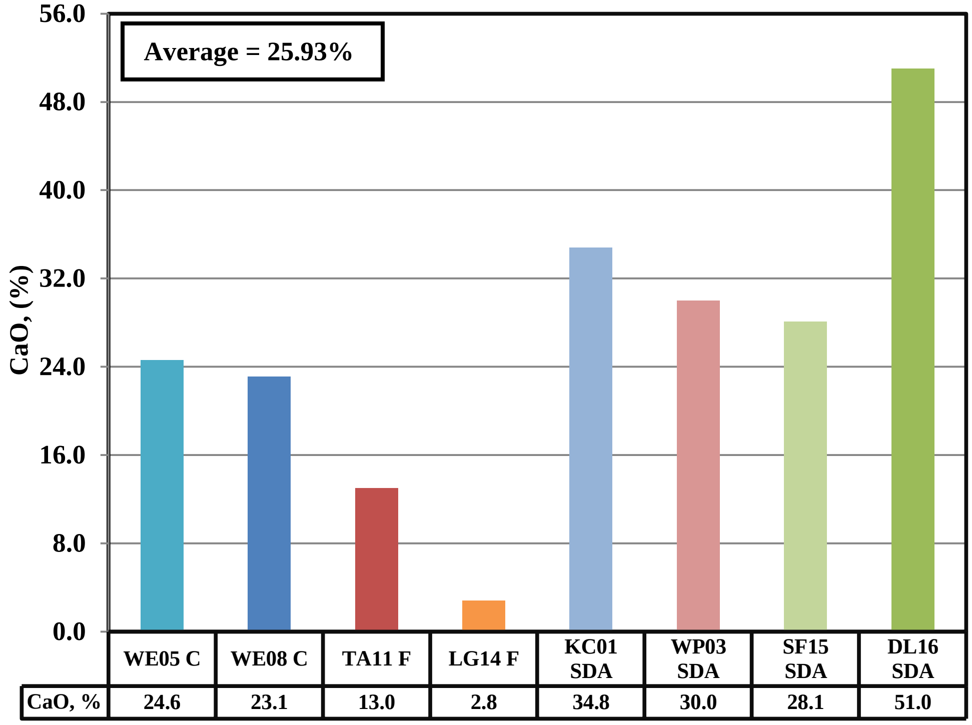


**Figure 4.4 CaO content for investigated CCPs**

As shown in Figure 4.5, both Classes C and F fly ash had a very small content of $SO_3$. On the other hand, SDA fillers had elevated quantities of $SO_3$ due to the presence of calcium sulfite. According to the information from the literature, all SDA fillers may demonstrate a higher stiffening effect due to higher $SO_3$ content.

Furthermore, the sulfur influence on the stiffness of asphalt binder was also reported by DeFoe, 1983; Liao & Huang, 2008; Wu, 2009.

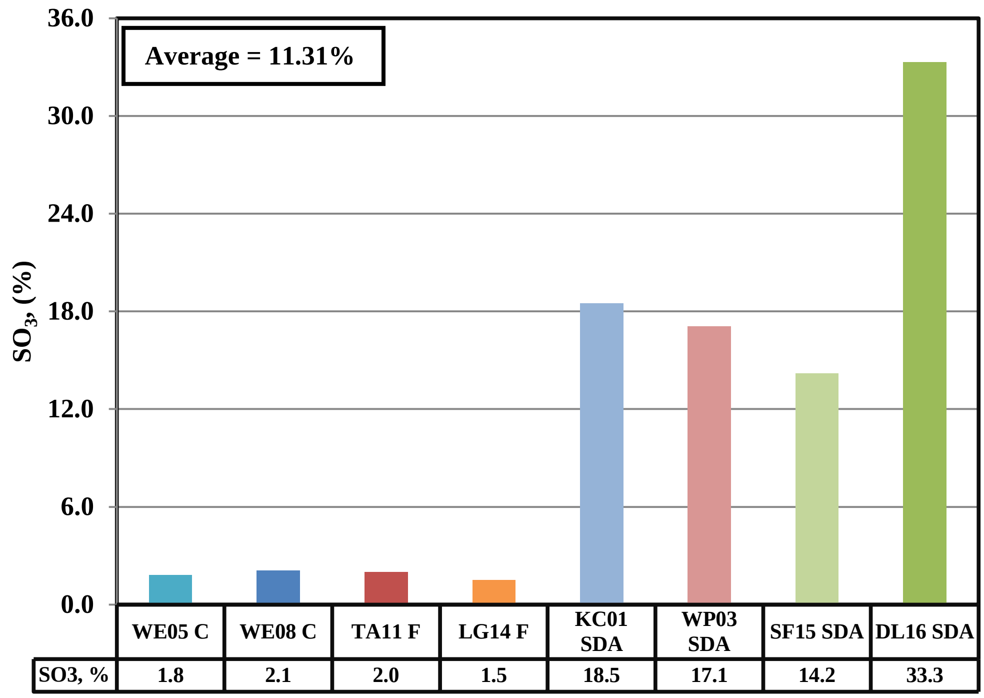


**Figure 4.5 $SO_3$ content for investigated CCPs/fillers**

### 4.1.1.1 Loss on Ignition (LOI)

The LOI results of the 8 CCP specimens are reported in Figure 4.6. The result for REF1 is omitted from this figure, since the LOI values for calcareous minerals differ significantly as demonstrated by LOI values of 42.4 for REF1.

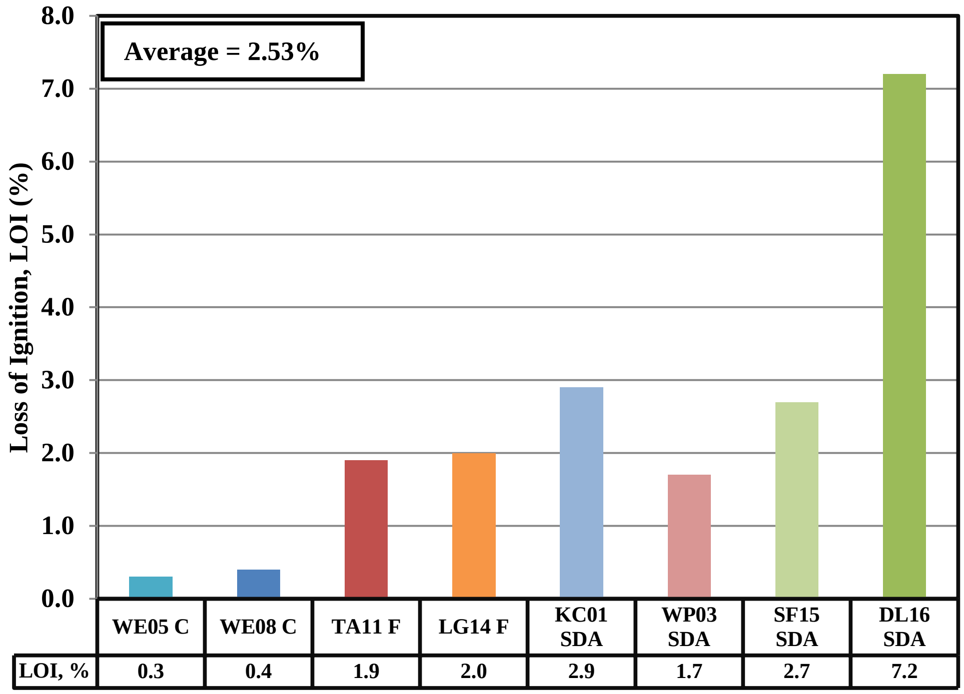


**Figure 4.6 Loss on ignition (LOI) for investigated CCPs**

This investigation demonstrated that CCPs had an average LOI of 2.53%; with minimal and maximal values of 0.3 and 7.2, respectively. As demonstrated by the test results Class C fly ashes have a very low LOI content. On the other hand, Class F ash and SDA had higher values of LOI compared to Class C.

### 4.1.2 Physical Properties

Specific gravity, particle size distribution, fineness modulus, $D_{10}$, $D_{50}$, $D_{90}$, surface area and volume of Rigden voids will be measure to characterize the physical properties of CCPs used in this research effort.

#### 4.1.2.1 Specific Gravity (SG)

The specific gravity (SG) was measured with the Helium Pycnometer test in accordance with ASTM D5550-06. Figure 4.7 reports on the specific gravity results.

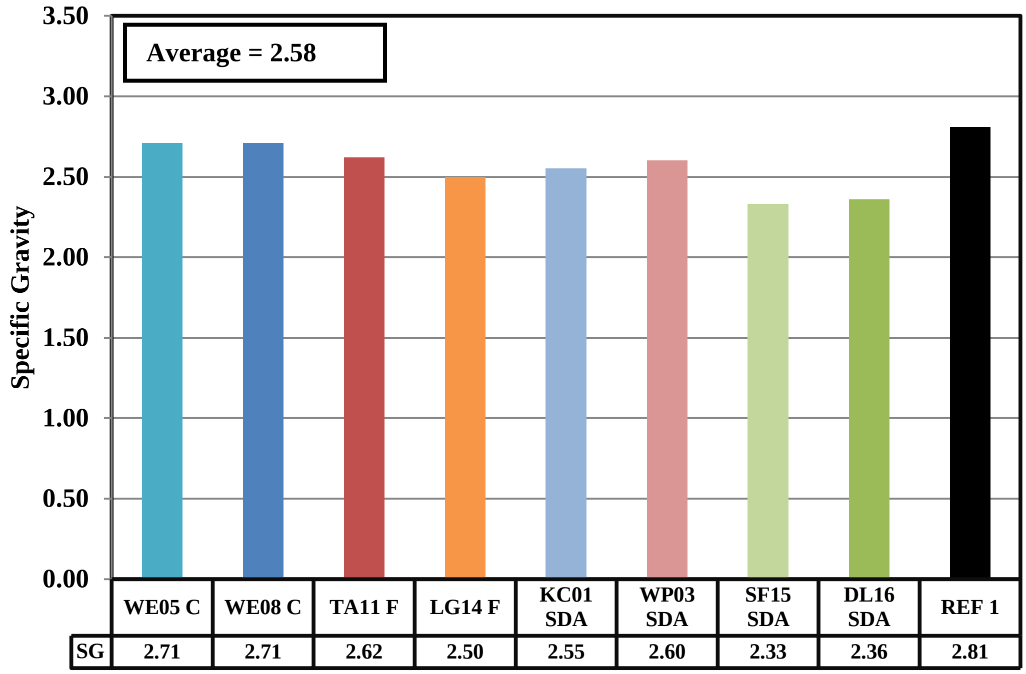


**Figure 4.7 Specific Gravity of investigated CCP/fillers**

The average SG for the CCPs is 2.58. The coefficient of variability of SG for all CCP classes and references filler is 6.24%; this translates in to a relatively low variability between all materials studied with reference limestone filler possessing the higher SG value of all fillers. The SG is an important parameter since it is used to calculate the Rigden voids and, also, for volume to mass conversion of the mastic blend.

### 4.1.2.2 Rigden Voids

The fractional void test, also known as the Rigden voids Test was developed by Rigden (1947), in order to obtain a simple filler characteristic which could be significant in predicting the effect of filler on the performance asphalt binders. In this research, Rigden voids tests were conducted according to the European Standard EN 1097-4. The Rigden voids results are shown in Figure 4.8.

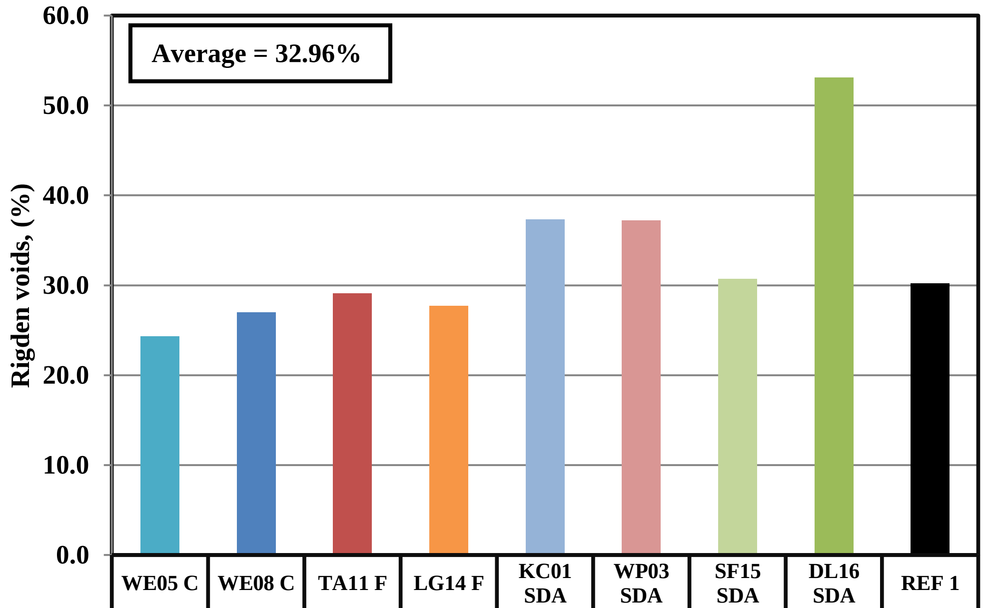


| | WE05 C | WE08 C | TA11 F | LG14 F | KC01 SDA | WP03 SDA | SF15 SDA | DL16 SDA | REF 1 |
|---|---|---|---|---|---|---|---|---|---|
| RV, % | 24.3 | 27.0 | 29.1 | 27.7 | 37.3 | 37.2 | 30.7 | 53.1 | 30.2 |

**Figure 4.8 The Rigden voids data for investigated CCPs/fillers**

The average value of Rigden voids for investigated CCPs is found to be 32.96%. The range of values represents a wide variation in packed particles void characteristics from 24.3% to 53.1% and can be considered as covering the ranges of fillers (and CCPs) used in the field. The lowest Rigden voids is for WE05 which is a Class C fly ash and highest is for DL16 SDA. The DL16 has a high sulfur content ($SO_3$) and a very low packing characterized by a high Rigden voids value (53.1%).

In terms of Rigden voids Class C fly ash specimens are mostly represented by the lower half of all CCPs specimens, WE05 and WE08 are below the Rigden voids average (32.96%). On the other hand, the lowest Rigden voids for Class F fly ash is for LG14. SDA specimens demonstrate values for Rigden voids that are higher than the average of all CCPs in this study with the exception of SF15. The reference limestone filler have Rigden voids values around the average value of all CCPs in this study.

#### 4.1.2.3 Particle Size Distribution (PSD)

The particle size distributions (PSD) of CCPs were determined using the laser diffraction according to ASTM D4464-10. This test method is capable of measuring the equivalent spherical diameter for particle sizes in the range of 1 to 300 µm. From the PSD curves, fineness modulus, $D_{10}$, $D_{50}$ and $D_{90}$ can be determined. The particle size distribution (PSD) of the 8 CCBs and the two reference fillers are presented in Figure 4.9, 4.10 and 4.11. The results were separated in three graphs, where the type of CCP was used for this separation and reference fillers were added for comparison. Maximum particle size of the reference limestone filler was around 80 µm. The fineness particles were found in Class C WE05 and WE08 fly ash. Class C fly ash (Figure 4.9) had a maximum particle size in a range of 30 to 50 µm. Particle sizes of all Class C fly ash were smaller than the reference fillers until a size of 6 µm and under.

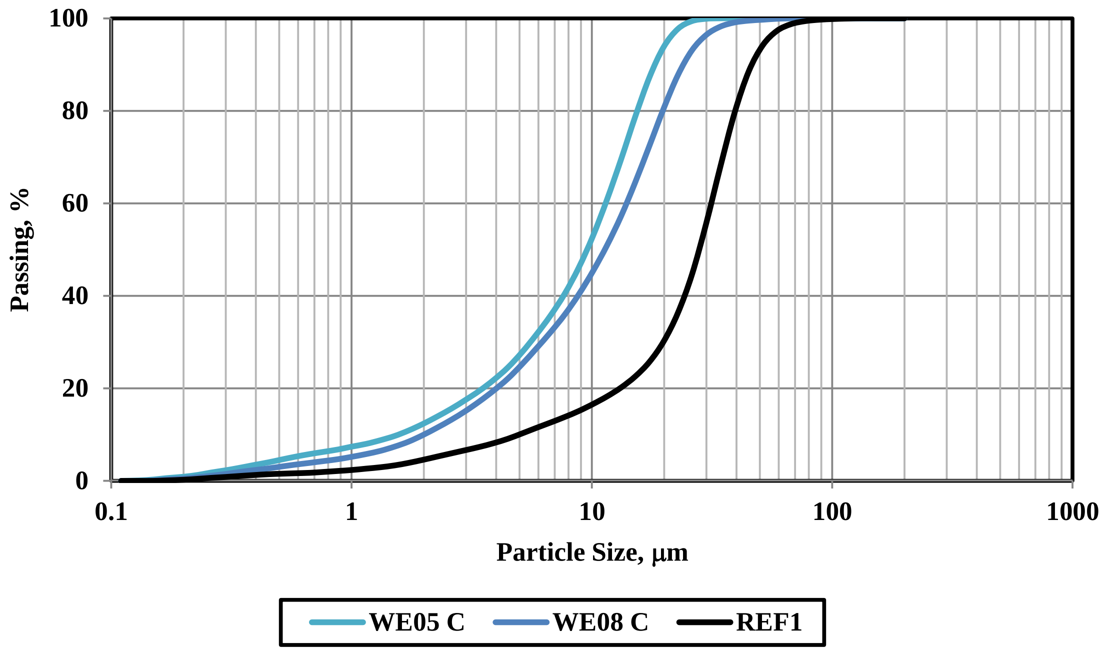


**Figure 4.9 PSDs of investigated Class C CCPs**

Class F TA11 fly ash (Figure 4.9) had bigger maximum size particles than Class C fly ash and the reference filler. Class F fly ash TA11 had maximum particle size in the range of 150 to 200 µm, and LG14 had maximum particle size in the range of 50 to 60 µm. Reference fillers had the same particle size distribution between the 2 and 50 µm sizes.

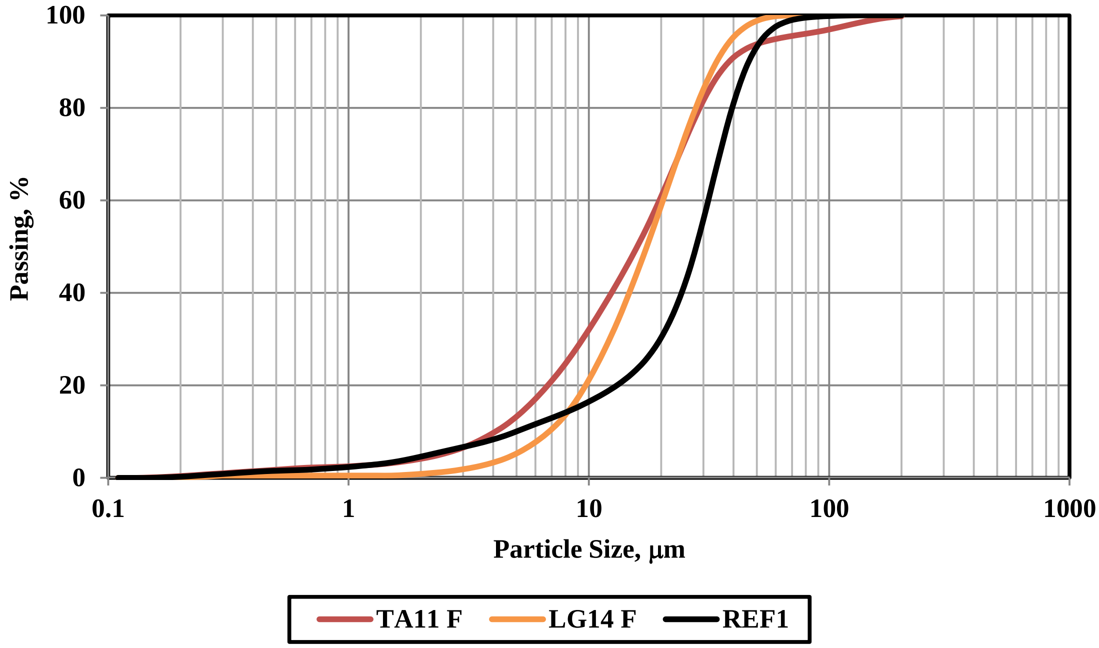


**Figure 4.10 PSD of investigated Class F CCPs**

Particle sizes of SDA ash were smaller than the reference filler until a size of 1 µm and smaller. All SDA ash (Figure 4.11) had a maximum particle size in a range of 25 to 35 µm. All SDA ash showed the same pattern of the curve of the particle size distribution as Class C fly ash, except for DL16 SDA ash. DL16 SDA ash had a maximum particle size of 10 to 15 µ m.

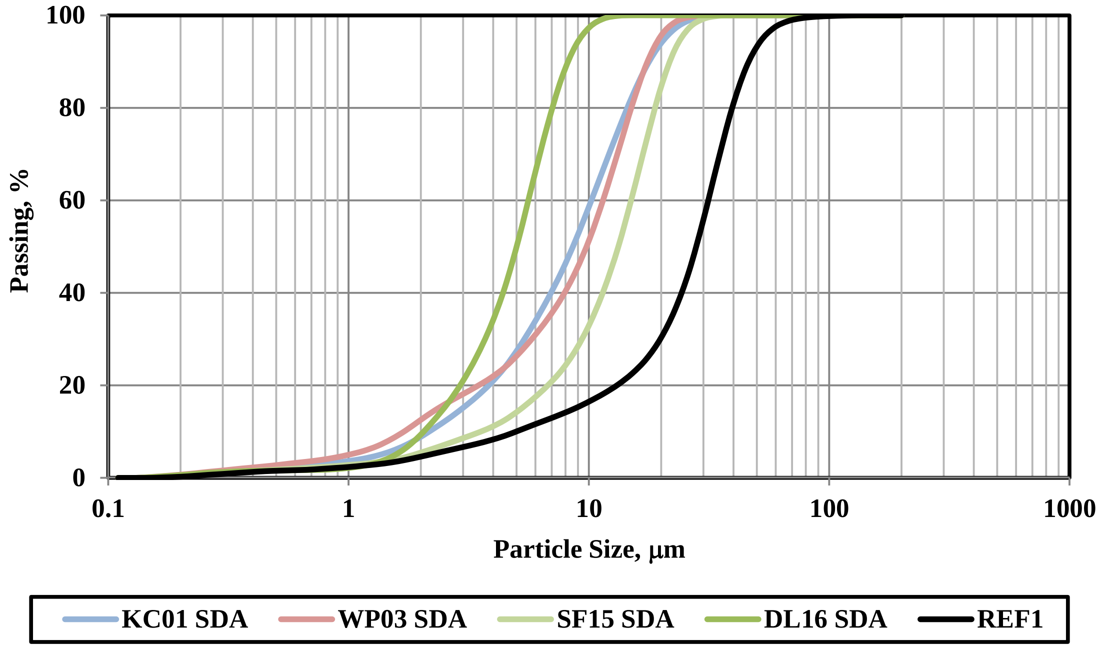


**Figure 4.11 PSD of investigated SDA CCPs**

From the PSD curves, fineness modulus (FM), $D_{10}$, $D_{50}$ and $D_{90}$ were determined as a measured of how fineness of the CCPs materials. The FM, $D_{10}$, $D_{50}$ and $D_{90}$ for investigated CCPs are demonstrated by Figures 4.12 to 4.14.

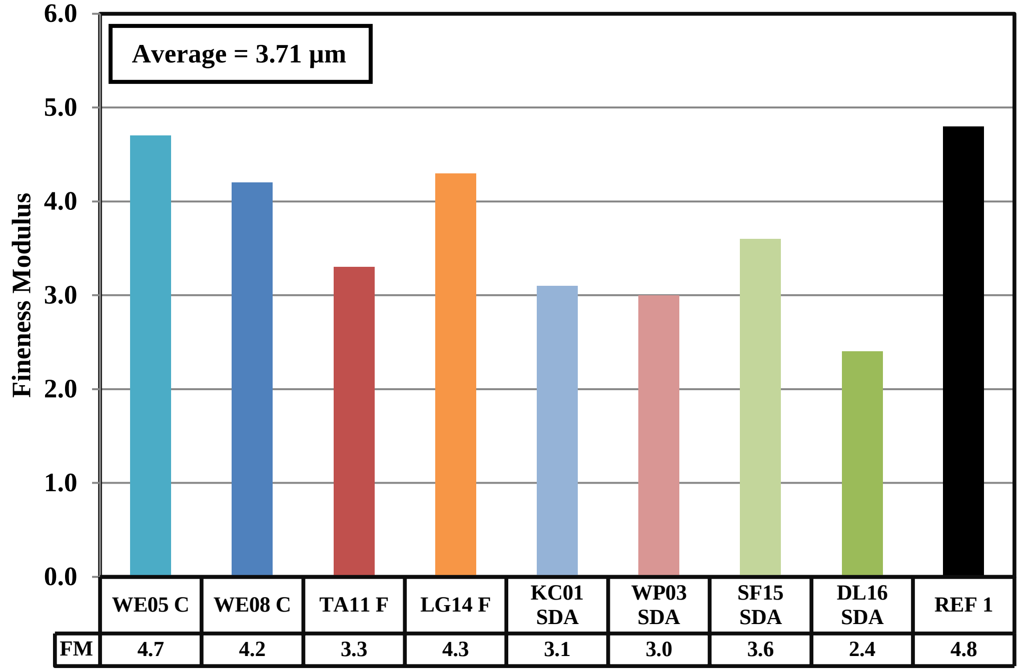


**Figure 4.12 The Fineness Modulus of investigated CCPs/fillers**

From the PSD curves (Figures 4.9 to 4.11) and the fineness modulus (Figure 4.12), Class C and SDA ash had smaller particles than both class F fly ash and reference fillers. Class F fly ash had the coarser particles with less than 5% of its particles smaller than 1 µm. DL16 SDA ash had the lower maximum particle size and from the shape of the particle distribution, it is also the finest material among all CCPs and reference filler.

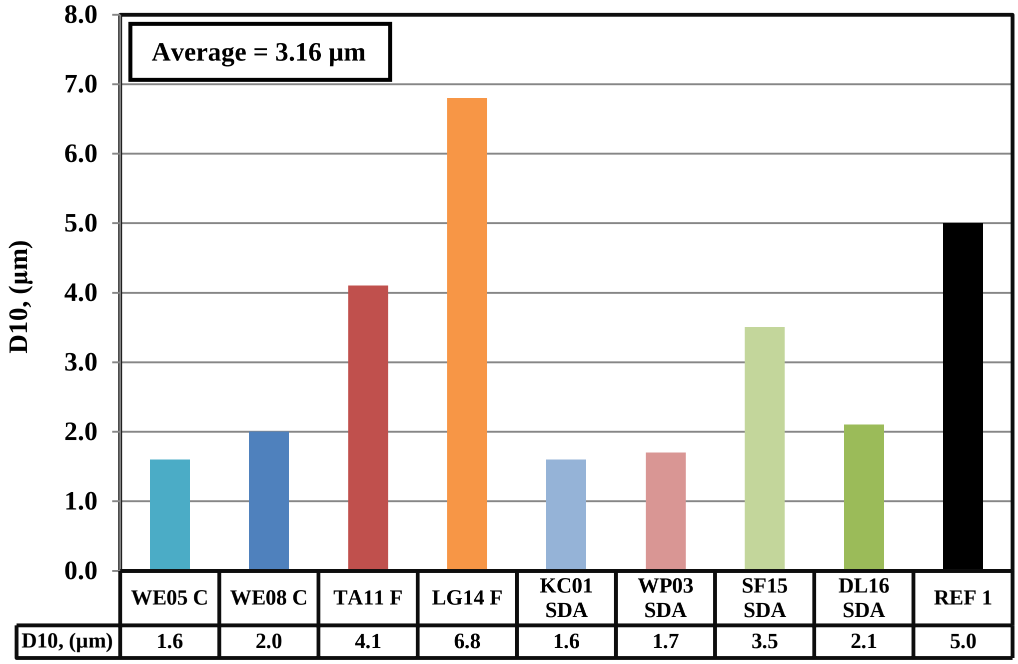


**Figure 4.13 The $D_{10}$ estimated from PSD curve**

Figures 4.13, 4.14 and 4.15 report the $D_{10}$, $D_{50}$ and $D_{90}$ as estimated from the particle size distribution data (Figure 4.9 to 4.11). Class C fly ash and SDA's are characterized by the presence of very small particles ($D_{10}$), mainly within the 1.6-3.5 µm size range, possibly due to contribution of fine lime (CaO) and sulfite ($SO_3$) particles.

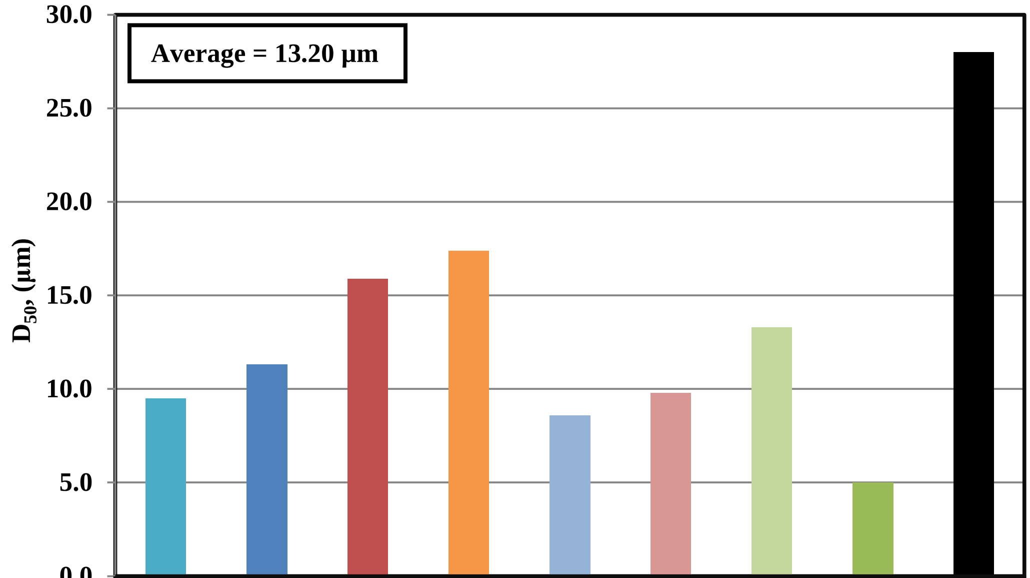


| | WE05 C | WE08 C | TA11 F | LG14 F | KC01 SDA | WP03 SDA | SF15 SDA | DL16 SDA | REF 1 |
|---|---|---|---|---|---|---|---|---|---|
| D50, (µm) | 9.5 | 11.3 | 15.9 | 17.4 | 8.6 | 9.8 | 13.3 | 5.0 | 28.0 |

**Figure 4.14 The $D_{50}$ estimated from PSD curve**

Similar trends were observed for $D_{50}$ and $D_{90}$. Class C fly ash had a very uniform particle size of approximately 10 µm corresponding to $D_{50}$. SDA materials were of similar average size, but with relatively high scatter from 5 to 13.3 µm. The reference filler were the coarsest materials in respect to $D_{50}$.

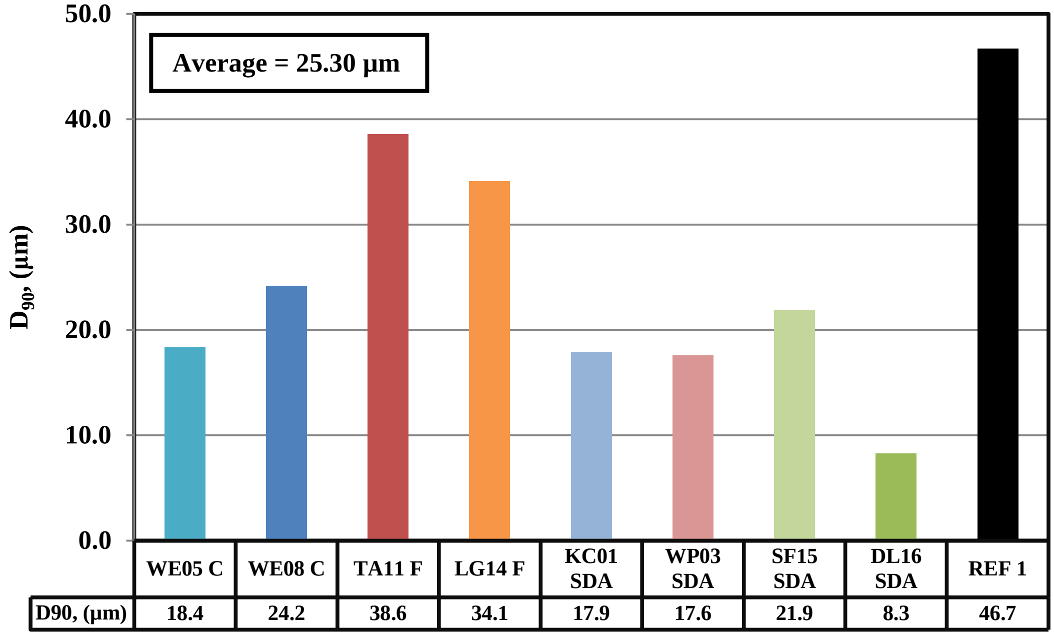


**Figure 4.15 $D_{90}$ calculated from PSD curve**

Considering all three size indicators ($D_{10}$, $D_{50}$, $D_{90}$), it can be concluded that the Class C fly ash and SDA materials are characterized by finer particle sizes compared to Class F ash which commonly has a wider range of relatively coarse particles. The $D_{10}$ – $D_{90}$ size range for Class F ash is from 4.1 µm to 38.6 µm. It can be promising to evaluate the interaction between Class F fly ash with binders given the wide range of PSDs.

#### 4.1.2.4 Surface Area

The surface area (SA) of particles is important because of contribution to the binder adsorption capacity. Generally, the SA of powder particles vary inversely with the particle size (Schure et al., 1985), the smaller the particle, the larger the surface area, as demonstrated by Figure 4.16). The surface area of Class F fly ash and reference fillers are below average. The finer groups: Class C fly ash and SDAs are demonstrating higher SA values, which will increase the binder adsorption capacity of these materials.

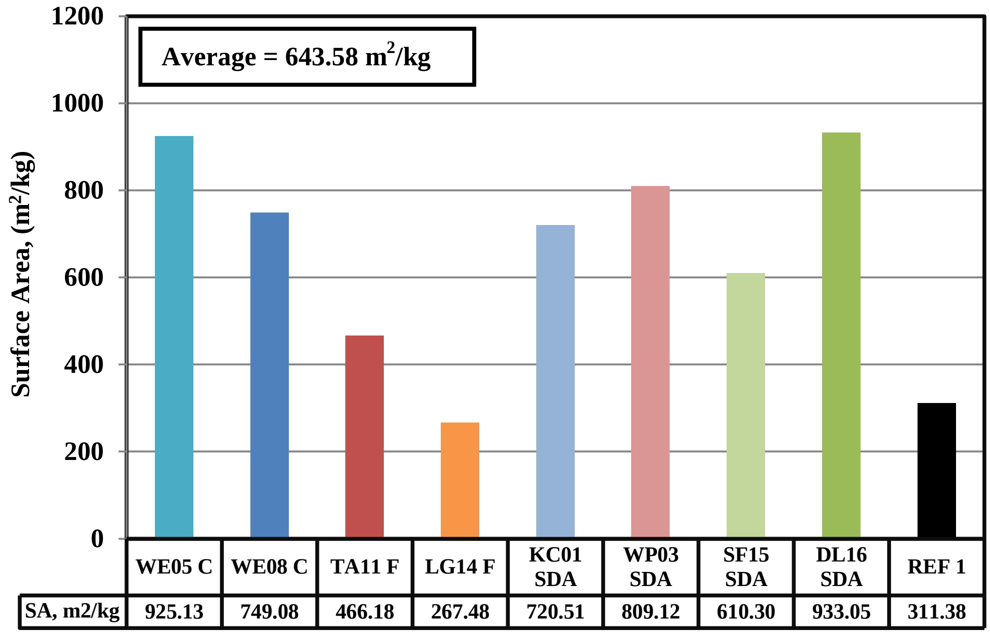


**Figure 4.16 Surface area of investigated CCPs and fillers**

### 4.1.3 Summary of CCPs Properties

The X-ray diffraction (XRD) was used for the chemical oxide composition of CCPs. Figure 4.17show the ternary compositional diagram of all CCPs in this research. This figure represents the distribution of silica, aluminum and calcium for all CCPs. As expected the Spray Dryer Absorbers (SDA) contain the highest amount of calcium oxide and lowest amount of silicon dioxide. Class F fly ash has the highest amount of silicon dioxide and type C fly ashes bridge the gap.

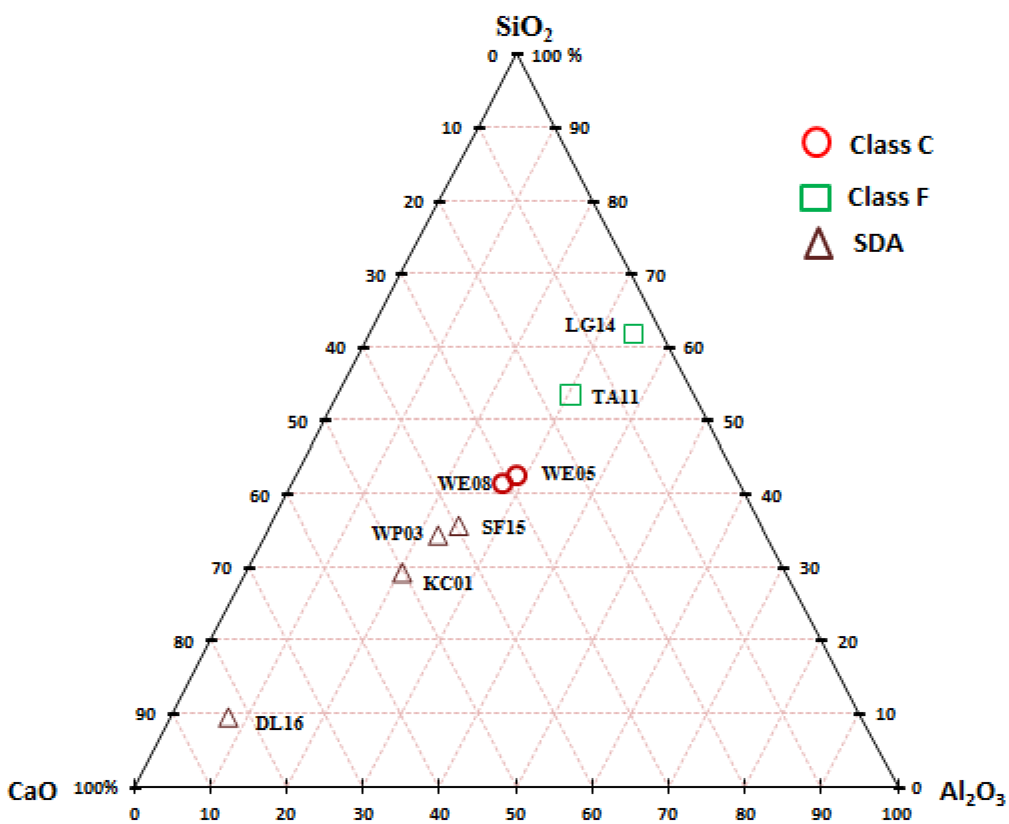


**Figure 4.17 Ternary diagram showing fly ash composition**

Table 4.1 reports on the summary of chemical composition of investigated CCPs. Class F and C fly ash meet the chemical requirements according to ASTM C618, where the $SO_3$ content is less than 5% and the sum of $SiO_2$ +$Al_2O_3$ +$Fe_2O_3$ is at least 70% for Class F fly ash and at least 50% for Class C fly ash. SDA's ashes were not compared to this standard because of the high concentrations of $SO_3$, CaO and low SAF. Table 4.2 reports on the summary of physical properties of the investigated CCPs.

**Table 4.1 Chemical composition of investigated CCPs**

| Materials ID | Class | $Al_2O_3$ | CaO | $Fe_2O_3$ | $SiO_2$ | $SO_3$ | SAF | LOI |
|---|---|---|---|---|---|---|---|---|
| WE05 | C | 22.3 | 24.6 | 5.4 | 32.9 | 1.8 | 60.6 | 0.3 |
| WE08 | C | 23.9 | 23.1 | 4.5 | 34.4 | 2.1 | 62.8 | 0.4 |
| TA11 | F | 24.5 | 13.0 | 9.0 | 42.9 | 2.0 | 76.4 | 1.9 |
| LG14 | F | 26.0 | 2.8 | 16.9 | 46.3 | 1.5 | 89.2 | 2.0 |
| KC01 | SDA | 14.2 | 34.8 | 4.5 | 20.2 | 18.5 | 38.9 | 2.9 |
| WP03 | SDA | 15.8 | 30.0 | 4.5 | 23.9 | 17.1 | 44.2 | 1.7 |
| SF15 | SDA | 17.5 | 28.1 | 4.4 | 25.2 | 14.2 | 47.1 | 2.7 |
| DL16 | SDA | 4.7 | 51.0 | 1.2 | 5.8 | 33.3 | 11.7 | 7.2 |

*SAF = $SiO_2$+ $Al_2O_3$+ $Fe_2O_3$

**Table 4.2 Physical properties of investigated CCPs and reference fillers**

| Materials ID | Class | Rigden Voids, % | Specific Gravity | Surface Area, $m^2/kg$ | Fineness Modulus | $D_{10}$, (μm) | $D_{50}$, (μm) | $D_{90}$, (μm) |
|---|---|---|---|---|---|---|---|---|
| WE05 | C | 24.35 | 2.71 | 925.13 | 4.75 | 1.87 | 9.55 | 18.43 |
| WE08 | C | 27.02 | 2.71 | 749.08 | 4.24 | 2.00 | 11.33 | 24.21 |
| TA11 | F | 29.15 | 2.62 | 466.18 | 3.32 | 4.08 | 15.91 | 38.56 |
| LG14 | F | 27.73 | 2.50 | 267.48 | 4.31 | 6.82 | 17.42 | 34.08 |
| KC01 | SDA | 37.27 | 2.55 | 720.51 | 3.09 | 1.65 | 8.58 | 17.90 |
| WP03 | SDA | 37.20 | 2.60 | 809.12 | 3.04 | 1.70 | 9.77 | 17.59 |
| SF15 | SDA | 30.74 | 2.33 | 610.30 | 3.61 | 3.55 | 13.27 | 21.90 |
| DL16 | SDA | 53.14 | 2.36 | 933.05 | 2.45 | 2.05 | 5.01 | 8.27 |
| REF 1 | Limestone | 30.22 | 2.81 | 311.38 | 4.80 | 4.98 | 27.96 | 46.66 |

## 4.2 NON-PERFORMANCE RELATED INDICATORS

### 4.2.1 Complex Shear Modulus, G*

The Dynamic Shear Rheometer (DSR) was used to measure a specimen's complex shear modulus or stiffness (G*) and phase angle ($\delta$) at the PG grade high temperature. The G* means the sample's total resistance to shear deformation when repeatedly sheared, while $\delta$, is the lag between the applied shear stress and the resulting shear strain. In this section, the results of the mastic complex modulus are presented. The results of this test are used to evaluate the interaction between the asphalt binders and the different fillers used. Since the asphalts are from different sources and modified in different ways, they may react with CCPs and fillers differently.

Figure 4.18 demonstrates the collected results for the G* for different fillers, at different concentrations when blended with unaged unmodified asphalt binder PG58-28. It is very clear that there is a wide range of stiffness values obtained depending on the type of filler. For the PG58-28 binder, depending on filler used, the G* value can increase by up to 73%.

It can be observed from Figure 4.18 that the increase in complex modulus starts with small increments up to 15% volume concentration of CCPs. At higher concentrations, the complex modulus increases rapidly. At 25% and 40% concentration (by volume) the complex modulus shows significant increments. For example, 15% addition of WE05 C increases the G* value by 55.6% compared to the plain unfilled binder. The increase in stiffness corresponding to 15% to 25% concentration increase is 68.6%. The increase in stiffness corresponding to 25% to 40% concentration increase is

84.4%. The results also suggest that the SDA mastics are the most interactive with this binder, while Class C ash based mastics are the least interactive. Class F ash was intermediate, and similar to the reference filler.

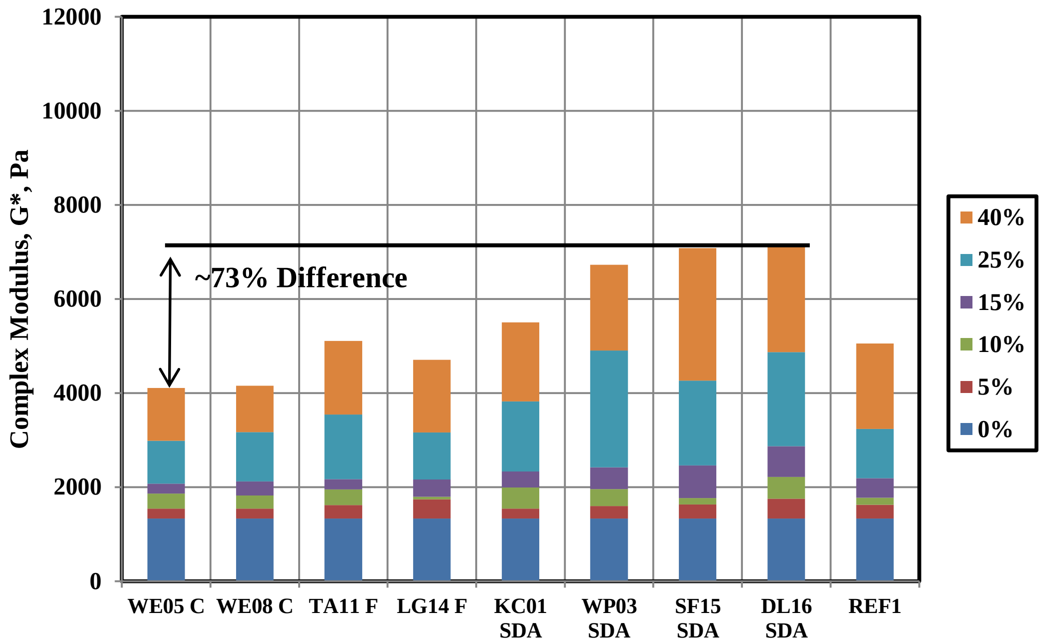


**Figure 4.18 Complex modulus, G* for different CCPs with PG58-28 (unmodified) binder at five concentrations by volume**

The effect the addition of CCPs to unaged PG64-28 (unmodified) binder on the complex modulus is presented in Figure 4.19. The results indicate very similar behavior in PG58-28 asphalt based mastics. Up to 15%, the increase per dosage is minor, but once the addition of CCPs goes to 25% and beyond, the complex modulus increases rapidly. Similarly to PG58-28 based mastics, the SDA materials were most interactive with the binder and the Class C ash was the least interactive.

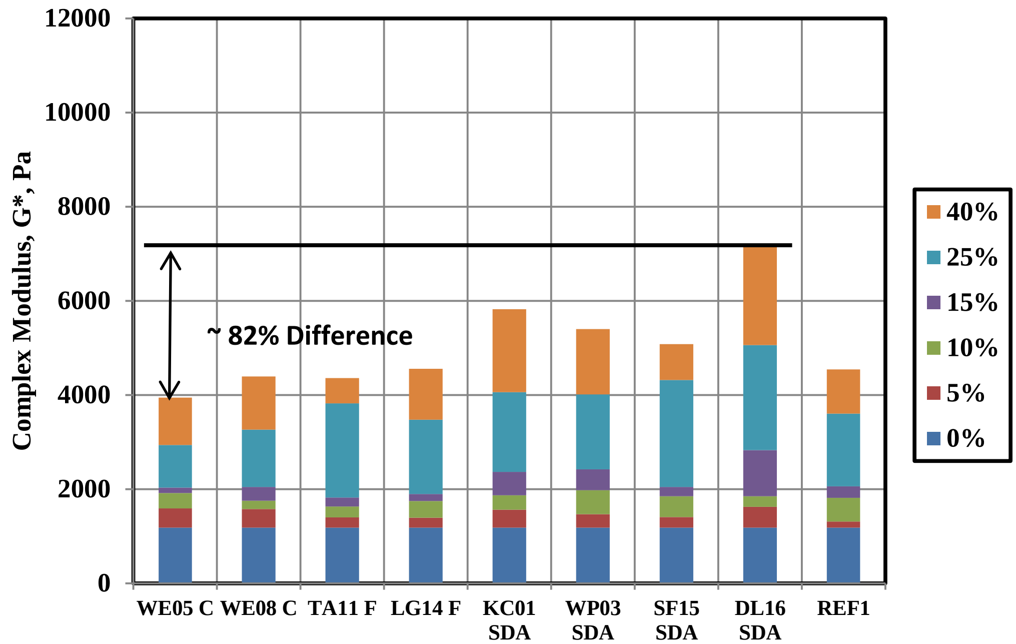


**Figure 4.19 Complex modulus, G* for different CCPs with PG64-28 (unmodified) binder at five concentrations by volume**

Figure 4.20 demonstrates the interaction of CCPs with unaged PG70-28 (modified) binder. As reported under section 2.1, the PG58-28 was modified with polymer to a performance grade PG70-28. Similar to the unmodified binders, the Class C fly ash was the least interactive, and the SDA CCP was the most. It is clear that one of the SDA CCPs (DL16) is highly sensitive to this binder compared to the other binders. It appears that there could be some level of synergy between this specific CCP and this specific binder.

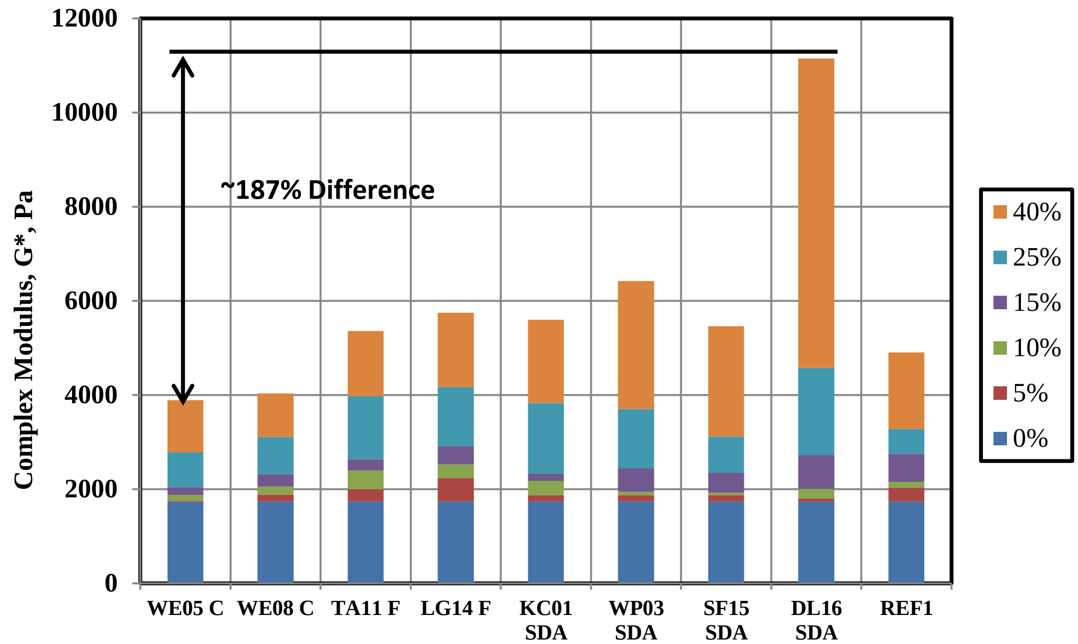


**Figure 4.20 Complex modulus, G* for different CCPs with PG70-28 (modified) binder at five concentrations by volume**

The above results do not provide detailed information regarding CCP contribution, but rather provide information on the level of interaction between the filler and the binder. The following sections of this report will clarify how these levels of interaction influence the performance levels tested by measuring asphalt binders performance indicators and, therefore, a better understanding can be achieved on the impact and contribution of selected CCPs on performance and the level of interaction.

#### 4.2.1.1 Relative Complex Shear Modulus, G*r

The measured complex modulus (G*) of the mastics made with CCPs and reference limestone filler were divided by the value of the G* of the corresponding unfilled asphalt binder to determine the complex modulus ratio or relative complex modulus (G*r).

It is theorized, that the increase in mastic G*r is linear until a certain critical filler volume concentration where the rate of increase becomes nonlinear and rapidly reaches an asymptotic linear trend (Faheem, 2009). The region where the mastic G*r increases linearly is known as the diluted region and it is influenced by the physical presence of fine and ultrafine particles with high potential energy and free asphalt content available that separates the filler particles. The free asphalt is defined as the portion of the asphalt available in the mastic that is not influenced by the filler particles. Filler concentration and particle size distribution are believed to be the two most important factors that can influence the increase in complex modulus of the mastics. As concentration increases, all the available asphalt in the mastic is influenced by the filler, the increase in G*r follows a linear rate trend similar to that of the diluted region but of higher slope value. This region is known as the concentrated region or jammed state and it is believed to be influenced by the physical-chemical interaction between the CCPs / fillers and the matrix that compounds the stiffening effect.

Figures 4.21 to 4.23 present the effect of all CCPs and reference materials mixed with 3 types of asphalt binders. The asphalt binders used under this task were PG58-28 (unmodified), PG64-28 (unmodified) and PG70-28 (modified). The comparison of the CCPs and fillers with these asphalt binders are made based on the relative complex modulus (G*r). The increase in complex modulus is linear with the addition of low volumes of CCPs. Up to 15% volume concentration the slope is small; however at concentrations from 25 to 40% a more pronounce increase of the slope is observed. It can be noted that the increase in complex modulus is not linear in this case; it is asymptotic linear from 25% to 40%.

Figures 4.21(a), 4.22(a) and 4.23(a) revealed that, at 40% addition, Class C fly ash demonstrated lower G*r with respect to the reference limestone filler. Figures 4.21(b), 4.22(b) and 4.22(b) demonstrate a very similar behavior observed for Class F fly ash and reference limestone filler. Linear increase in G*r with the addition of Class C and F fly ash indicates the potential increase in rutting resistance. The use of SDA makes the asphalt binder stiffer as demonstrated by a higher increase of the G*r vs. reference limestone filler (Figures 4.21(c), 4.22(c) and 4.23(c)). Very high increase of the G*r is characteristic for the SDA based materials at dosages higher than 15%; this indicates materials that are more difficult to compact. The results demonstrate that the increase in relative complex modulus is not binder dependent but filler dependent.

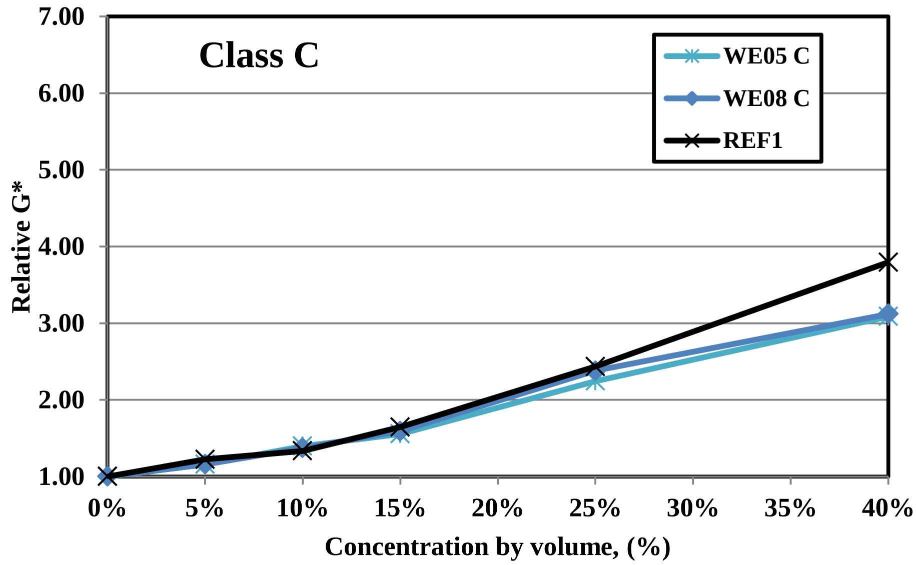


**(a)**

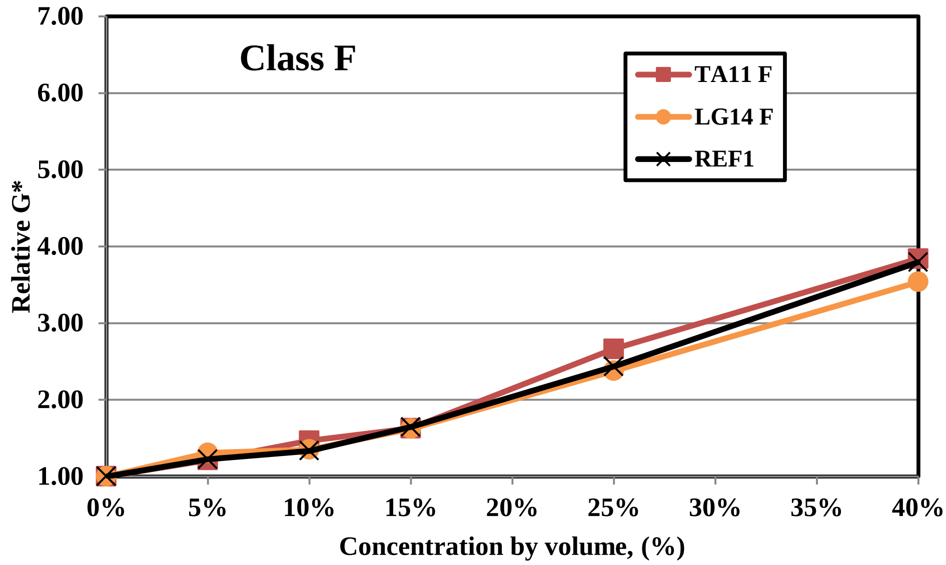


(b)

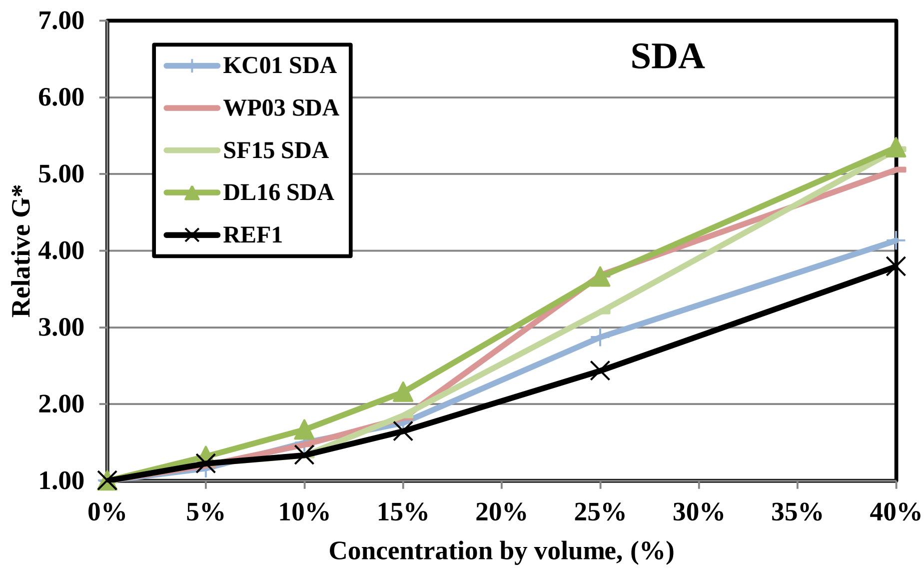


(c)

**Figure 4.21 The effect of CCP on relative G* of PG58-28 (unmodified) mastics at 58°C for: (a) Class C ash, (b) Class F ash and (c) SDA material**

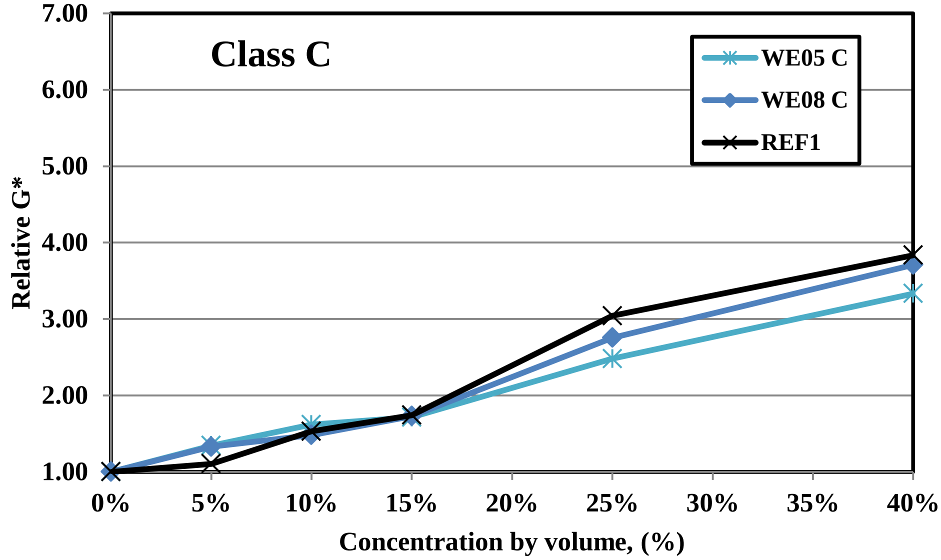
Class C
WE05 C
WE08 C
REF1
Relative G*
7.00
6.00
5.00
4.00
3.00
2.00
1.00
0%
5%
10%
15%
20%
25%
30%
35%
40%
Concentration by volume, (%)

**(a)**

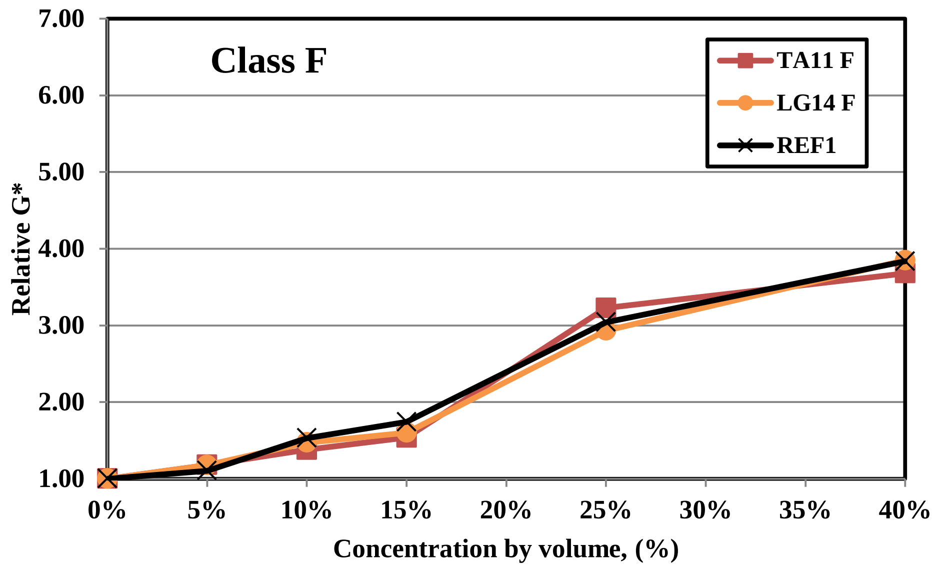
Class F
TA11 F
LG14 F
REF1
Relative G*
7.00
6.00
5.00
4.00
3.00
2.00
1.00
0%
5%
10%
15%
20%
25%
30%
35%
40%
Concentration by volume, (%)

**(b)**

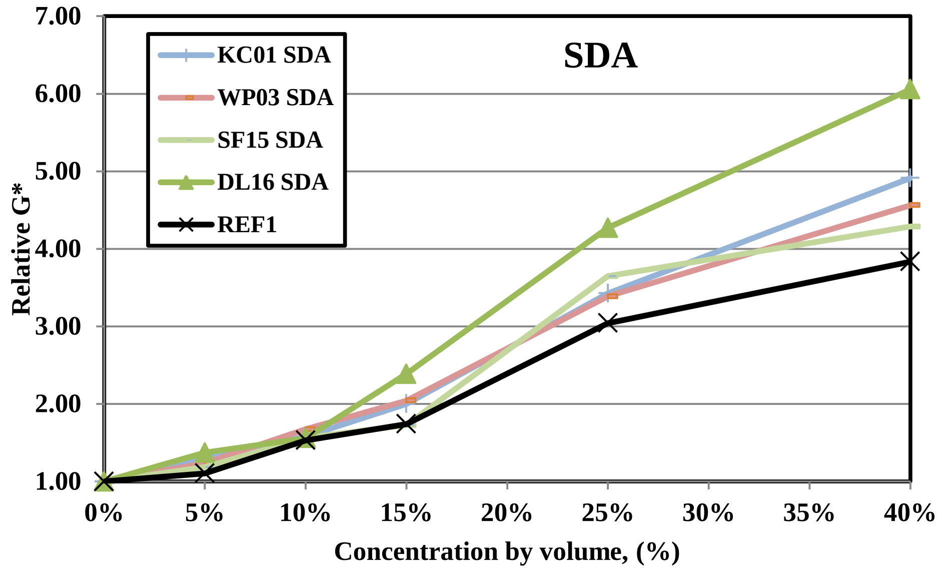


**(c)**

**Figure 4.22 The effect of CCP on relative G* of PG64-28 (unmodified) mastics at 64°C for: (a) Class C ash, (b) Class F ash and (c) SDA material**

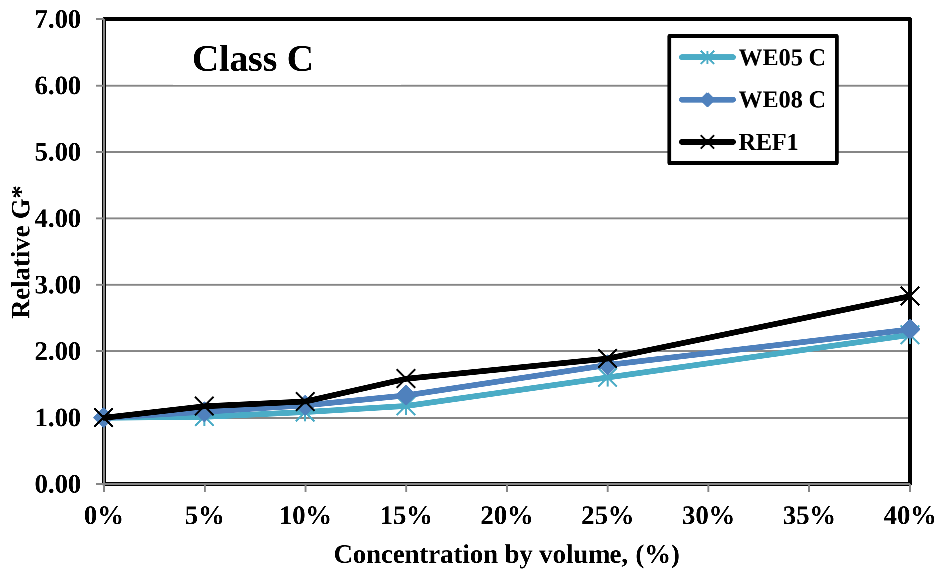


**(a)**

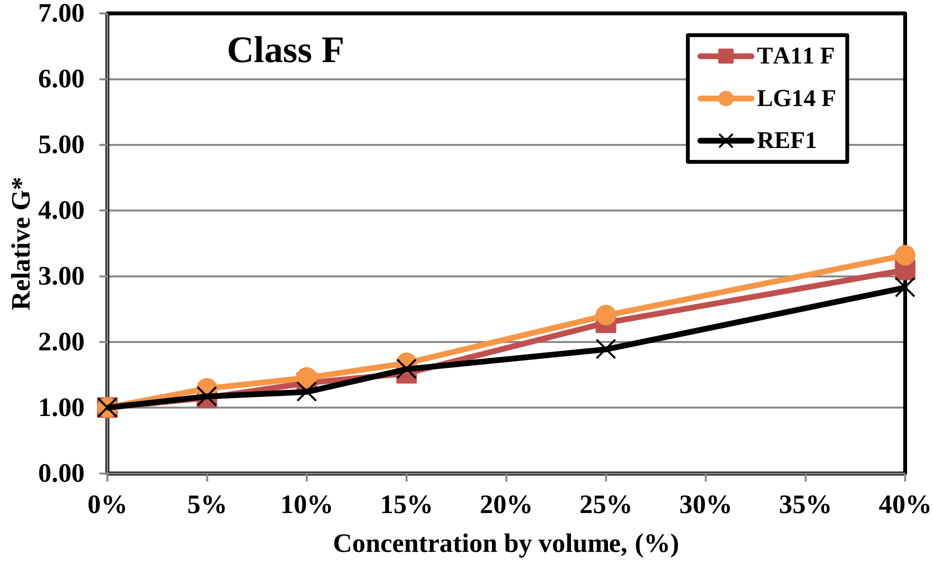


**(b)**

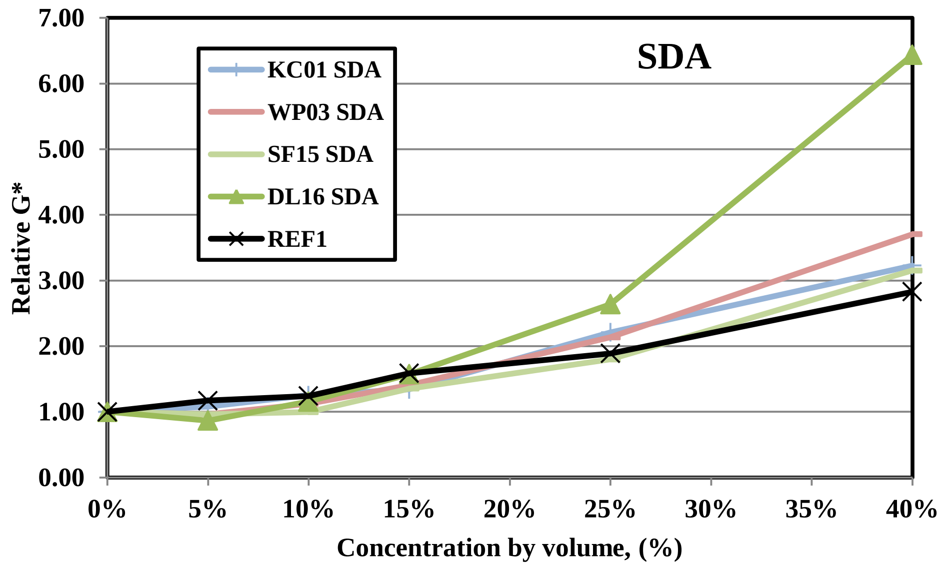


**(c)**

**Figure 4.23 The effect of CCP on relative G* of PG70-28 (modified) mastics at 70°C for: (a) Class C ash, (b) Class F ash and (c) SDA material**

#### 4.2.1.2 Relative Phase angle, δr

The relative phase angle ($\delta_r$) for the mastics prepared with both binders, PG58-28, PG64-28 and PG70-28 at the PG grade temperature are presented in Tables 4.3 to 4.5 . Similar to the relative stiffness, the phase angle of the mastic is divided over the binder phase angle as an indication of the change induced by the addition of CCPs. The phase angle is an indication of elastic or viscous performance of a material. The lower the phase angle the more elastic the material is. It can be observed in Table 4.3 and 4.4 that the phase angle has a small variation for the entire range of investigated mastics based on unmodified tested binders. Modified binders phase angle variations were also small with the exception of DL16 at 40% concentration. This is a clear indication that there is no significant effect of the CCPs type or dosage on the phase angle.

**Table 4.3 The effect of CCP on relative phase angle (δ) of PG58-28 (unmodified) mastics at 58°C**

| Materials ID | Class | Relative Phase Angle ($\delta_r$) | | | | | |
|---|---|---|---|---|---|---|---|
| | | **0%** | **5%** | **10%** | **15%** | **25%** | **40%** |
| WE05 | C | 1.000 | 0.997 | 0.997 | 0.997 | 1.003 | 1.004 |
| WE08 | C | 1.000 | 0.995 | 0.996 | 0.997 | 1.007 | 1.002 |
| TA11 | F | 1.000 | 0.996 | 0.997 | 0.997 | 1.006 | 1.004 |
| LG14 | F | 1.000 | 0.997 | 0.997 | 0.998 | 1.007 | 1.008 |
| KC01 | SDA | 1.000 | 0.996 | 0.997 | 0.997 | 1.001 | 1.000 |
| WP03 | SDA | 1.000 | 0.996 | 0.997 | 0.997 | 1.010 | 1.007 |
| SF15 | SDA | 1.000 | 0.996 | 0.996 | 0.997 | 1.011 | 1.009 |
| DL16 | SDA | 1.000 | 0.996 | 0.997 | 0.999 | 1.007 | 1.005 |
| REF 1 | Limestone | 1.000 | 0.997 | 0.996 | 0.997 | 1.001 | 1.006 |

**Table 4.4 The effect of CCP on relative phase angle (δ) of PG64-28 (unmodified) mastics at 64°C**

| Materials ID | Class | Relative Phase Angle ($\delta_r$) | | | | | |
|---|---|---|---|---|---|---|---|
| | | **0%** | **5%** | **10%** | **15%** | **25%** | **40%** |
| WE05 | C | 1.000 | 1.007 | 1.003 | 1.002 | 1.010 | 1.008 |
| WE08 | C | 1.000 | 1.003 | 1.001 | 1.001 | 1.013 | 1.013 |
| TA11 | F | 1.000 | 0.999 | 0.998 | 0.999 | 1.016 | 1.005 |
| LG14 | F | 1.000 | 1.000 | 1.002 | 1.001 | 1.016 | 1.012 |
| KC01 | SDA | 1.000 | 1.000 | 1.000 | 1.002 | 1.012 | 1.008 |
| WP03 | SDA | 1.000 | 1.001 | 1.001 | 1.003 | 1.009 | 1.007 |
| SF15 | SDA | 1.000 | 1.000 | 1.001 | 1.001 | 1.015 | 1.007 |
| DL16 | SDA | 1.000 | 1.000 | 0.996 | 1.007 | 1.019 | 1.016 |
| REF 1 | Limestone | 1.000 | 0.999 | 1.001 | 1.003 | 1.014 | 1.008 |

**Table 4.5 The effect of CCP on relative phase angle (δ) of PG70-28 (modified) mastics at 70°C**

| Materials ID | Class | Relative Phase Angle ($\delta_r$) | | | | | |
|---|---|---|---|---|---|---|---|
| | | **0%** | **5%** | **10%** | **15%** | **25%** | **40%** |
| WE05 | C | 1.000 | 1.004 | 0.983 | 0.975 | 0.981 | 0.985 |
| WE08 | C | 1.000 | 0.985 | 0.989 | 0.985 | 0.998 | 1.001 |
| TA11 | F | 1.000 | 0.984 | 0.996 | 0.992 | 1.005 | 0.997 |
| LG14 | F | 1.000 | 1.014 | 1.005 | 1.007 | 1.018 | 1.013 |
| KC01 | SDA | 1.000 | 0.999 | 0.997 | 1.007 | 1.015 | 1.049 |
| WP03 | SDA | 1.000 | 0.984 | 0.997 | 1.005 | 1.031 | 1.097 |
| SF15 | SDA | 1.000 | 0.987 | 0.993 | 1.006 | 1.035 | 1.083 |
| DL16 | SDA | 1.000 | 1.000 | 1.015 | 1.052 | 1.106 | 1.353 |
| REF 1 | Limestone | 1.000 | 0.998 | 1.009 | 1.012 | 1.009 | 1.018 |

The change in the phase angle is very small that it could be within the machine error tolerance. Therefore, it is difficult to draw conclusion on the phase angle results.

## 4.3 PERFORMANCE RELATED INDICATORS

All testing conducted on the mastics followed the Superpave binder testing requirements. While these tests where not developed to characterize mastics, they are used for comparison, and capturing fundamental properties of the mastics. Therefore, the Superpave limits are not followed in this study, but rather qualitative and quantitative analysis of the effect of the different CCPs on asphalt binders. Based on the research plan all tests were conducted as duplicate measurements. Coefficient of variations (CV) within duplicates were calculated and those values were not greater than 15%.

### 4.3.1 Constructability

To ensure that asphalt binders, especially modified asphalts, can be pumped and handled at the hot mixing facility the Superpave® binder specification measures the viscosity of the unaged asphalt binder as an indication of constructability or workability. The Rotational Viscometer is used under the Superpave® testing protocol to measure the asphalt viscosity at high construction temperatures (above 100°C). At such temperatures, the behavior of most asphalt binders is totally viscous, and a viscosity measurement is sufficient to represent the workability of the asphalt. The Superpave® binder specification sets the viscosity limit for unfilled unaged asphalts at a maximum of 3 Pa.s at 135°C plant mixing temperature.

Under this research effort the viscosity of mastics was measured at 135°C using a # 27 spindle. The comparisons of the CCPs and fillers were performed based on the relative viscosity in order to evaluate the effect of CCPs on constructability of mastics. This parameter was calculated by dividing the viscosity of the mastic by the viscosity of the unfilled asphalt binder at the test temperature, similarly to the relative stiffness presented on section 4.1.1.1. Work conducted on mastics with natural fillers under the NCRHP 9-45 research project sets the limit of relative viscosity to 5 (Bahia et al. 2011). Beyond this limit an additional effort to compact the coarse asphalt mixes is required. The mastic limit was set based on a linear relationship between the coarse mixtures number of gyrations to reach 92% $G_{mm}$ and relative viscosity of mastic with natural fillers. $G_{mm}$ is defined as the maximum theoretical density; a 92% $G_{mm}$ means the mix is compacted to 8% air void content.

#### 4.3.1.1 Relative viscosity

Figures 4.24 to 4.26 describe the performance of the 8 selected CCPs and reference filler materials mixed with 3 types of asphalt binders. The asphalt binders used under this task were PG58-28 (unmodified), PG64-28M (modified) and PG70-28 (modified). A favorable performance is demonstrated by lower relative viscosity value, which relates to the ability of the asphalt to coat the aggregate, and easy compaction in the field. In order to evaluate the influence of the CCPs on the binder, the relative viscosity values are compared to the reference fillers (which can be considered as a representative of natural filler). In the following plots, the relative viscosity values of CCP mastics that are lower than the reference filler are marked with shaded rectangles.

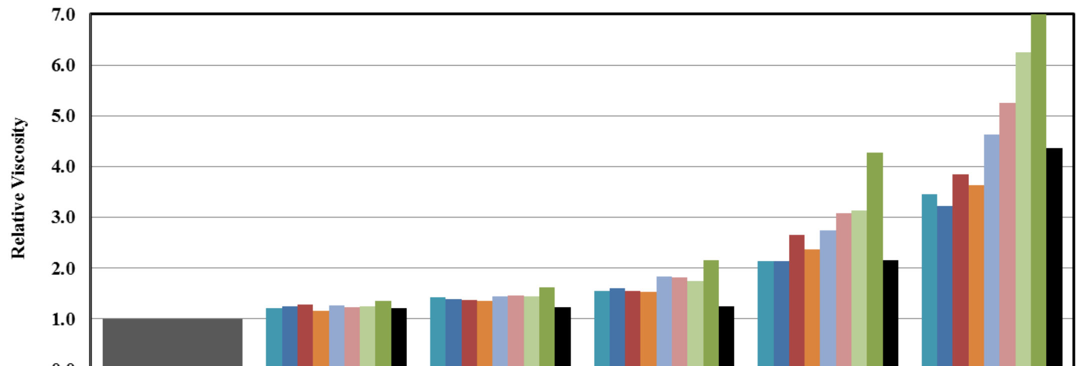


| | 0% | 5% | 10% | 15% | 25% | 40% |
|---|---|---|---|---|---|---|
| WE05 C | 1.00 | 1.21 | 1.43 | 1.54 | 2.14 | 3.46 |
| WE08 C | 1.00 | 1.23 | 1.38 | 1.60 | 2.13 | 3.22 |
| TA11 F | 1.00 | 1.28 | 1.37 | 1.55 | 2.66 | 3.85 |
| LG14 F | 1.00 | 1.15 | 1.35 | 1.53 | 2.36 | 3.64 |
| KC01 SDA | 1.00 | 1.26 | 1.45 | 1.83 | 2.74 | 4.64 |
| WP03 SDA | 1.00 | 1.22 | 1.46 | 1.81 | 3.08 | 5.26 |
| SF15 SDA | 1.00 | 1.23 | 1.45 | 1.74 | 3.14 | 6.24 |
| DL16 SDA | 1.00 | 1.34 | 1.62 | 2.15 | 4.28 | 13.26 |
| REF 1 | 1.00 | 1.20 | 1.23 | 1.25 | 2.14 | 4.36 |

**Figure 4.24 The Relative Viscosity values for PG58-28 (unmodified) mastics with CCPs and reference filler at 135°C**

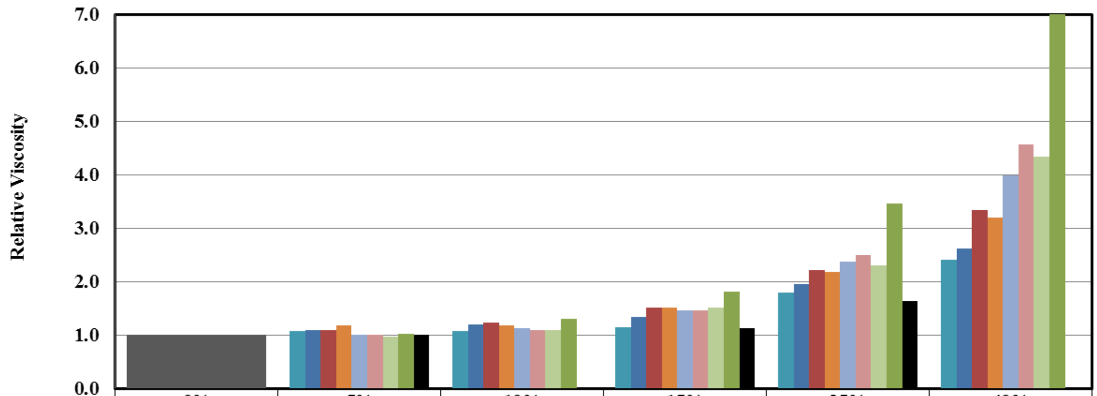


| | 0% | 5% | 10% | 15% | 25% | 40% |
|---|---|---|---|---|---|---|
| WE05 C | 1.00 | 1.08 | 1.08 | 1.14 | 1.79 | 2.41 |
| WE08 C | 1.00 | 1.10 | 1.20 | 1.34 | 1.96 | 2.62 |
| TA11 F | 1.00 | 1.10 | 1.23 | 1.51 | 2.21 | 3.34 |
| LG14 F | 1.00 | 1.18 | 1.18 | 1.52 | 2.18 | 3.20 |
| KC01 SDA | 1.00 | 1.00 | 1.13 | 1.46 | 2.38 | 3.99 |
| WP03 SDA | 1.00 | 1.01 | 1.10 | 1.46 | 2.49 | 4.58 |
| SF15 SDA | 1.00 | 0.97 | 1.10 | 1.51 | 2.31 | 4.35 |
| DL16 SDA | 1.00 | 1.03 | 1.30 | 1.82 | 3.46 | 16.76 |
| REF 1 | 1.00 | 1.01 | | 1.13 | 1.63 | |

**Figure 4.25 The Relative Viscosity values for PG64-28M (modified) mastics with CCPs and reference filler at 135°C**

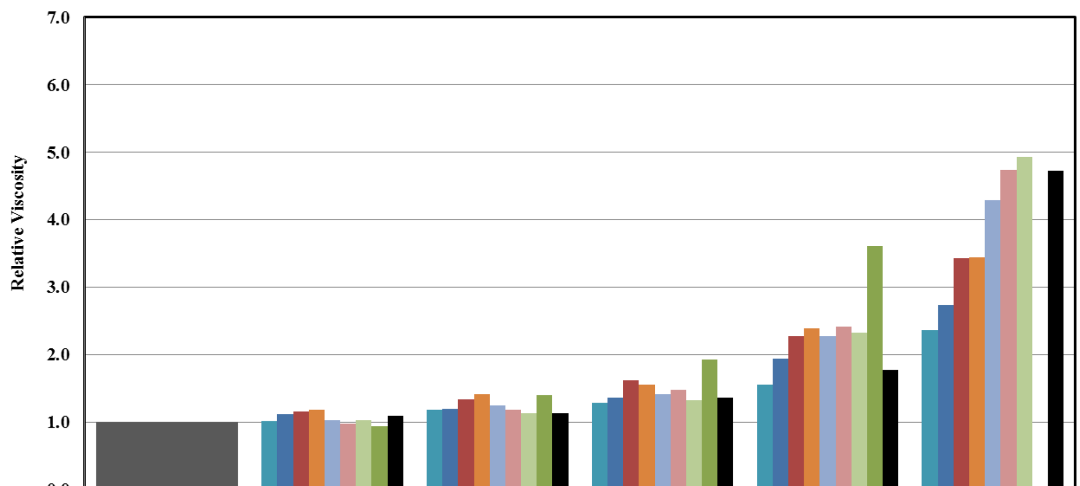


| | 0% | 5% | 10% | 15% | 25% | 40% |
|---|---|---|---|---|---|---|
| WE05 C | 1.00 | 1.02 | 1.19 | 1.29 | 1.56 | 2.37 |
| WE08 C | 1.00 | 1.12 | 1.20 | 1.37 | 1.94 | 2.74 |
| TA11 F | 1.00 | 1.16 | 1.33 | 1.62 | 2.28 | 3.44 |
| LG14 F | 1.00 | 1.18 | 1.41 | 1.55 | 2.39 | 3.45 |
| KC01 SDA | 1.00 | 1.03 | 1.25 | 1.42 | 2.28 | 4.30 |
| WP03 SDA | 1.00 | 0.98 | 1.19 | 1.48 | 2.42 | 4.73 |
| SF15 SDA | 1.00 | 1.03 | 1.14 | 1.33 | 2.32 | 4.94 |
| DL16 SDA | 1.00 | 0.94 | 1.40 | 1.94 | 3.61 | 0.00 |
| REF 1 | 1.00 | 1.09 | 1.14 | 1.37 | 1.77 | 4.73 |

NA

**Figure 4.26 The Relative Viscosity values for PG70-28 (modified) mastics with CCPs and reference filler at 135°C**

The above figures will be used to identify the CCPs with favorable influence on performance.

**4.3.2 Rutting resistance**

The response of asphalt binder to load consists of two components: elastic (recoverable) and viscous (non-recoverable). Rutting is the accumulation of the non-recoverable component of the responses to load repetitions at high service temperatures.

Asphalt rutting is a high pavement service temperature distress that occurs at the surface as a depression under the wheel path. In this report, in order to demonstrate the rutting resistance behavior, the Superpave® rutting factor $G^*/\sin\delta$ was calculated. The purpose of estimating $G^*/\sin\delta$ of mastics is to assess the effect of the addition of CCPs on possible increase in rutting resistance of asphalt mastics. This specification measures the rheological parameters $G^*$ and $\delta$ in the linear range. For viscous materials flow is linear even under high stress and strain. On the other hand, at high stress and strains, the response of polymer modified binders is not linear. To minimize the rutting, $G^*/\sin\delta$ must be a minimum of 1.00 kPa for the original asphalt binder and 2.20 kPa after RTFO aging. High values of $G^*$ and low values of $\delta$ are considered desirable from the standpoint of rutting resistance. Superpave® promotes the use of stiff, elastic binders (unaged and RTFO aged) to address the rutting resistance.

Furthermore, binder results within the linear regions have been found not to correlate with high temperature mix failure unless the binder is a viscous fluid at those temperatures. To be able to address asphalt mix failure accurately the non-linear properties of the asphalt binders must be measured. For this reason in recent years the asphalt industry started looking into alternatives to better quantify the behavior of polymer modified materials. The G*/sinδ test is considered as not sufficient to characterize the rutting resistance of polymer modified binders, and it is usually coupled with the Multiple Stress Creep Recovery (MSCR) test to characterize the deformation resistance and recovery influenced by the polymer modification (D'Angelo 2009). The MSCR test was also conducted as a part of this research effort to investigate the effect of the addition of CCPs on possible increase in rutting resistance of asphalt mastics in terms of the non-recoverable compliance ($J_{nr}$) and percent of recovery.

#### 4.3.2.1 Superpave® rutting factor, G*/sinδ

The Superpave® binder specification considers the G*/sinδ as the rutting performance parameter.  Table 4.6 presents the G*/sinδ values for unfilled binders and Tables 4.7, 4.8 and 4.9 report on the G*/sinδ results for mastics based on PG58-28, PG64-28 and PG70-28 binders, respectively.

The G*/sinδ values greater than or equal to 1.0 kPa are desired as they indicate a higher potential of rutting resistance.  For example, according to the specifications, for an unaged binder PG58-28 at a PG grade temperature of 58°C, the G*/sinδ value should be greater than or equal to 1.0 kPa. It is evident from Table 4.2 that G*/sinδ for the unfilled unaged binder PG58-28 is 1.33, which above the Superpave® threshold meaning that at the test temperature (PG grade) the asphalt binder can resist rutting.  All mastics results presented in this section were under the unaged condition.

**Table 4.6 The effect of CCPs on unfilled, unaged binders rutting resistance**

| | PG58-28 (unmodified) | PG64-28 (unmodified) | PG70-28 (modified) |
|---|---|---|---|
| **Testing Temperature (°C)** | **58** | **64** | **70** |
| **G*/Sinδ (kPa)** | 1.33 | 1.19 | 1.90 |

Note: Superpave® binder specifications sets value of unfilled binder G*/sinδ to be greater or equal to 1.0 kPa

For all asphalt mastics results, it is clear that the addition of CCPs increases the rutting resistance as compared to the corresponding unfilled binder. For example, at all CCP concentrations the G*/sinδ results for mastics based on unaged PG58-28 and PG64-28 are above the corresponding unfilled binders results. These results clearly indicate that the addition of CCPs (and reference filler) to unmodified asphalt binders increase the rutting resistance as measured by G*/sinδ. On the other hand, PG70-28 polymer modified binders also demonstrate an increase on rutting resistance with all CCPs at all addition levels with the exceptions of mixtures with 5% of WP03 SDA and SF15 SDA, and DL16 SDA at up to 10% concentration (by volume). These exceptions are an indication of a softening effect at low concentrations of these SDA materials. A softening effect is an indicator of an extension of the asphalt binder. This is a very important observation that should be carried over to the mixture testing to prove the ability of the CCPs to replace some of the asphalt binder without any adverse effect on the performance.

**Table 4.7 The effect of CCPs on PG58-28 (unmodified) Superpave® rutting performance (values are G*/sinδ in kPa)**

| | | PG58-28 (unmodified) test at 58°C | | | | |
|---|---|---|---|---|---|---|
| **Materials ID** | **Class** | **5%** | **10%** | **15%** | **25%** | **40%** |
| **WE05** | **C** | 1.54 | 1.86 | 2.04 | 2.99 | 4.12 |
| **WE08** | **C** | 1.54 | 1.83 | 2.12 | 3.17 | 4.16 |
| **TA11** | **F** | 1.62 | 1.95 | 2.17 | 3.55 | 5.12 |
| **LG14** | **F** | 1.74 | 1.80 | 2.16 | 3.17 | 4.72 |
| **KC01** | **SDA** | 1.55 | 1.99 | 2.34 | 3.83 | 5.51 |
| **WP03** | **SDA** | 1.60 | 1.96 | 2.42 | 4.91 | 6.74 |
| **SF15** | **SDA** | 1.63 | 1.77 | 2.46 | 4.28 | 7.10 |
| **DL16** | **SDA** | 1.75 | 2.22 | 2.87 | 4.88 | 7.13 |
| **REF 1** | **Limestone** | 1.63 | 1.78 | 2.19 | 3.24 | 5.06 |

**Table 4.8 The effect of CCPs on PG64-28 (unmodified) Superpave® rutting performance (values are G*/sinδ in kPa)**

| | | PG64-28 (unmodified) test at 64°C | | | | |
|---|---|---|---|---|---|---|
| **Materials ID** | **Class** | **5%** | **10%** | **15%** | **25%** | **40%** |
| **WE05** | **C** | 1.60 | 1.92 | 2.03 | 2.95 | 3.96 |
| **WE08** | **C** | 1.58 | 1.76 | 2.05 | 3.27 | 4.41 |
| **TA11** | **F** | 1.40 | 1.64 | 1.82 | 3.84 | 4.37 |
| **LG14** | **F** | 1.40 | 1.75 | 1.90 | 3.49 | 4.57 |
| **KC01** | **SDA** | 1.56 | 1.87 | 2.37 | 4.07 | 5.83 |
| **WP03** | **SDA** | 1.47 | 1.98 | 2.42 | 4.02 | 5.42 |
| **SF15** | **SDA** | 1.41 | 1.85 | 2.05 | 4.34 | 5.09 |
| **DL16** | **SDA** | 1.63 | 1.85 | 2.83 | 5.08 | 7.20 |
| **REF 1** | **Limestone** | 1.31 | 1.82 | 2.07 | 3.61 | 4.55 |

**Table 4.9 The effect of CCPs on PG70-28 (modified) Superpave® rutting performance (values are G*/sinδ in kPa)**

| | | PG70-28 (modified) test at 70°C | | | | |
|---|---|---|---|---|---|---|
| **Materials ID** | **Class** | **5%** | **10%** | **15%** | **25%** | **40%** |
| **WE05** | **C** | 1.93 | 2.04 | 2.21 | 3.02 | 4.23 |
| **WE08** | **C** | 2.05 | 2.24 | 2.52 | 3.40 | 4.43 |
| **TA11** | **F** | 2.17 | 2.61 | 2.88 | 4.36 | 5.87 |
| **LG14** | **F** | 2.47 | 2.77 | 3.20 | 4.61 | 6.34 |
| **KC01** | **SDA** | 2.05 | 2.38 | 2.56 | 4.23 | 6.29 |
| **WP03** | **SDA** | 1.82 | 2.16 | 2.68 | 4.12 | 7.41 |
| **SF15** | **SDA** | 1.81 | 1.88 | 2.58 | 3.48 | 6.26 |
| **DL16** | **SDA** | 1.65 | 2.21 | 3.07 | 5.31 | 14.85 |
| **REF 1** | **Limestone** | 2.22 | 2.37 | 3.03 | 3.61 | 5.43 |

#### 4.3.2.2 Non-recoverable compliance, $J_{nr}$

Non-recoverable compliance ($J_{nr}$) was tested following AASHTO T350-14; in this experiment, the 0.1 kPa was used as a conditioning stress, while 3.2 and 10 kPa levels were used to characterize the damage resistance of the mastic. Figure 4.27 demonstrates the correlation between the non-recoverable compliance ($J_{nr}$) at 3.2 kPa and 10 kPa for all mastics at all concentrations. This figure can be used to compare the results obtained at high stress levels and to demonstrate the stress sensitivity of the tested mastics.

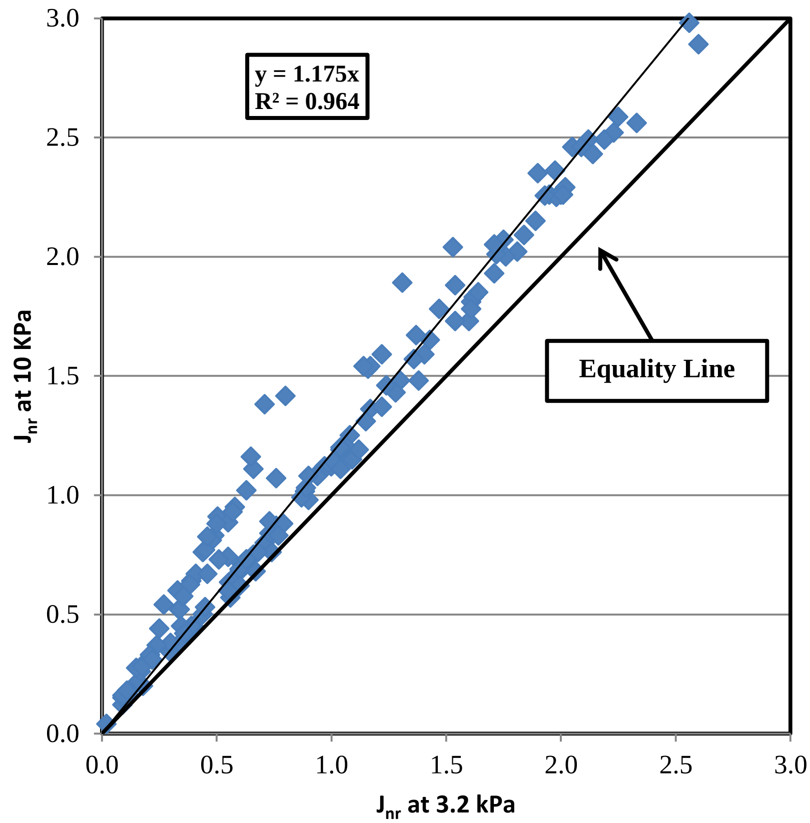


**Figure 4.27 The correlation between Jnr tested at 3.2 kPa and 10 kPa**

The trend shows that when all the mastics are compared, the $J_{nr}$ values for 10 kPa are on average about 17.5% higher than $J_{nr}$ at 3.2 kPa, as shown by the slope of the correlation line (1.175). It is clear that with the strong linear correlation observed (96.4%), the change in stress level results in a constant shift in the calculated $J_{nr}$. Therefore, the stress dependency of the results can be ignored in further analysis. These results are characteristic of classical Newtonian behavior of the asphalt binders and mastics. Based on these results, the remainder of the analysis will utilize the results obtained at 3.2 kPa loading.

Figures 4.28 to 4.31 demonstrates the 3.2 kPa - $J_{nr}$ for mastics prepared with Class C, Class F, SDA CCPs and reference filler based on PG58-28 (unmodified), PG64-28 (unmodified), PG64-28 (modified) and PG70-28 (modified) asphalt binders, respectively. It is important to note that as the $J_{nr}$ **decreases** the rutting resistance **increases.**

Figure 4.28 clearly shows that all CCPs improve the rutting resistance as demonstrated by the decreasing trend of the $J_{nr}$ values with increasing CCP concentration. While all the CCPs increase the rutting resistance, those causing further decrease of the $J_{nr}$ below the reference filler are marked with shaded rectangles for the purpose of identifying the best performimg CCPs.

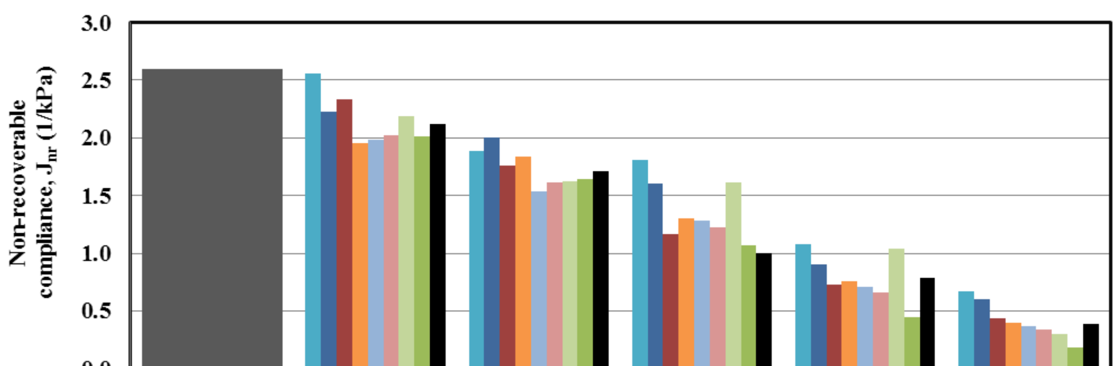


| | 0% | 5% | 10% | 15% | 25% | 40% |
|---|---|---|---|---|---|---|
| WE05 | 2.60 | 2.56 | 1.89 | 1.81 | 1.08 | 0.67 |
| WE08 | 2.60 | 2.23 | 2.00 | 1.60 | 0.90 | 0.60 |
| TA11 | 2.60 | 2.33 | 1.76 | 1.17 | 0.73 | 0.44 |
| LG14 | 2.60 | 1.95 | 1.84 | 1.30 | 0.76 | 0.40 |
| KC01 | 2.60 | 1.98 | 1.54 | 1.28 | 0.71 | 0.37 |
| WP03 | 2.60 | 2.02 | 1.61 | 1.22 | 0.66 | 0.34 |
| SF15 | 2.60 | 2.19 | 1.62 | 1.61 | 1.04 | 0.30 |
| DL16 | 2.60 | 2.01 | 1.64 | 1.07 | 0.45 | 0.18 |
| REF 1 | 2.60 | 2.12 | 1.71 | 1.00 | 0.79 | 0.39 |

**Figure 4.28 The $J_{nr}$ values for PG58-28 (unmodified) mastics with CCPs and reference filler at 58°C**

The unmodified asphalt binder PG64-28 based mastics had very similar behavior as mastics based on PG58-28 as observed in Figure 4.29. Mastics based on Class F fly ash were similar in behavior tomastics prepared with the reference filler. On the other hand, Class C fly ash shows the least effect on the $J_{nr}$ value.

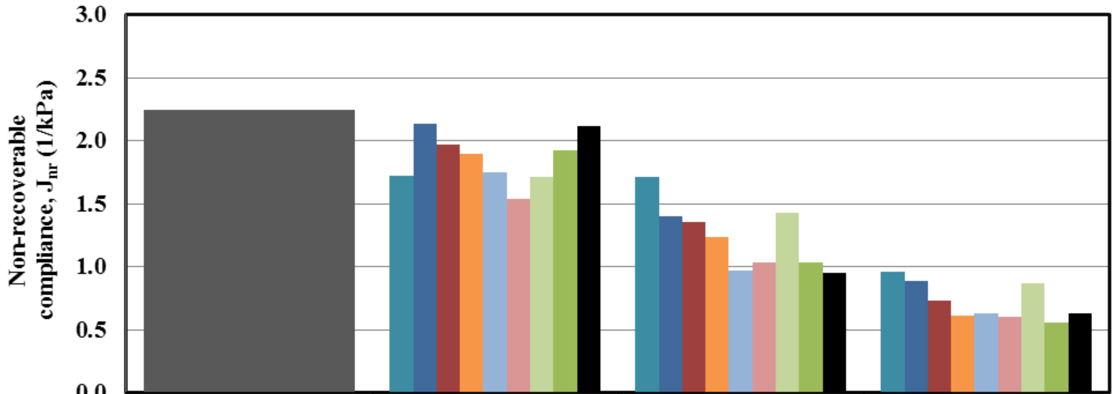


| | 0% | 5% | 15% | 25% |
|---|---|---|---|---|
| WE05 | 2.25 | 1.72 | 1.71 | 0.96 |
| WE08 | 2.25 | 2.14 | 1.41 | 0.89 |
| TA11 | 2.25 | 1.98 | 1.36 | 0.74 |
| LG14 | 2.25 | 1.90 | 1.24 | 0.61 |
| KC01 | 2.25 | 1.75 | 0.97 | 0.63 |
| WP03 | 2.25 | 1.54 | 1.04 | 0.60 |
| SF15 | 2.25 | 1.71 | 1.43 | 0.87 |
| DL16 | 2.25 | 1.93 | 1.04 | 0.56 |
| REF 1 | 2.25 | 2.12 | 0.95 | 0.63 |

**Figure 4.29 The $J_{nr}$ values for PG64-28 (unmodified) mastics with CCPs and reference filler at 64°C**

Figures 4.30 and 4.31 demonstrate the Jnr plots for mastics with CCPs based on **modified** asphalt binders PG64-28M and PG70-28. The unfilled modified binder had a $J_{nr}$ value of 1.31. For PG64-28M, the addition of the fillers decreases the $J_{nr}$ value to a minimum of 0.55 for mastics with DL16 SDA CCP. As reported for the unmodified binders, Class C fly ash had the least effect on the $J_{nr}$ value. The increase in the CCPs concentration shifts the curves downwards, but at a lower rates compared to the unmodified binders.

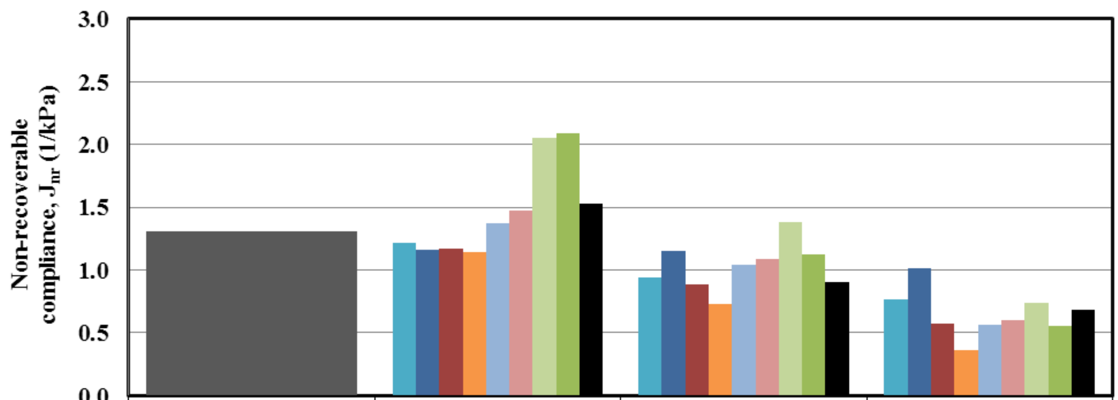


| | 0% | 5% | 15% | 25% |
|---|---|---|---|---|
| WE05 | 1.31 | 1.22 | 0.94 | 0.77 |
| WE08 | 1.31 | 1.16 | 1.15 | 1.01 |
| TA11 | 1.31 | 1.17 | 0.89 | 0.57 |
| LG14 | 1.31 | 1.14 | 0.73 | 0.36 |
| KC01 | 1.31 | 1.37 | 1.04 | 0.56 |
| WP03 | 1.31 | 1.47 | 1.09 | 0.60 |
| SF15 | 1.31 | 2.05 | 1.38 | 0.74 |
| DL16 | 1.31 | 2.09 | 1.12 | 0.55 |
| REF 1 | 1.31 | 1.53 | 0.90 | 0.68 |

**Figure 4.30 The $J_{nr}$ values for PG64-28 (modified) mastics with CCPs and reference filler at 64°C**

Figure 4.30 demonstrates a very interesting trend. At lower concentrations, the Class C and Class F fly ash had greater improvement when compared with the reference filler. On the other hand, at 5% the DL16 and SF15 materials deteriorate the rutting resistance of the binder. As concentration increases, the effect of fly ash becomes more comparable to the reference filler (but still improves the rutting resistance), and the SDA's improvement becomes more pronounced beyond the reference filler.

Figure 4.31 demonstrates the $J_{nr}$ for PG70-28 mastics with CCPs. The unfilled modified binder had a $J_{nr}$ value of 0.50. The addition of fillers decreases the value of the $J_{nr}$ to a minimum of 0.02 for mastics with the DL16 SDA CCP. Again, as observed with previous results, Class C fly ash had the least effect on the $J_{nr}$ value. Similarly with the PG64-28 modified asphalt binder, the increase in the CCPs concentration shifts the curves downwards, but at a lower rate compared to the unmodified binders. This may be attributed to the polymer modification of PG64-28M and PG70-28 asphalt binders.

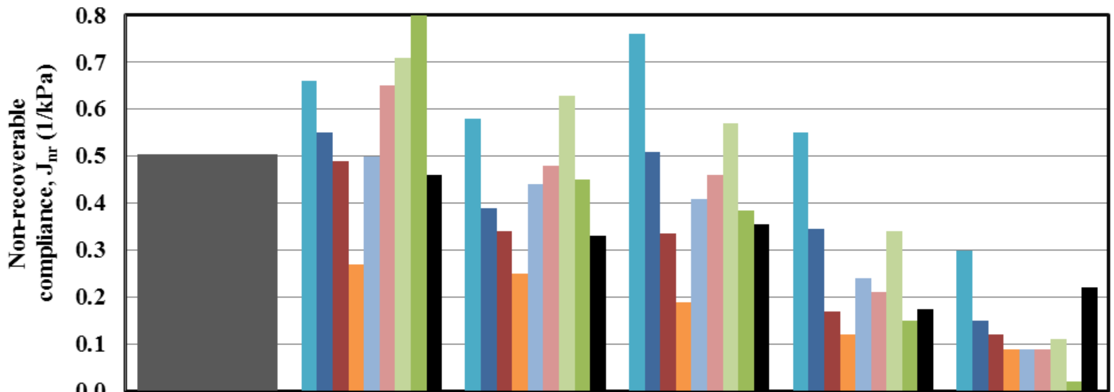


| | 0% | 5% | 10% | 15% | 25% | 40% |
|---|---|---|---|---|---|---|
| WE05 | 0.51 | 0.66 | 0.58 | 0.76 | 0.55 | 0.30 |
| WE08 | 0.51 | 0.55 | 0.39 | 0.51 | 0.35 | 0.15 |
| TA11 | 0.51 | 0.49 | 0.34 | 0.34 | 0.17 | 0.12 |
| LG14 | 0.51 | 0.27 | 0.25 | 0.19 | 0.12 | 0.09 |
| KC01 | 0.51 | 0.50 | 0.44 | 0.41 | 0.24 | 0.09 |
| WP03 | 0.51 | 0.65 | 0.48 | 0.46 | 0.21 | 0.09 |
| SF15 | 0.51 | 0.71 | 0.63 | 0.57 | 0.34 | 0.11 |
| DL16 | 0.51 | 0.80 | 0.45 | 0.39 | 0.15 | 0.02 |
| REF 1 | 0.51 | 0.46 | 0.33 | 0.36 | 0.18 | 0.22 |

**Figure 4.31 The $J_{nr}$ values for PG70-28 (modified) mastics with CCPs and reference fillers at 70°C**

In general, the addition of fillers increases the damage resistance as measured by the $J_{nr}$. The trend is that an increase in CCPs (or filler) volume leads to a decrease in $J_{nr}$ value and, consequently, to an increase of the rutting resistance. The SDA category consistently displays the most sensitivity to modified binders. The extent of its effect varies significantly based on the dosage and binder type.

#### 4.3.2.3 Percent recovery

Table 4.10 presents the percent recovery of mastics based on unmodified asphalt binders PG58-28 and PG64-28 and modified asphalt binders PG64-28 and PG70-28 tested at 3.2 kPa stress level. This test was originally developed for modified binders to quantify the added elasticity. Typically, unmodified binders at the high PG testing temperature do not possess any recovery after loading.

Although CCPs blends with unmodified asphalt binders had significantly improved the recovery values (by more than 100%), these results can be considered negligible. For example, the percent recovery for mastics with 25% DL16 SDA increased from 1.44% (for the unfilled binder) to 4.16%. This is an increase of 189%, yet the recovery is still at too low a level to cause any real change in the performance. These results suggest little improvement in recovery.

For modified binders the recovery is highly depended on the type of modification, and the integrity of the polymer modifiers within the binder. Therefore, the first concern when using CCPs is to make sure that the recovery is not hindered by the presence of the CCPs. If any added recovery is observed, this is a substantial impact as it indicates a good compatibility between the CCPs and the polymer.

**Table 4.10 The %Recovery for tested asphalt binder and mastics**

| Material | Filler type | Concentration, % | % Recovery | | | | Relative Recovery | | | |
|---|---|---|---|---|---|---|---|---|---|---|
| | | | PG58-28 | PG64-28 | PG64-28P | PG70-28 | PG58-28 | PG64-28 | PG64-28M | PG70-28P |
| - | - | 0 | 1.44 | 2.14 | 26.89 | 59.35 | 1.00 | 1.00 | 1.00 | 1.00 |
| WE05 | Class C | 5 | 1.46 | 2.38 | 26.73 | 56.63 | 1.01 | 1.11 | 0.99 | 0.95 |
| | | 10 | 1.88 | - | - | 62.19 | 1.31** | - | - | 1.05 |
| | | 15 | 1.91 | 2.35 | 24.53 | 49.46 | 1.33** | 1.10 | 0.91 | 0.83 |
| | | 25 | 2.70 | 3.84 | 24.79 | 53.38 | 1.88** | 1.79** | 0.92 | 0.90 |
| | | 40 | 3.52 | - | - | 55.96 | 2.44* | - | - | 0.94 |
| WE08 | Class C | 5 | 1.65 | 1.96 | 27.49 | 58.94 | 1.15 | 0.92 | 1.02 | 0.99 |
| | | 10 | 1.92 | - | - | 64.34 | 1.33** | - | - | 1.08 |
| | | 15 | 1.95 | 2.64 | 24.65 | 56.35 | 1.35** | 1.23** | 0.92 | 0.95 |
| | | 25 | 3.04 | 3.71 | 24.27 | 58.90 | 2.11* | 1.73** | 0.90 | 0.99 |
| | | 40 | 3.66 | - | - | 67.88 | 2.54* | - | - | 1.14 |
| TA11 | Class F | 5 | 1.57 | 2.13 | 26.97 | 60.12 | 1.09 | 1.00 | 1.00 | 1.01 |
| | | 10 | 2.07 | - | - | 67.43 | 1.44** | - | - | 1.14 |
| | | 15 | 2.34 | 2.68 | 27.62 | 63.08 | 1.63** | 1.25** | 1.03 | 1.06 |
| | | 25 | 3.37 | 4.19 | 29.30 | 71.17 | 2.34* | 1.96** | 1.09 | 1.20** |
| | | 40 | 4.27 | - | - | 68.70 | 2.97* | - | - | 1.16** |
| LG14 | Class F | 5 | 2.04 | 2.48 | 29.03 | 73.73 | 1.42** | 1.16** | 1.08 | 1.24** |
| | | 10 | 2.14 | - | - | 70.66 | 1.49** | - | - | 1.19** |
| | | 15 | 2.93 | 3.49 | 32.10 | 72.61 | 2.03* | 1.63** | 1.19** | 1.22** |
| | | 25 | 4.90 | 6.36 | 36.54 | 76.24 | 3.40* | 2.97* | 1.36** | 1.28** |
| | | 40 | 6.03 | - | - | 72.59 | 4.19* | - | - | 1.22** |
| KC01 | SDA | 5 | 1.94 | 2.40 | 23.24 | 63.74 | 1.35** | 1.12 | 0.86 | 1.07 |
| | | 10 | 2.04 | - | - | 64.23 | 1.42** | - | - | 1.08 |
| | | 15 | 2.39 | 3.54 | 21.81 | 63.26 | 1.66** | 1.65** | 0.81 | 1.07 |
| | | 25 | 2.91 | 4.10 | 24.88 | 67.30 | 2.02* | 1.92** | 0.93 | 1.13 |
| | | 40 | 3.78 | - | - | 74.03 | 2.63* | - | - | 1.25** |
| WP03 | SDA | 5 | 1.84 | 2.66 | 22.19 | 59.45 | 1.28** | 1.24** | 0.83 | 1.00 |
| | | 10 | 2.00 | - | - | 63.27 | 1.39** | - | - | 1.07 |
| | | 15 | 2.35 | 3.22 | 21.52 | 58.16 | 1.63** | 1.50** | 0.80 | 0.98 |
| | | 25 | 3.66 | 3.97 | 25.12 | 67.57 | 2.54* | 1.86** | 0.93 | 1.14 |
| | | 40 | 3.84 | - | - | 72.60 | 2.67* | - | - | 1.22** |
| SF15 | SDA | 5 | 1.65 | 2.59 | 19.50 | 62.50 | 1.15 | 1.21** | 0.73 | 1.05 |
| | | 10 | 2.02 | - | - | 57.38 | 1.40** | - | - | 0.97 |
| | | 15 | 1.60 | 2.38 | 20.70 | 60.25 | 1.11 | 1.11 | 0.77 | 1.02 |
| | | 25 | 2.78 | 3.00 | 22.18 | 63.37 | 1.93** | 1.40** | 0.82 | 1.07 |
| | | 40 | 4.00 | - | - | 70.90 | 2.78* | - | - | 1.19 |
| DL16 | SDA | 5 | 1.56 | 2.04 | 18.51 | 56.89 | 1.08 | 0.95 | 0.69 | 0.96 |
| | | 10 | 2.05 | - | - | 64.04 | 1.42** | - | - | 1.08 |
| | | 15 | 2.34 | 3.23 | 23.31 | 63.57 | 1.63** | 1.51** | 0.87 | 1.07 |
| | | 25 | 4.16 | 3.94 | 28.04 | 74.98 | 2.89* | 1.84** | 1.04 | 1.26** |
| | | 40 | 5.32 | - | - | 91.04 | 3.69* | - | - | 1.53** |
| REF1 | Limestone | 5 | 1.66 | 1.96 | 26.35 | 64.43 | 1.15 | 0.92 | 0.98 | 1.09 |
| | | 10 | 2.12 | - | - | 68.61 | 1.47** | - | - | 1.16 |
| | | 15 | 2.54 | 3.11 | 29.33 | 65.52 | 1.76** | 1.45** | 1.09 | 1.10 |
| | | 25 | 2.74 | 5.45 | 29.09 | 69.23 | 1.90** | 2.55* | 1.08 | 1.17 |
| | | 40 | 4.06 | - | - | 62.65 | 2.82* | - | - | 1.06 |

* Highlighted and bold numbers indicate more than 100% increase in recovery
** Highlighted and bold numbers indicate more than 15% increase in recovery

The mastics based on two modified binders used in this study had a minor change in the recovery when Class C fly ash was used. The mastics with SDA and PG64-28M had a severe deterioration in the recovery; and a minor change if recovery was reported for PG70-28 mastics with less than 25% of SDA. For the mastics based on acid modified binder (PG64-28M) and Class F only minor change in the recovery were observed. The polymer modified PG70-28 and Class F blends had the most significant improvement in the percent recovery.

The mechanism by which polymers and CCPs interact is still under investigation, but at this stage it is believed that the CCP can bridge the polymer chains, which explains why the effect is only observed in the damage resistance rather than recovery. The effect of the different CCPs when compared to the reference filler vary. Some of the CCPs outperform the reference filler depending on the asphalt grade and concentration. Further investigation must be performed to maximize the beneficial effect of the CCPs.

### 4.3.3 Fatigue resistance

The Superpave® binder specification systems uses a fatigue factor, $G^*\sin\delta$, to measure the fatigue damage resistance of binder at intermediate pavement service temperatures using the DSR. Since the fatigue generally occurs at low to moderate pavement temperatures after the pavement has been in service for a period of time, the Superpave® binder specification addresses this phenomenon using the binder aged in both the RTFO and PAV. Likewise, for the $G^*/\sin\delta$ factor the fatigue factor is measured by applying an oscillating load to the asphalt binder at a relatively low shear strain within the linear viscoelastic region. Unaged and PAV aged asphalt cement were tested under the dynamic loading at the intermediate pavement service temperature.

The Superpave® binder testing protocol limits G*sinδ for PAV asphalt biner to equal or less than 5,000 kPa at the intermediate temperature. Low values of G* and δ are considered desirable from the standpoint of fatigue resistance. Superpave® promotes the use of compliant, elastic PAV aged binders to address the fatigue resistance.

4.3.3.1 Superpave® fatigue resistance factor, G*sinδ

Figures 4.32 to 4.34 demonstrate the fatigue damage resistance results for mastics prepared with Class C, Class F, SDA CCPs and reference filler combined with PG58-28 (unmodified), PG64-28 (unmodified), and PG70-28 (modified) asphalt binders, respectively. The fatigue tests were conducted to evaluate the effects of CCPs on the resistance to fatigue at intermediate temperatures: 19°C for PG58-28, 22°C for PG64-28 and 25°C for PG70-28.

The results show that for both unmodified binders, the stiffness of the mastics increases rapidly beyond the 5,000kPa limit. Figure 4.32 demonstrates that PG58-28 mastics with up to 15% of WE08 C, LG14 F, and SF15 SDA CCPs can still meet the binder specifications.  The PG64-28 mastics up to 5% of CCP continue to meet the binder specification. Only PG64-28 mastic with 15% of WE05 C can meet the binder specification.  On the other hand, for mastics based on PG70-28 modified binder, the increase in the stiffness is more gradual. All mastics with PG70-28 still meet the binder specifications as demonstrated by Figure 4.34.

PG58-28 based mastics (with the exception of those prepared with 5% and 15% of Class C CCP WE05) had the G*sinδ results which are lower than these for corresponding mastics with reference limestone filler. It is important to note that the reference filler had the most rapid rate of increase while the Class C fly ash based mastics had the least increase in rate. *This could indicate that CCP based mastics are less prone to fatigue damage in terms of G*sinδ when compared to the reference limestone filler.*

A unique behavior was noticed for mastics based on PG64-28 and PG70-28 and 5% of SF15 SDA. It is evident from Figures 4.33c and 4.34c, that the addition of lower dosages of SF15 SDA reduces the intermediate temperature stiffness indicating the potential for the CCP to extend the asphalt binder, especially, in the polymer modified systems.

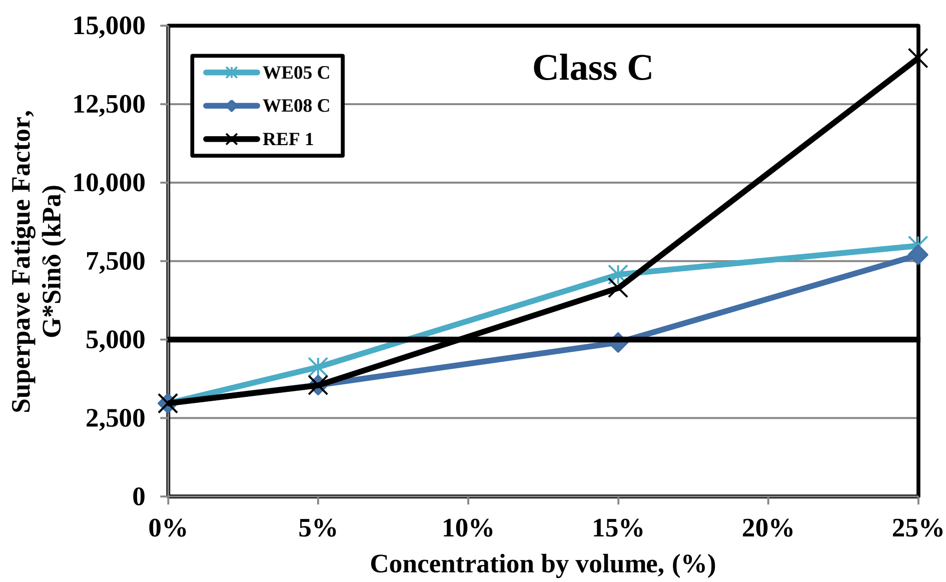


a)

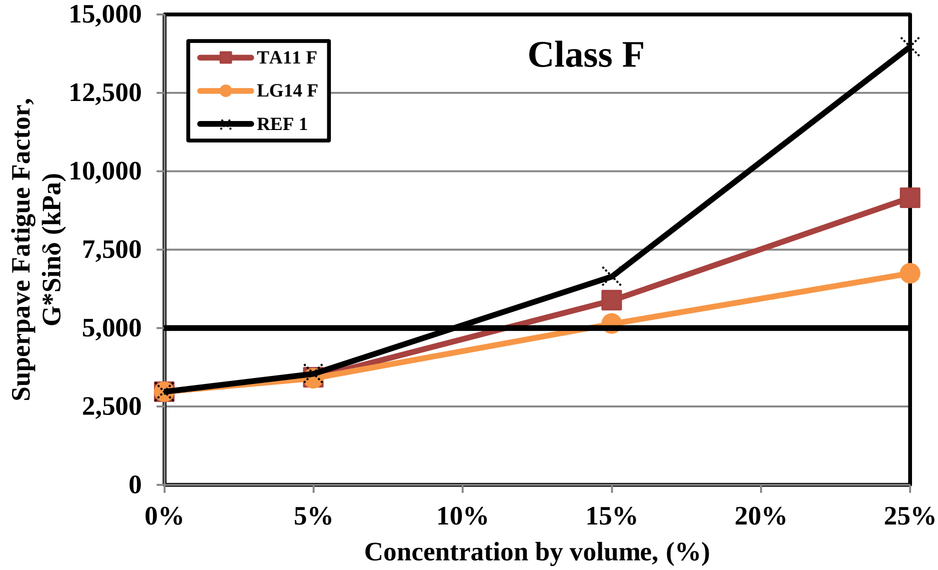


b)

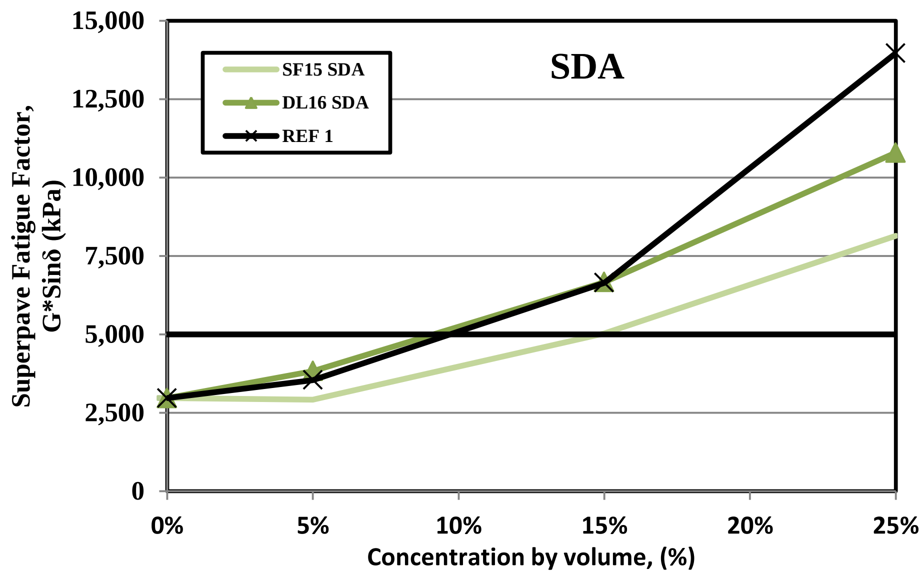


c)

**Figure 4.32 The Superpave® Fatigue G*Sin δ parameter for PG58-28 (unmodified) mastics with CCPs and reference fillers at 19°C for: (a) Class C, (b) Class F and (c) SDA**

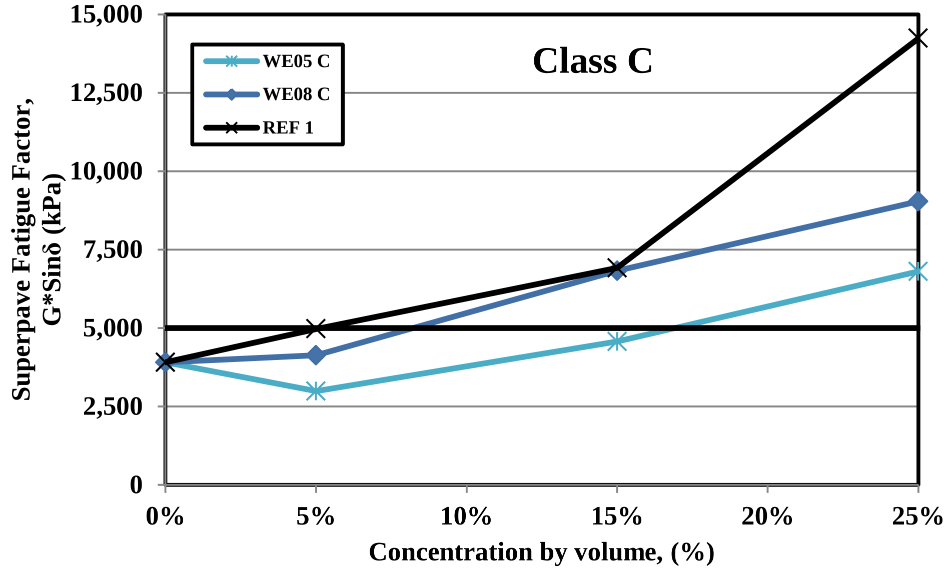
15,000
12,500
10,000
7,500
5,000
2,500
0
Superpave Fatigue Factor, G*Sinδ (kPa)
Class C
WE05 C
WE08 C
REF 1
0%
5%
10%
15%
20%
25%
Concentration by volume, (%)

a)

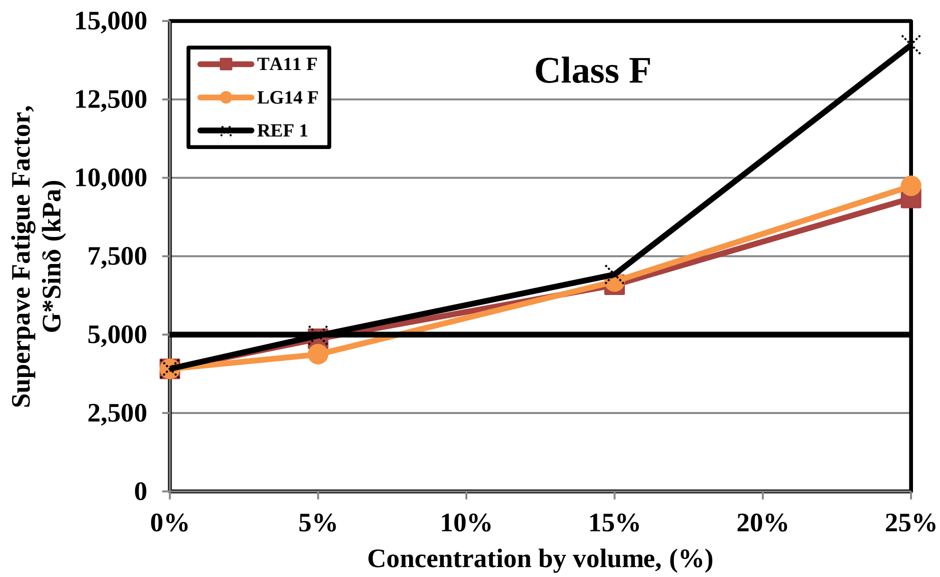
15,000
12,500
10,000
7,500
5,000
2,500
0
Superpave Fatigue Factor, G*Sinδ (kPa)
Class F
TA11 F
LG14 F
REF 1
0%
5%
10%
15%
20%
25%
Concentration by volume, (%)

b)

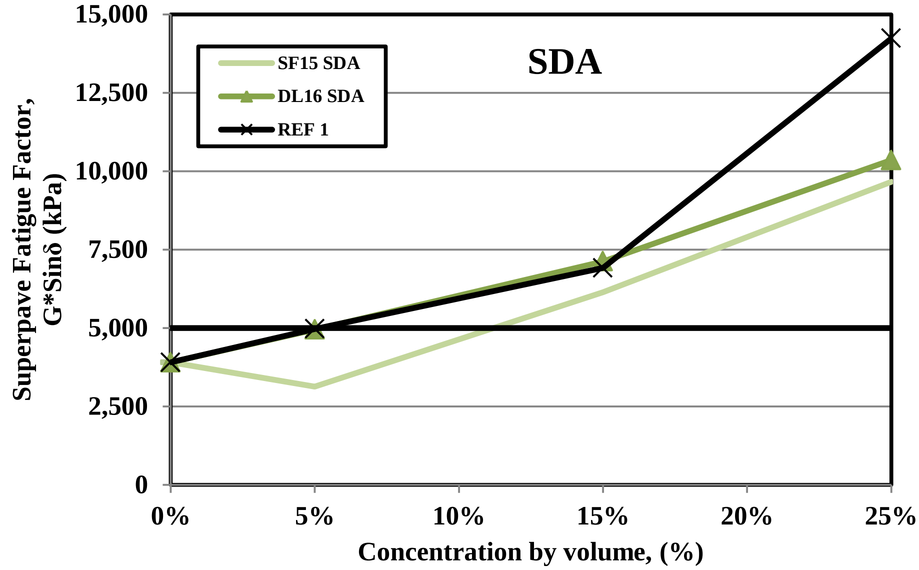


c)

**Figure 4.33 The Superpave® Fatigue G*Sin δ parameter for PG64-28 (unmodified) mastics with CCPs and reference fillers at 22°C for: (a) Class C, (b) Class F and (c) SDA**

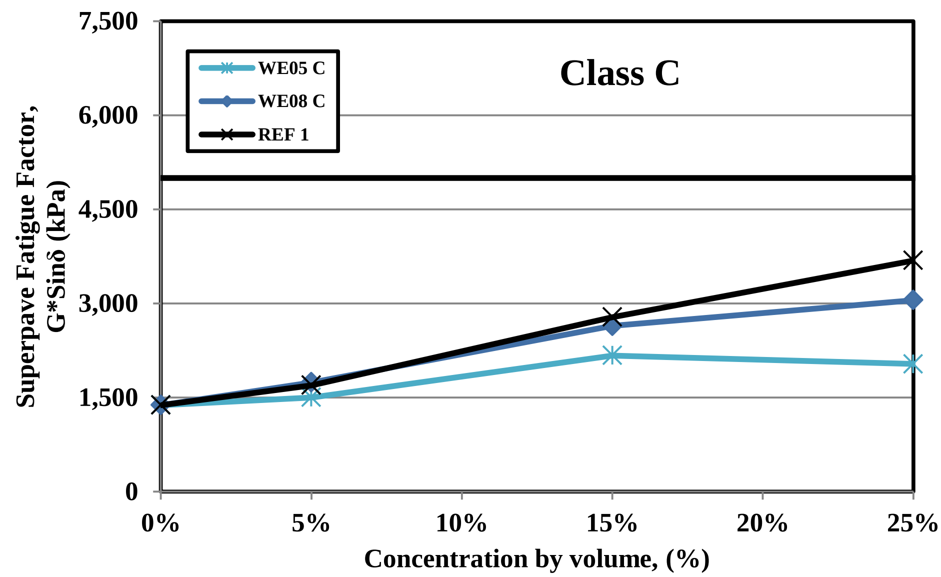


a)

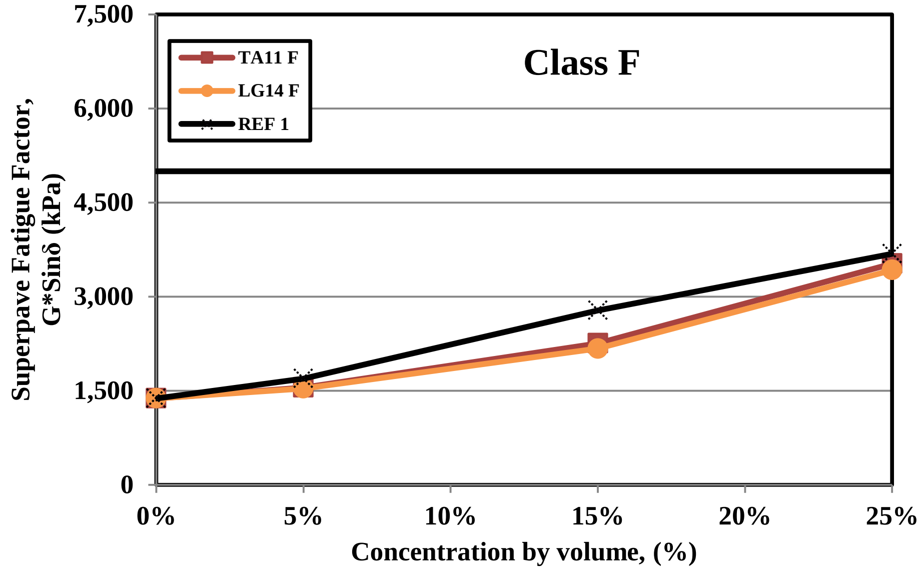


b)

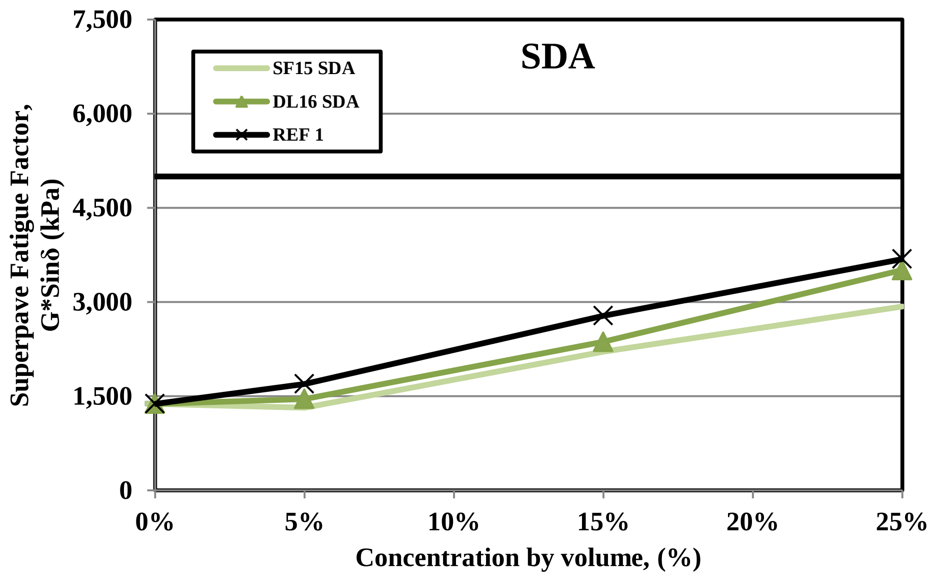


c)

**Figure 4.34 The Superpave® Fatigue G*Sin δ parameter for PG70-28 (modified) mastics with CCPs and reference fillers at 25°C for: (a) Class C, (b) Class F and (c) SDA**

This test does not provide the information on how the fatigue life of the mastics is changed. Therefore, the results obtained are not conclusive. The following section will shed some light of the potential improvement in the fatigue life of the mastics.

### 4.3.4 Aging resistance

In this section the increase in G* due to PAV aging for mastics is compared to the increase of G* of unaged mastics tested at intermediate temperature to calculate the aging index. The goal of this comparison is to verify if some CCPs can reduce the extent of the aging as compared to the reference limestone filler. Lower aging indexes demonstrate a reduction (delay) of the aging.  Figures 4.35 to 4.37 demonstrate the aging index results for PG58-28 (unmodified), PG64-28 (unmodified), and PG70-28 (modified) asphalt binders, respectively.

Figure 4.35 indicates that for PG58-28 unmodified binder with SG15 SDA CCPs the aging index is less than the aging index for the reference filler at all concentration levels. With the exception of WE05 C at 15% concentration all mastics demonstrate lower aging index compare to the reference filler at 15% and 25% concentration,

For PG64-28 unmodified binder, Figure 4.36 indicates that with WE05C and SF15 SDA CCPs the aging index is less than the aging index of the reference fillers at all concentrations levels. With the exception of LG14 C at 25% concentration all mastics demonstrate lower aging index compare to the reference filler at 15% and 25% concentration with PG64-28.

For PG70-28 modified binder, Figure 4.37 indicates that with DL16 SDA CCP the aging index is less than the aging index of the reference fillers at all concentrations levels. For the polymer modified binder, the SDA CCPs appears to retard the effect of the aging significantly and Class C and F fly ash show similar trends in unmodified binder systems. At 15% and 25% concentrations of CCP, all mastics demonstrate lower aging index than the reference filler.

From the aging index results it is evident that the increase in the aging index in mastics with reference filler was proportional to filler concentration indicating that with the increase in concentration, the mastics are more sensitive to aging. In general, the CCPs did not show the same trend. For example, the aging index for SDA and the polymer modified binder blends (Figure 4.35) does not change with the increment in concentration, but rather stays close to the value of the unfilled binder. It can be concluded at this stage that the addition of the CCP causes some retardation in aging compared to the natural fillers. This conclusion must be confirmed through further testing and analysis.

Further testing to identify the significance of aging retardation and failure mechanisms should be conducted since most of the cracking in asphalt pavements is attributed to aging. In addition, filler properties will be evaluated to highlight the influencing factors on the reported observations. As discussed in the literature, the inclusion of any particulate is expected to increase the stiffness with increase in concentration. The observed results raise a very important question for future research; how much of the observed increase in G* is due to aging compared to particulate inclusion.

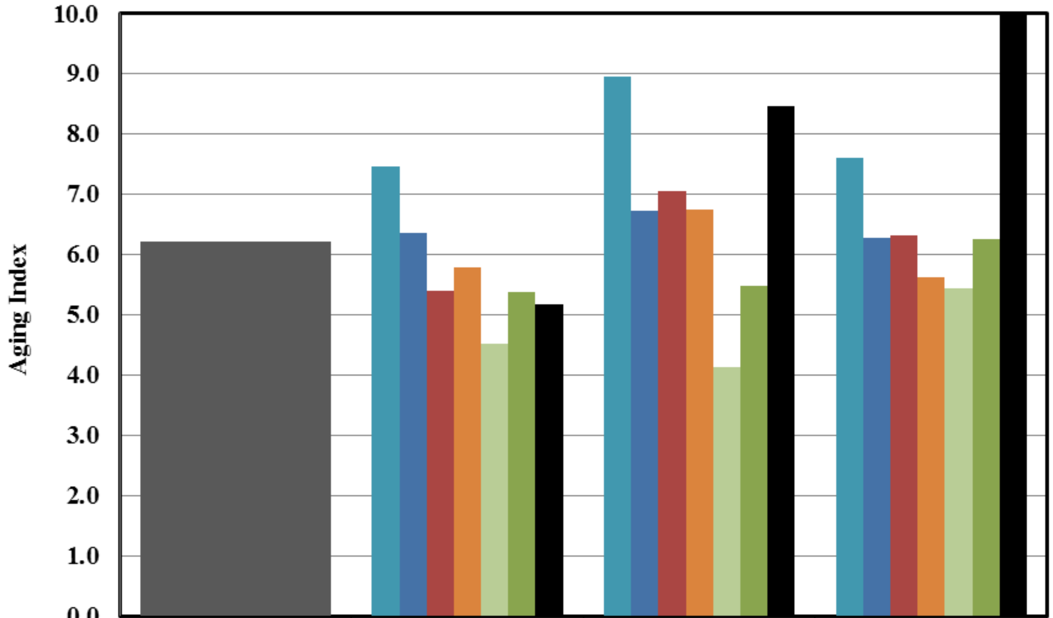


| | 0% | 5% | 15% | 25% |
|---|---|---|---|---|
| WE05 C | 6.23 | 7.46 | 8.96 | 7.61 |
| WE08 C | 6.23 | 6.36 | 6.74 | 6.27 |
| TA11 F | 6.23 | 5.40 | 7.05 | 6.32 |
| LG14 F | 6.23 | 5.78 | 6.75 | 5.62 |
| SF15 SDA | 6.23 | 4.53 | 4.13 | 5.44 |
| DL16 SDA | 6.23 | 5.38 | 5.49 | 6.26 |
| REF 1 | 6.23 | 5.18 | 8.46 | 10.03 |

**Figure 4.35 The Aging Index for PG58-28 (unmodified) based mastics**

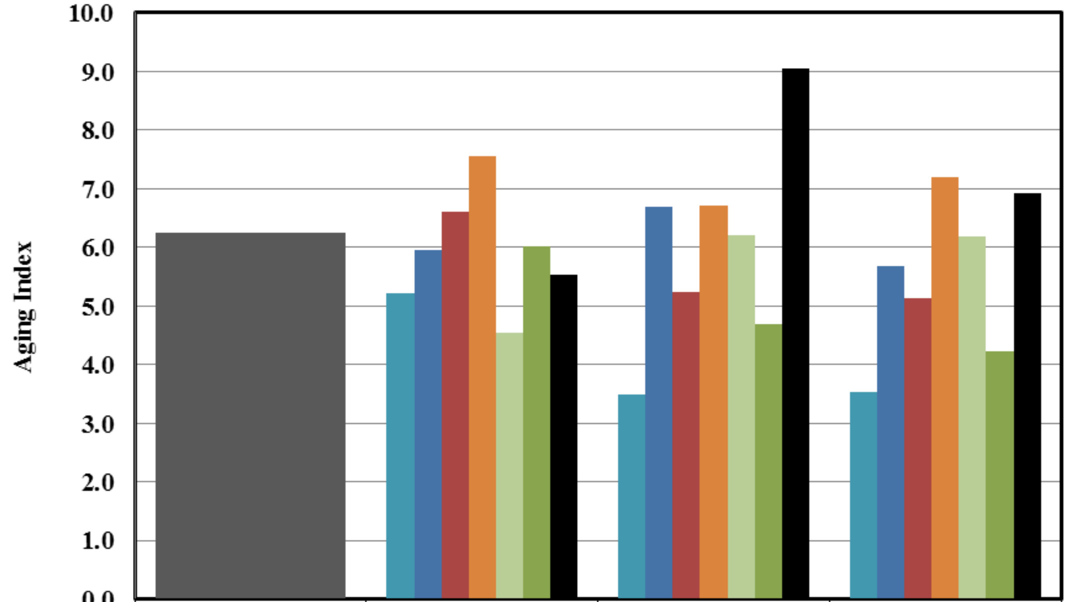


| | 0% | 5% | 15% | 25% |
|---|---|---|---|---|
| WE05 C | 6.26 | 5.22 | 3.50 | 3.54 |
| WE08 C | 6.26 | 5.95 | 6.68 | 5.67 |
| TA11 F | 6.26 | 6.61 | 5.23 | 5.13 |
| LG14 F | 6.26 | 7.55 | 6.71 | 7.20 |
| SF15 SDA | 6.26 | 4.54 | 6.21 | 6.18 |
| DL16 SDA | 6.26 | 6.01 | 4.69 | 4.22 |
| REF 1 | 6.26 | 5.53 | 9.06 | 6.92 |

**Figure 4.36 The Aging Index for PG64-28 (unmodified) based mastics**

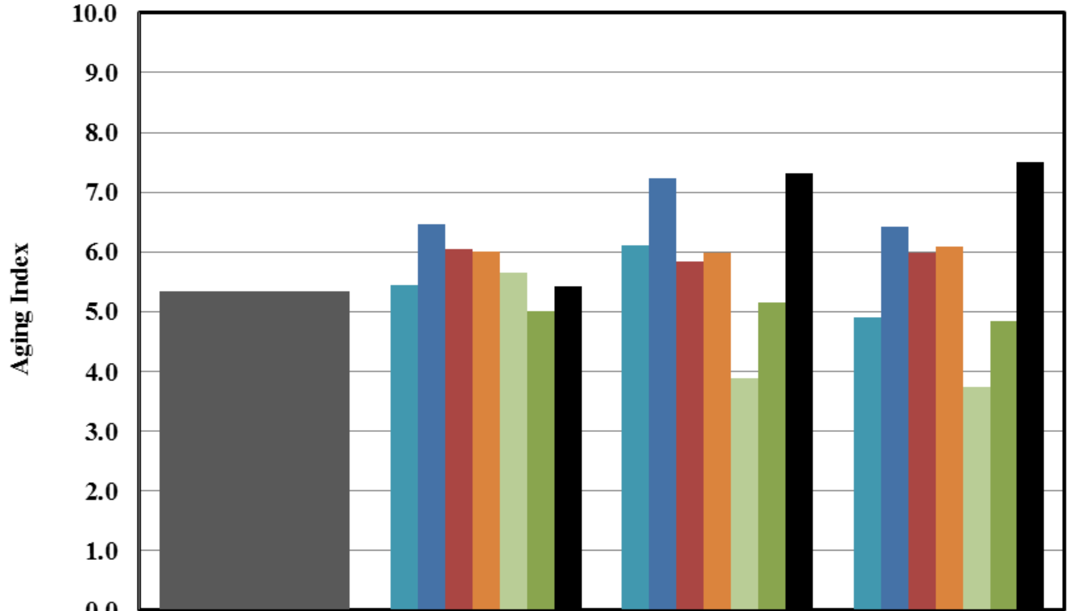


| | 0% | 5% | 15% | 25% |
|---|---|---|---|---|
| WE05 C | 5.33 | 5.45 | 6.10 | 4.90 |
| WE08 C | 5.33 | 6.46 | 7.24 | 6.42 |
| TA11 F | 5.33 | 6.04 | 5.83 | 5.99 |
| LG14 F | 5.33 | 6.01 | 5.98 | 6.08 |
| SF15 SDA | 5.33 | 5.65 | 3.88 | 3.74 |
| DL16 SDA | 5.33 | 5.01 | 5.15 | 4.84 |
| REF 1 | 5.33 | 5.42 | 7.31 | 7.51 |

**Figure 4.37 The Aging Index for PG70-28 (modified) based mastics**

### 4.3.5 The thermal cracking resistance

As the pavement temperature drops, asphalt concrete shrinks and the asphalt binder contracts to a much greater degree than the aggregate in the asphalt mixture. This causes thermal stresses to develop in the pavements. Low temperature cracks develop when the stress exceeds the tensile strength of the asphalt mixture. Low temperature cracking is generally found in older pavements since the asphalt has been exposed to the environment and has become more brittle; therefore, this test is typically performed on PAV long-term aged material.

The Superpave® binder specification use the Bending Beam Rheometer (BBR) to measure the asphalt tendency to develop thermal stresses at a specified temperature by measuring the creep stiffness (St) and the m-value. The creep stiffness (St) is defined as the binders' resistance to load. If the creep stiffness (St) is too high, the asphalt binder behaves in a brittle manner and, therefore, is more prone to cracking at low temperatures. According to Superpave® binder specifications, the creep stiffness (St) of the asphalt binder should be below 300 MPa to prevent thermal cracking. The m-value is an estimation of the rate at which the binder creep stiffness (St) changes with time at low temperatures. According to Superpave® binder specifications, the m-value should be 0.300 or higher. A high m-value is desirable, because the asphalt binder will respond as a material that is less stiff as the temperature decreases and contraction occurs.

The test is conducted at low PG temperature plus 10°C, the time temperature superposition is applied to calculate the response at low PG temperature; this allows for shorter testing times (Ng Puga, 2013). For mastics based on asphalt binders PG58-28, PG64-28 and PG70-28 the test was conducted at -18°C rather than -28 =°C.

#### 4.3.5.1 Creep stiffness, $S_t$

This section presents the low temperature creep stiffness of mastics based on 2 unmodified and one modified binders. The Bending Beam Rheometer tests were conducted to evaluate the effects of CCPs addition on the resistance to thermal cracking at -18°C for asphalt binders. Figures 4.38 to 4.40 demonstrate the creep stiffness for PG 58-28 (unmodified), PG64-28(unmodified) and PG70-28 (modified) binders, respectively.

For binders PG58-28 and PG70-28 with up to 5% of CCP, the stiffness of all mastics are still within the Superpave® limit for binders of 300 MPa. On the other hand, the stiffness of the PG64-28 unfilled binder is right at the limit and, subsequently, mastics with CCPs or fillers exceed the Superpave® binder limit. For the evaluation of the influence of the CCPs, the focus will be on the CCP ability to maintain the thermal relaxation rather than abiding by the Superpave® limits. This is because it is expected that the stiffness of the binders will increase due to the inclusion of particulates. Therefore, the complete evaluation will include the evaluation of the rate of increase of the stiffness combined with the relaxation modulus (m-value).

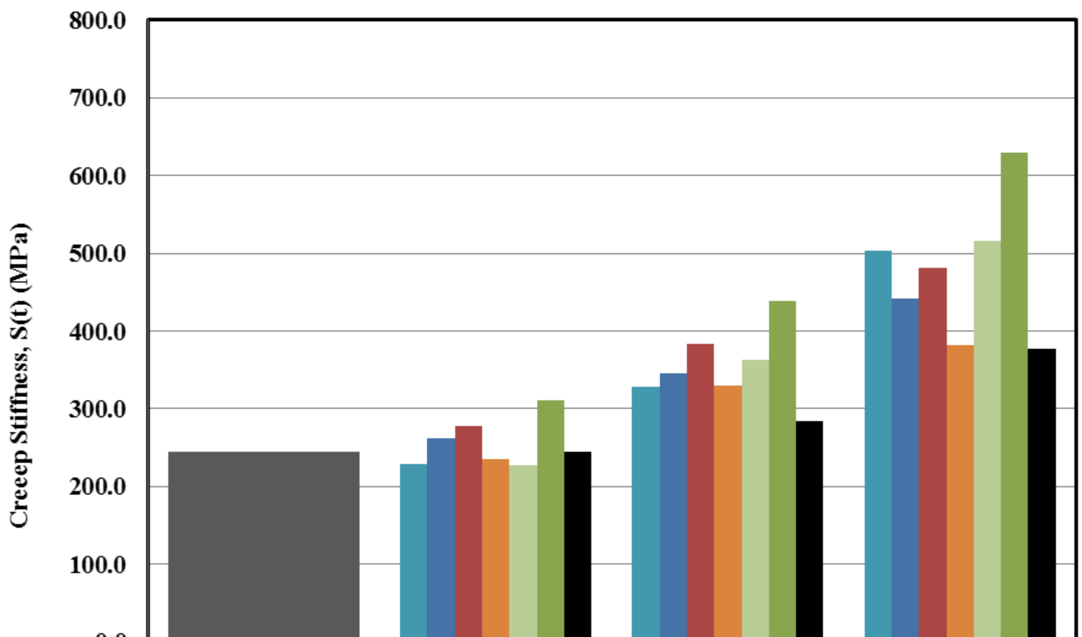


| | 0% | 5% | 15% | 25% |
|---|---|---|---|---|
| WE05 C | 244.00 | 229.00 | 327.50 | 502.50 |
| WE08 C | 244.00 | 262.50 | 345.50 | 441.50 |
| TA11 F | 244.00 | 277.50 | 384.00 | 480.50 |
| LG14 F | 244.00 | 235.00 | 330.00 | 382.50 |
| SF15 SDA | 244.00 | 226.50 | 363.50 | 516.00 |
| DL16 SDA | 244.00 | 310.50 | 439.00 | 630.00 |
| REF 1 | 244.00 | 244.00 | 283.50 | 377.50 |

**Figure 4.38 Creep Stiffness for PG58-28 (unmodified) mastics**

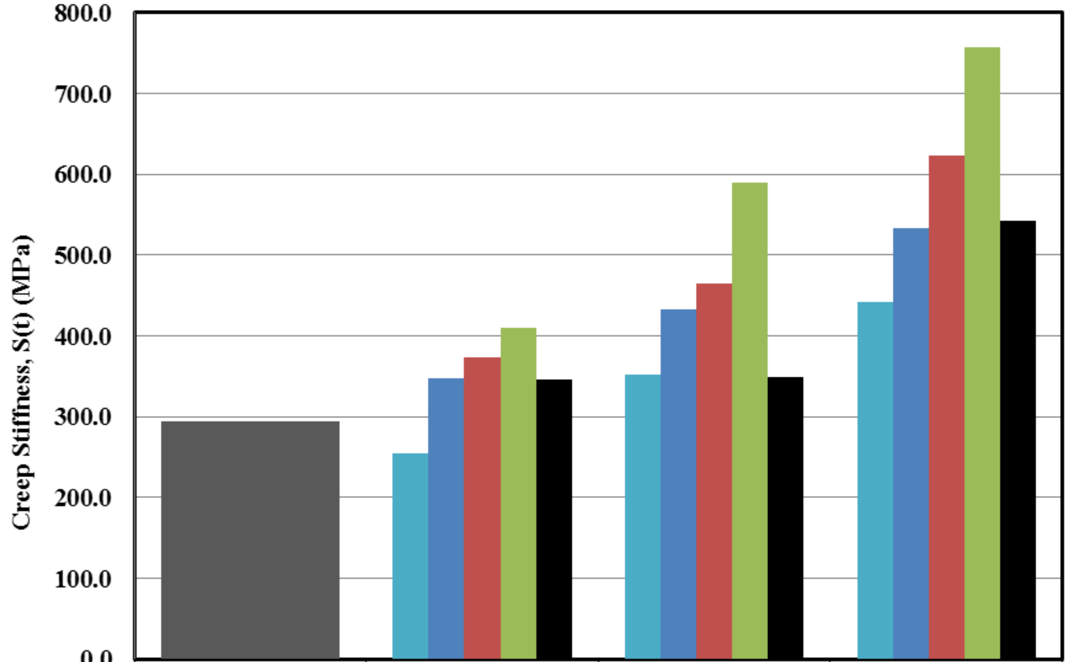


| | 0% | 5% | 15% | 25% |
|---|---|---|---|---|
| WE05 C | 294.50 | 255.50 | 352.00 | 441.50 |
| WE08 C | 294.50 | 348.00 | 433.00 | 534.00 |
| TA11 F | 294.50 | 373.50 | 464.50 | 622.50 |
| DL16 SDA | 294.50 | 410.00 | 589.50 | 757.00 |
| REF 1 | 294.50 | 345.50 | 349.50 | 542.00 |

**Figure 4.39 Creep Stiffness for PG64-28 (unmodified) mastics**

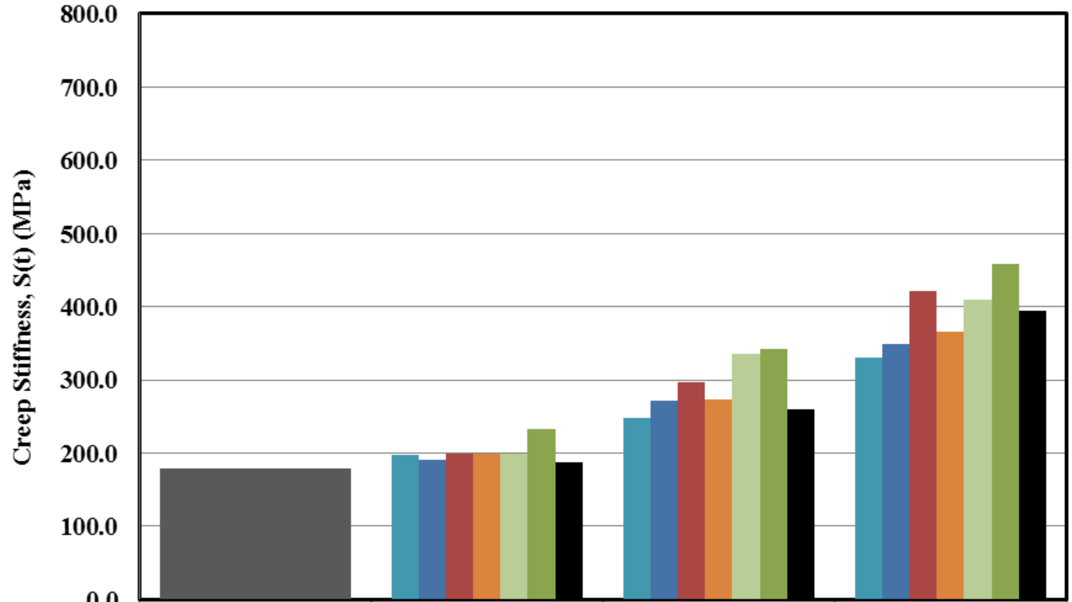


| | 0% | 5% | 15% | 25% |
|---|---|---|---|---|
| WE05 C | 178.50 | 197.00 | 248.50 | 330.50 |
| WE08 C | 178.50 | 190.00 | 271.00 | 349.00 |
| TA11 F | 178.50 | 200.00 | 297.50 | 422.00 |
| LG14 F | 178.50 | 200.00 | 272.50 | 366.50 |
| SF15 SDA | 178.50 | 199.50 | 335.50 | 410.00 |
| DL16 SDA | 178.50 | 233.50 | 343.00 | 458.50 |
| REF 1 | 178.50 | 188.00 | 260.50 | 395.00 |

**Figure 4.40 Creep Stiffness for PG70-28 (modified) mastics**

The previous results demonstrated that the addition of WE05 C is consistently reducing the stiffness of the mastics below that of the plain binder for PG58-28 and PG64-28 for the 5% concentration. Also, for 5% of SF15 SDA mastics, the low temperature stiffness is reduced for the PG58-28 asphalt, while it was able to maintain a relatively low stiffening rate when other binders were tested. For example, the Class F fly ash does not demonstrate significant increase in the stiffness, while the DL16 SDA had an extreme increase in the stiffness.

4.3.5.2 m-value

In this section the m-value for mastics prepared with 2 unmodified and one modified asphalt binders are reported. As stated previously, a higher m-value is desired as this indicates a higher ability to relax the stresses. The Superpave® binder testing protocol limits the m-value to greater than or equal to 0.300 for unfilled binders at low testing temperature. Figures 4.41 to 4.43 demonstrate m-value for PG 58-28 (unmodified), PG64-28(unmodified) and PG70-28 (modified) based mastics, respectively.

Figure 4.41 indicates that the m-value for PG58-28 unmodified binder blends with WE05 C, WE08 C, LG14 F, and SF15 SDA CCPs is higher than that of the reference fillers at all concentrations levels. At 15% concentration WE05 C had a higher m-value than the corresponding mastic based on reference filler. On the other hand, at 25% concentration, WE05 C and TA11 F fly ash had higher m-value than the corresponding mastic based on a reference filler.

For PG64-28 unmodified binder, Figure 4.42 indicates that mastics with WE05 C are higher than the reference filler at all concentrations. Mastics with 5% of WE05 C, WE08 C, and TA11 F CCPs m-value is higher than that reported for reference fillers. At 15% concentration level WE05 C is the only mastics that shows higher m-value than the corresponding reference filler based mastic. On the other hand, at 25% concentration WE05 C, WE08 C and TA11 F fly ash demonstrate higher m-value than the corresponding mastic based on reference filler.

Figure 4.43 presents the m-value results for mastics based on PG70-28 modified binder and CCPs. Mastics with WE05 C, and WE08 C have higher m-values than the reference filler at all concentrations. At 5% levels all CCPs demonstrate a higher m-value than that of the reference filler (at the same concentration). Mastics with 15% of WE08 C had a similar m-value as the obtained for corresponding reference mastics; with the rest of CCPs resulting in lower m-values. On the other hand, mastics with 25% of WE05 C had a higher m-value than mastics based on WE08 C, LG14F, DL16 SDA and reference filler.

These are interesting results, as it was evident that the most of CCPs based mastics had higher creep stiffness than the reference filler mastics; but the m-value results demonstrate that, in some cases, these CCPs based mastics can to relax the stresses better than the reference filler. It is difficult to analyze the effect of the CCPs on the stiffness limits for the Superpave® as these limits are developed for binders only. Furthermore, this test is not designed to characterize the resistance to thermal cracking, but rather to evaluate the stiffness as surrogate to potential prediction for cracking performance.

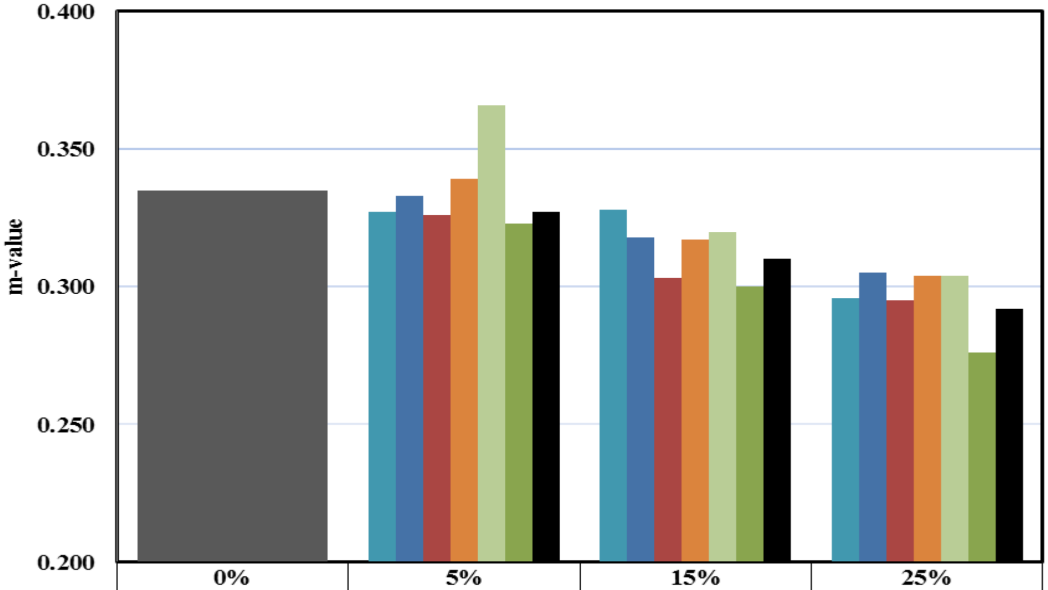


| | 0% | 5% | 15% | 25% |
|---|---|---|---|---|
| WE05 C | 0.335 | 0.327 | 0.328 | 0.296 |
| WE08 C | 0.335 | 0.333 | 0.318 | 0.305 |
| TA11 F | 0.335 | 0.326 | 0.303 | 0.295 |
| LG14 F | 0.335 | 0.339 | 0.317 | 0.304 |
| SF15 SDA | 0.335 | 0.366 | 0.320 | 0.304 |
| DL16 SDA | 0.335 | 0.323 | 0.300 | 0.276 |
| REF 1 | 0.335 | 0.327 | 0.310 | 0.292 |

**Figure 4.41 m-value for PG58-28 (unmodified) mastics with CCPs and reference**

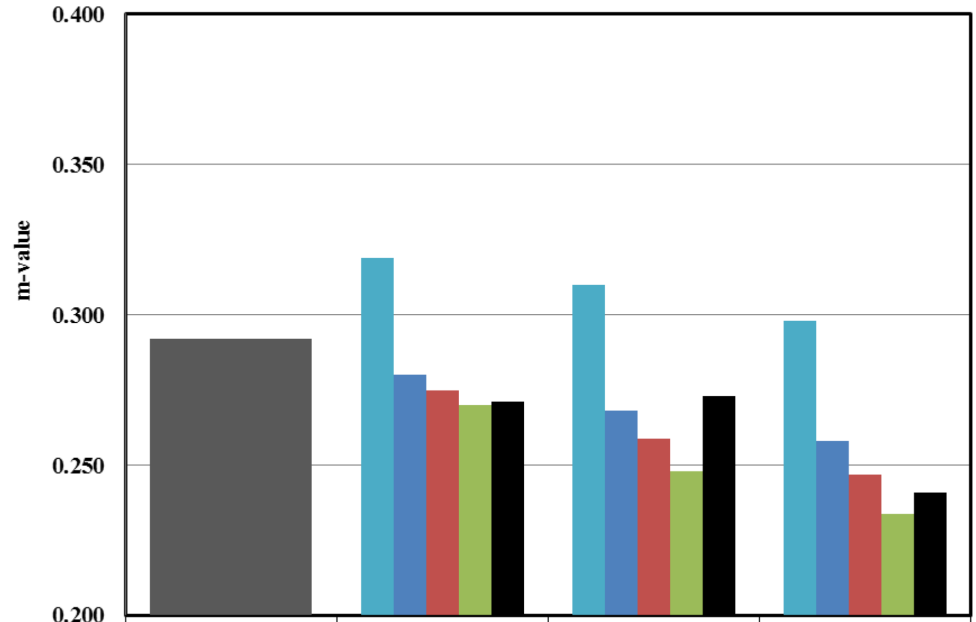


| | 0% | 5% | 15% | 25% |
|---|---|---|---|---|
| WE05 C | 0.292 | 0.319 | 0.310 | 0.298 |
| WE08 C | 0.292 | 0.280 | 0.268 | 0.258 |
| TA11 F | 0.292 | 0.275 | 0.259 | 0.247 |
| DL16 SDA | 0.292 | 0.270 | 0.248 | 0.234 |
| REF 1 | 0.292 | 0.271 | 0.273 | 0.241 |

**Figure 4.42 m-value for PG64-28 (unmodified) mastics with CCPs and reference**

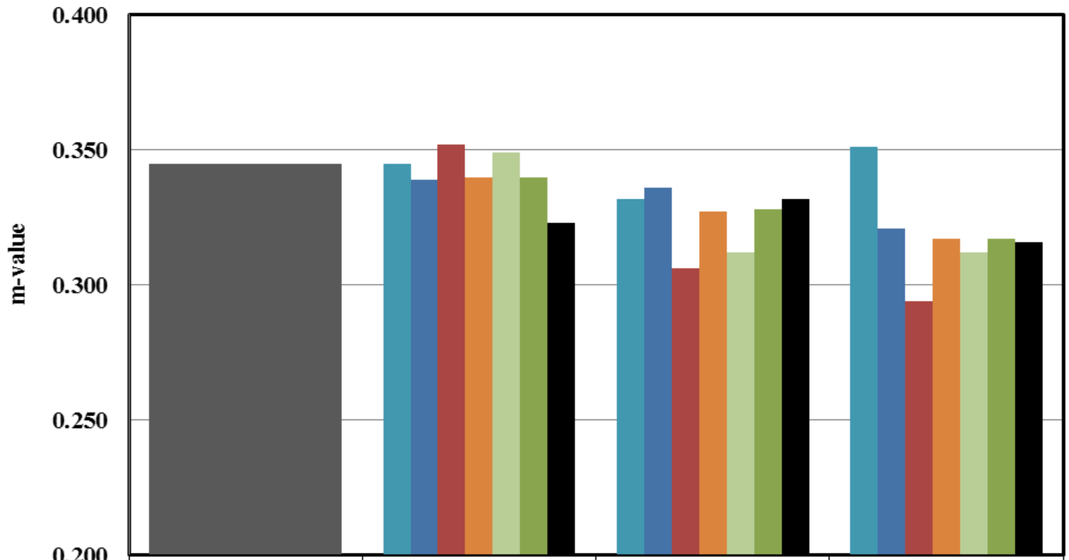


| | 0% | 5% | 15% | 25% |
|---|---|---|---|---|
| WE05 C | 0.345 | 0.345 | 0.332 | 0.351 |
| WE08 C | 0.345 | 0.339 | 0.336 | 0.321 |
| TA11 F | 0.345 | 0.352 | 0.306 | 0.294 |
| LG14 F | 0.345 | 0.340 | 0.327 | 0.317 |
| SF15 SDA | 0.345 | 0.349 | 0.312 | 0.312 |
| DL16 SDA | 0.345 | 0.340 | 0.328 | 0.317 |
| REF 1 | 0.345 | 0.323 | 0.332 | 0.316 |

**Figure 4.43 m-value for PG70-28 (modified) mastics with CCPs and reference**

For thermal relaxation, Class C and Class F materials are able to maintain an acceptable level of relaxation (above the Superpave® limit of 0.300) for all binders and at most concentrations. Class C fly ash, and, especially, WE05 improve the relaxation modulus of the binders at 5% dosage and maintain the same level of relaxation at higher concentrations. However, for the PG64-28 binder, the plain unfilled binder itself did not meet the limits indicating that it was mis-graded by the supplier as PG64-28 when the test results show that it is actually PG64-22. Yet, with the help of Class C WE05 fly ash, the binder low temperature limit was extended from -22°C to -28°C.

## 4.4 SUMMARY OF RESULTS

Based on the results presented above, the following table is compiled to examine the influence of the CCPs on all the performance indicators tested. The arrows in the table represent the effect of the CCP on the binder performance indicators. As such, an arrow pointing upwards indicate favorable influence, downwards indicate unfavorable influence, and horizontal indicate no change.

**Table 4.11 Summary of performance related results**

| CCP | Workability | Rutting Resistance | Recovery | Aging Resistance | Low Temp Resistance |
|---|---|---|---|---|---|
| **WE05 C** | ↑ | ↔ | ↔ | ↔ | ↑ |
| **WE08 C** | ↑ | ↔ | ↔ | ↔ | ↔ |
| **TA11 F** | ↔ | ↑ | ↑ | ↑ | ↔ |
| **LG14 F** | ↔ | ↑ | ↑ | ↑ | ↔ |
| **KC01 SDA** | ↔ | ↑ | ↓ | NT | NT |
| **WP03 SDA** | ↔ | ↑ | ↓ | NT | NT |
| **SF15 SDA** | ↑ | * | * | ↑ | ↑ |
| **DL16 SDA** | ↓ | * | * | ↑ | ↓ |

*depends on dosage and type of binder
NT: not tested yet

Table 4.11 shows that Class F is the most beneficial CCP material improving the rutting, elastic recovery, and aging. At the same time it maintains the performance of the binder for workability and low temperature resistance without detrimental effects. Class C fly ash demonstrates improved workability, and low temperature resistance (WE05) without causing any determinate effects on the other performance indicators. Due to extreme variability (SF15 vs. DL16), the SDA CCPs have different responses and it is difficult to predict the contribution to the performance as these materials are sensitive to the type of binder and dosage. Further investigation is needed to understand the potential synergy between this category of CCPs and polymer modified binders.

# CHAPTER 5.

# MODELING CCP EFFECT ON ASPHALT MASTICS

Various studies have demonstrated that properties of mineral fillers have a significant effect on the performance of asphalt mixtures. Physico-chemical properties of CCPs materials vary; therefore, the influence of these materials on the properties of HMA mixtures also varies (Kandhal, 1981). It is important to characterize CCPs so that the resulting materials performance parameters, such as rutting, are not compromised.

Rutting is defined as a creep failure, which implies that it is time dependent. Therefore, the modulus is equivalent to the deviator stress over the total strain. For visco-elastic materials the reciprocal of the modulus, known as compliance, is used because it allows for the separation of different strain components at constant stress levels. This research evaluated rutting behavior of the asphalt mastics by measuring the non-recoverable compliance (Jnr) using the Multiple Stress Creep and Recovery (MSCR) test other. Research demonstrated that Jnr is highly correlated with pavement rutting (D'Angelo, 2009). As the asphalt binder becomes stiffer, the Jnr decreases indicating the increase in rutting resistance.

This chapter covers the regression analysis used to find the correlations between physical and chemical properties of CCPs and mastic behavior. As a first step, the correlation between physical properties and chemical characteristics was established and stiffening rate ($S_R$) based on the research results of mastics produced at 5 volume concentrations and 3 different asphalt binders. Based on multi-scale approach, the mastic properties are considered as a bridge indicator between the filler or CCP properties and asphalt mixture performance.

As a second step, the most important CCPs properties identified, the multiple linear regressions analyzes (MLRA) were conducted to develop the models that relate the mastics rutting, as measured by the Jnr, to reference unfilled binder and CCP properties. Two models were developed: one for unmodified binders and a second for modified binders. The models were developed based on mastics results at 5%, 15% and 25% CCP concentration levels. The models for the mastic Jnr were developed considering the PG grade temperature.

## 5.1 THE EFFECT OF CCP PROPERTIES ON STIFFENING RATE

The stiffening rate ($S_R$) is defined as the slope of relative complex modulus with respect to concentration (Eq. 5.1). This is an indication of the effect of CCPs on increasing the relative stiffening modulus:

$$S_R = \frac{(\text{Relative } G^* - 1)}{Concentration} \qquad 5.1$$

where:

- Relative G*,the ratio of mastic G* to binder G*,
- Concentration, volume of CCP as related to the asphalt binder

The $S_R$ rate can be utilized to quantify the CCPs and binder interaction and as a numerical parameter in the analysis of the test results. The correlations between the CCP's physical and chemical properties and mastics stiffening were developed using linear regression analysis. Based on develop models the desirable levels of interaction can be identify and used for the design and performance assessment of ASHphalt. The results of stiffening rate of mastics are reported in Tables 5.1 to 5.3.

**Table 5.1 The stiffening rate of CCP of PG58-28 (unmodified) mastics at 58°C**

| Materials ID | Class | Stiffening Rate ($S_r$) | | | | |
|---|---|---|---|---|---|---|
| | | 5% | 10% | 15% | 25% | 40% |
| WE05 | C | 3.19 | 3.97 | 3.71 | 4.97 | 5.22 |
| WE08 | C | 3.18 | 3.71 | 3.94 | 5.52 | 5.30 |
| TA11 | F | 4.27 | 4.66 | 4.19 | 6.65 | 7.10 |
| LG14 | F | 6.13 | 3.51 | 4.15 | 5.51 | 6.35 |
| KC01 | SDA | 3.23 | 4.95 | 5.03 | 7.49 | 7.83 |
| WP03 | SDA | 4.00 | 4.72 | 5.45 | 10.73 | 10.14 |
| SF15 | SDA | 4.48 | 3.27 | 5.66 | 8.82 | 10.80 |
| DL16 | SDA | 6.34 | 6.65 | 7.71 | 10.63 | 10.87 |
| REF 1 | Limestone | 4.46 | 3.34 | 4.31 | 5.73 | 6.99 |

**Table 5.2 The stiffening rate of CCP of PG64-28 (unmodified) mastics at 64°C**

| Materials ID | Class | Stiffening Rate ($S_r$) | | | | |
|---|---|---|---|---|---|---|
| | | 5% | 10% | 15% | 25% | 40% |
| WE05 | C | 6.88 | 6.18 | 4.76 | 5.92 | 5.83 |
| WE08 | C | 6.59 | 4.82 | 4.85 | 7.02 | 6.77 |
| TA11 | F | 3.59 | 3.78 | 3.58 | 8.91 | 6.70 |
| LG14 | F | 3.55 | 4.73 | 4.01 | 7.73 | 7.12 |
| KC01 | SDA | 6.36 | 5.77 | 6.67 | 9.70 | 9.78 |
| WP03 | SDA | 4.75 | 6.72 | 6.95 | 9.55 | 8.90 |
| SF15 | SDA | 3.70 | 5.60 | 4.83 | 10.59 | 8.22 |
| DL16 | SDA | 7.40 | 5.59 | 9.24 | 13.08 | 12.64 |
| REF 1 | Limestone | 2.10 | 5.30 | 4.94 | 8.16 | 7.09 |

**Table 5.3 The stiffening rate of CCP of PG70-28 (modified) mastics at 70°C**

| Materials ID | Class | Stiffening Rate ($S_r$) | | | | |
|---|---|---|---|---|---|---|
| | | 5% | 10% | 15% | 25% | 40% |
| WE05 | C | 0.26 | 0.84 | 1.19 | 2.42 | 3.12 |
| WE08 | C | 1.76 | 1.85 | 2.24 | 3.18 | 3.32 |
| TA11 | F | 3.06 | 3.79 | 3.48 | 5.17 | 5.24 |
| LG14 | F | 5.86 | 4.57 | 4.53 | 5.62 | 5.80 |
| KC01 | SDA | 1.62 | 2.54 | 2.28 | 4.84 | 5.57 |
| WP03 | SDA | -0.71 | 1.23 | 2.72 | 4.54 | 6.76 |
| SF15 | SDA | -0.76 | -0.05 | 2.36 | 3.20 | 5.38 |
| DL16 | SDA | -2.63 | 1.57 | 3.83 | 6.56 | 13.59 |
| REF 1 | Limestone | 3.42 | 2.42 | 3.91 | 3.56 | 4.58 |

Table 5.4 presents the correlation matrix between the characteristics of CCP and stiffening rate of mastics. The correlation was establish using the Pearson's method and the statistical significance, p is reported in the table. The strength and direction of the association was measured by the Pearson (r) coefficient which varies from -1 to 1. The properties of CCPs and stiffening rate of mastics were linearly associated. The significance of correlation is measured by the p value, and for 90% significance (or confidence) level selected for this study the p value must be lower than 0.1. In other words, when the p value is less than 0.1 (for 90% confidence level), the correlation is statistically significant. This level is selected given the nature of the materials used. In the Table 5.4, the bold numbers represent the correlations which are statistically significant.

Good correlations were obtained between the CCPs characteristics and stiffening rate for mastics with 15% CCP based on plain unmodified asphalt binders. However, very few CCPs parameters correlate significantly ($p < 0.1$) with the stiffening rate up to 10% volume addition of CCP. This indicates that at low concentrations the characteristics of CCPs have no significant effect on the stiffening rate. Based on the analysis of mastics based on unmodified asphalt binders PG58-28 and PG64-28 with 15% CCP, the Rigden voids (RV) strongly correlate with the stiffening rate. For example, the $S_R$ relationship of CCP mastics based on binder PG58-28 had the parameter of $r = 0.89$ and $p<0.0001$ and the PG64-28 based mastics were characterized by $r = 0.84$ and $p<0.0001$. It is evident that the stiffening rate increases with the increase of the Rigden voids parameter. Following the Rigden voids, $Al_2O_3$, CaO, $SiO_2$, $SO_3$, SAF ($SiO_2$+ $Al_2O_3$+ $Fe_2O_3$), LOI (Loss on Ignition), and $D_{10}$ parameters have significant contribution on the stiffening rate as it is evident from the (r) correlation and p values listed in Table 5.4. An increase in

$Al_2O_3$, $SiO_2$, SAF and $D_{10}$ leads to a decrease of the stiffening rate of mastics based on unmodified binders, which is an indication of plasticizing (softening effect). On the other hand, higher RV, CaO, $SO_3$ and LOI values result in an increase in the stiffening rate which results in stiffer mastics. Overall, the amount of CaO and the Rigden Voids are the most influential factors.

Looking into the correlations for the PG70-28 modified asphalt binder it can be concluded that there are statistically significant correlation between CCP parameters and $S_R$. For example, the $S_{R5\%}$ vs. CaO correlation coefficient is is -0.895 (indicating a negative relationship (i.e., as the CaO increases, the $S_R$ decrease). For mastics based on PG70-28 binder the Rigden voids parameter did not have any correlation at up to 15% CCP concentration. For 25% and 40% concentrations the parameters related to chemical composition ($Al_2O_3$, $Fe_2O_3$, $SiO_2$ and $SO_3$) and physical properties (Rigden voids) provided the highest correlation values.

**Table 5.4 The correlation matrix between the properties of CCP and stiffening rate of mastics**

| | PG58-28 | | | | | PG64-28 | | | | | PG70-28 | | | | |
|---|---|---|---|---|---|---|---|---|---|---|---|---|---|---|---|
| | $SR_{5\%}$ | $SR_{10\%}$ | $SR_{15\%}$ | $SR_{25\%}$ | $SR_{40\%}$ | $SR_{5\%}$ | $SR_{10\%}$ | $SR_{15\%}$ | $SR_{25\%}$ | $SR_{40\%}$ | $SR_{5\%}$ | $SR_{10\%}$ | $SR_{15\%}$ | $SR_{25\%}$ | $SR_{40\%}$ |
| **$Al_2O_3$** | -0.331 | **-0.809** | **-0.936** | **-0.819** | **-0.768** | -0.505 | -0.497 | **-0.954** | **-0.855** | **-0.951** | **0.794** | 0.427 | -0.062 | -0.448 | **-0.837** |
| | 0.453 | **0.015** | **0.001** | **0.013** | **0.026** | 0.202 | 0.210 | **0.0002** | **0.007** | **0.0003** | **0.019** | 0.292 | 0.883 | 0.266 | **0.010** |
| **CaO** | 0.026 | **0.733** | **0.804** | **0.695** | 0.616 | **0.692** | 0.547 | **0.905** | **0.689** | **0.815** | **-0.895** | -0.612 | -0.239 | 0.170 | **0.652** |
| | 0.950 | **0.038** | **0.016** | **0.056** | 0.104 | **0.057** | 0.160 | **0.002** | **0.059** | **0.014** | **0.003** | 0.107 | 0.569 | 0.688 | **0.079** |
| **$Fe_2O_3$** | 0.333 | -0.496 | -0.547 | -0.544 | -0.456 | **-0.652** | -0.502 | **-0.664** | -0.448 | -0.511 | **0.911** | **0.778** | 0.545 | 0.197 | -0.320 |
| | 0.421 | 0.211 | 0.160 | 0.164 | 0.256 | **0.080** | 0.205 | **0.073** | 0.266 | 0.195 | **0.002** | **0.023** | 0.162 | 0.641 | 0.440 |
| **$SiO_2$** | -0.139 | **-0.722** | **-0.870** | **-0.766** | **-0.708** | -0.605 | -0.583 | **-0.937** | **-0.762** | **-0.882** | **0.865** | 0.578 | 0.135 | -0.254 | **-0.752** |
| | 0.743 | **0.043** | **0.005** | **0.027** | **0.050** | 0.112 | 0.129 | **0.001** | **0.028** | **0.004** | **0.006** | 0.133 | 0.750 | 0.544 | **0.046** |
| **$SO_3$** | 0.381 | **0.783** | **0.959** | **0.866** | **0.826** | 0.396 | 0.462 | **0.939** | **0.904** | **0.976** | **-0.738** | -0.366 | 0.164 | 0.518 | **0.861** |
| | 0.352 | **0.022** | **0.0002** | **0.006** | **0.012** | 0.332 | 0.249 | **0.001** | **0.002** | **<0.0001** | **0.037** | 0.373 | 0.697 | 0.188 | **0.006** |
| **SAF** | -0.101 | **-0.732** | **-0.860** | **-0.768** | **-0.704** | -0.609 | -0.565 | **-0.925** | **-0.757** | **-0.864** | **0.888** | 0.596 | 0.164 | -0.232 | **-0.701** |
| | 0.811 | **0.039** | **0.006** | **0.026** | **0.051** | 0.109 | 0.145 | **0.001** | **0.030** | **0.006** | **0.003** | 0.119 | 0.698 | 0.581 | **0.053** |
| **LOI** | **0.697** | **0.794** | **0.927** | **0.680** | **0.708** | 0.250 | 0.058 | **0.765** | **0.917** | **0.922** | -0.487 | -0.045 | 0.501 | **0.746** | **0.958** |
| | **0.055** | **0.019** | **0.001** | **0.063** | **0.049** | 0.550 | 0.892 | **0.027** | **0.001** | **0.001** | 0.221 | 0.916 | 0.206 | **0.034** | **0.0002** |
| **Rigden Voids, %** | 0.504 | **0.896** | **0.941** | **0.813** | **0.732** | 0.402 | 0.282 | **0.931** | **0.893** | **0.981** | -0.620 | -0.146 | 0.356 | **0.699** | **0.947** |
| | 0.203 | **0.003** | **0.001** | **0.014** | **0.039** | 0.324 | 0.498 | **0.001** | **0.003** | **<0.0001** | 0.101 | 0.729 | 0.387 | **0.054** | **0.0004** |
| **$D_{10}$, µm** | 0.585 | -0.427 | -0.269 | -0.348 | -0.174 | -0.592 | -0.592 | -0.576 | -0.147 | -0.320 | **0.745** | **0.661** | **0.697** | 0.309 | -0.087 |
| | 0.128 | 0.291 | 0.520 | 0.398 | 0.681 | 0.123 | 0.123 | 0.135 | 0.728 | 0.439 | **0.034** | **0.074** | **0.055** | 0.457 | 0.837 |

Note: Top values are Pearson correlations coefficients R and bottom values are significance levels P in each cell. Bold numbers indicates strong correlation among chemical and physical properties and stiffening rate as evident by high R values and p-values $\leq 0.1$ for a 90% confidence level

In general, the correlation results (Table 5.4) confirm the reported postulations made earlier. At low concentrations, all CCPs act as physical inclusions causing an overall increase in stiffness irrespective of the CCP physical or chemical properties. As CCP concentration increases, the influence of the individual properties becomes significant. This proves that the interaction between the binder and CCP starts to appear as a significant factor contributing to the mastic performance. The research results and statistical evaluation prove that at 15% concentration (by volume), the chemical and physical properties of CCP start to control the interaction as measured by the stiffening rate. Accordingly, $Al_2O_3$, CaO, $SiO_2$, $SO_3$, LOI, and Rigden Voids are the CCP properties that can be used for further analysis to determine the optimal CCP make up required for the best HMA performance.

## 5.2 MULTIPLE LINEAR REGRESSION ANALISYS

The predictor variables for the regression analysis were based on the correlation analysis conducted for the association between the characteristics of CCP and the stiffening rate (Table 5.4). The primary properties of CCPs that affected the behavior of the mastics were $Al_2O_3$, CaO, $SiO_2$, $SO_3$, LOI, and Rigden Voids. Therefore, the same variables were considered for modeling the Jnr of mastic. Multiple regression analysis was conducted separately for mastics based on unmodified and modified asphalt.

The CCP properties, concentration (CONC) and asphalt binder non-recoverable compliance (ACJnr) were used as experimental variables and mastic Jnr was the response variable. Moreover, the Jnr asphalt cements (ACJnr) and CCP concentrations (CONC) were selected as the primary experimental variables and the physical and chemical CCPs properties were selected as secondary experimental variables. The two primary experimental variables were used as a part of the regression equations with the purpose of developing multiple regression models that can predict the Jnr of mastic different concentrations based on the properties of unfilled asphalt binder and the properties of CCPs. The concentration was defined as a categorical independent variable because this variable can take some positive values from 0.05 to 0.40. In regression analysis these variables are known as indicator variables and for a variable with *n* categories there are *n-1* indicator variables. For example, in this study CCPs were added at 3 concentrations levels this means there are 2 indicator variables.

The Rigden voids (RV), also known as a void content in fine powder materials compacted to a maximum density, was selected as the main physical parameter because it characteristic of compacted powders. This parameter is also a relatively inexpensive test and it is and integral characteristic governed by other basic filler properties: particle shape, particle size, particle size distribution, and surface area. Loss of ignition was not considered as a parameter. On the other hand, significant evidence was collected on the potential effects of calcium compounds; therefore, CaO was considered as a parameter.

In order to confirm the independence a correlation analysis of the variables was conducted among the predictor variables. Table 5.5 presents the correlation matrix between the selected properties and correlation factors based on the stiffening rate analysis.

**Table 5.5 Correlation matrix for CCPs parameters and Jnr**

| | ACJnr | CONC | Rigden Voids, % | $Al_2O_3$ | CaO | $SiO_2$ | $SO_3$ | SAF | LOI |
|---|---|---|---|---|---|---|---|---|---|
| **ACJnr** | 1.000 | -0.044<br>0.473 | -0.027<br>0.659 | 0.047<br>0.423 | -0.058<br>0.335 | 0.058<br>0.341 | -0.044<br>0.470 | 0.058<br>0.339 | -0.011<br>0.850 |
| **CONC** | | 1.000 | -0.006<br>0.925 | -0.001<br>0.992 | 0.009<br>0.882 | -0.006<br>0.915 | -0.001<br>0.9848 | -0.007<br>0.9049 | -0.012<br>0.837 |
| **Rigden Voids, %** | | | 1.000 | **-0.942<br><.0001** | **0.813<br><.0001** | **-0.861<br><.0001** | **0.957<br><.0001** | **-0.852<br><.0001** | **0.924<br><.0001** |
| **$Al_2O_3$** | | | | 1.000 | **-0.937<br><.0001** | **0.975<br><.0001** | **-0.989<br><.0001** | **0.967<br><.0001** | **-0.850<br><.0001** |
| **CaO** | | | | | 1.000 | **-0.983<br><.0001** | **0.889<br><.0001** | **-0.992<br><.0001** | **0.672<br><.0001** |
| **$SiO_2$** | | | | | | 1.000 | **-0.947<br><.0001** | **0.997<br><.0001** | **-0.736<br><.0001** |
| **$SO_3$** | | | | | | | 1.000 | **-0.935<br><.0001** | **0.872<br><.0001** |
| **SAF** | | | | | | | | 1.000 | **-0.719<br><.0001** |
| **LOI** | | | | | | | | | 1.000 |

Note: In each cell top values are Pearson correlations coefficients R and bottom values are significance levels P. Bold numbers indicate strong correlation as evident by high r values and significance with p-values ≤ 0.1 for a 90% confidence level

The correlations analysis proves that all selected parameters of CCP based on the stiffening rate analysis are highly correlated thus leading to multicollinearity among the predictor variables used to build the multiple regression models of unmodified and modified asphalt mastics with CCP.

In order to identify and reduce the collinear variables, the variance inflation factor (VIF) was calculated to quantify the degree of multicollinearity. A rule of thumb dictates that any VIF greater than 10 represents high multicollinearity. In this study, the strategy to identify the collinear variables was to calculate VIF for a regression model that included 8 variables (Full Model) and to select the 4 variables with the lowest VIF (i.e., ACJNR, RV, CaO, and $AL_2O_3$; Table 5.6). It is important to mention that VIF values were calculated based on the entire dataset (n=209 observations) including duplicates.

Variance inflation factors for unmodified (n=113 observations) and modified (n=96 observations) asphalt datasets are described in detail by Tables 5.7 and 5.8.

**Table 5.6. Variance inflation factor calculated for experimental variables included in Full Model (8 variables) and Reduced Models (2 or 3 variables)[1]**

| Variable | Full Model | Reduced Models | | | |
|---|---|---|---|---|---|
| | | 2 variables | | | 3 variables |
| ACJNR | 1.0074 | 1.0011 | 1.0025 | 1.0024 | 1.0029 |
| LOI | 12.0544 | | | | |
| RV | 128.6770 | 1.0009 | | | 2.9652 |
| $AL_2O_3$ | 296.9593 | | | 1.0023 | |
| SIO | 325.8679 | | | | |
| SO3 | 1305.9607 | | | | |
| CaO | 2326.5416 | | 1.0022 | | 2.9689 |
| SAF | 3511.4939 | | | | |

[1] Variance Inflation Factor values were calculated based on the entire dataset (n=209)

As demonstrated by Table 5.6, VIF was calculated for multiple regression analysis using the combination of 2 or 3 variables (Reduced Models) which showed that the VIF was reduced to values close or lower than 10. In order to compare and select the best Model that predicted the mastic Jnr, the Goodness of Fit for the reduced models was analyzed based on $R^2$, adjusted $R^2$, Mallows Cp and Root Mean Square Error (RMSE) as reported in Tables 5.7 and 5.8. The RMSE measures the difference between the predicted and estimated values based on the regression analysis; therefore, lower difference implies a better fit. Mallows Cp was used to calculate the effect of the predictors of a regression model in order to avoid overfitting in which the residual sum of squares gets smaller as more variables are added to a model. Lesser Mallows Cp values are always preferred.

**Table 5.7 Best parameters for subsets of regression fir Jnr of mastics based on unmodified asphalts**

| Vars | $R^2$ | $R^2$adj | Mallows Cp | Root MSE | ACJnr | CONC | RV | CaO | $Al_2O_3$ |
|---|---|---|---|---|---|---|---|---|---|
| 3 | 0.890 | 0.886 | 5 | 0.187 | x | x | x | | |
| 3 | 0.853 | 0.848 | 5 | 0.216 | x | x | | x | |
| 3 | 0.872 | 0.867 | 5 | 0.202 | x | x | | | x |
| 4 | 0.913 | 0.909 | 6 | 0.168 | x | x | x | x | |
| 4 | 0.903 | 0.899 | 6 | 0.176 | x | x | x | | x |
| 4 | 0.907 | 0.903 | 6 | 0.173 | x | x | | x | x |
| 5 | 0.914 | 0.909 | 7 | 0.167 | x | x | x | x | x |

The best model that predicted unmodified mastic Jnr included following variables: AC Jnr, RV and CONC (Table 5.7). The $R^2$ for the model using these parameters is 0.886. The regression equation is represented by Eq. 5.2. The Rigden voids predictor coefficient of -0.014 suggests that if all other variables are held fixed each unit of increase in RV decreases unmodified mastic Jnr by -0.014. This clearly is in line with the literature and experimental findings that an increase in Rigden voids increase the rutting resistance (as higher resistance to rutting is given by lower value of Jnr).

<u>Regression Equation for Unmodified Mastics</u>

$$\text{Mastic Jnr} = 0.197 + 0.414\ \text{ACJnr} + 1.263\ \text{CONC}_{0.05} + 0.572\ \text{CONC}_{0.15} - 0.014\ \text{RV} \qquad \text{Eq.5.2}$$

| Predictor | Estimate | Standard Error | P | VIF |
|---|---|---|---|---|
| Constant | 0.197 | 0.253 | <0.0001 | 0.000 |
| ACJnr | 0.414 | 0.097 | <0.0001 | 1.005 |
| $\text{CONC}_{0.5}$ | 1.263 | 0.044 | <0.0001 | 1.346 |
| $\text{CONC}_{0.15}$ | 0.572 | 0.043 | <0.0001 | 1.346 |
| RV | -0.014 | 0.002 | <0.0001 | 1.005 |

This model was selected based on the best combination of the lowest root MSE, Mallows Cp and difference between $R^2$ and adjusted $R^2$. Model estimates, p-values and VIF are described for all the variables used in the regression equation. It is important to notice that all VIF are lower than 10 and that all the variables included in the model are statistically significant.

**Table 5.8. Best parameters for subsets of regression fir Jnr of mastics based on modified asphalts**

| Vars | $R^2$ | $R^2$adj | Mallows Cp | Root MSE | ACJnr | CONC | RV | CaO | $Al_2O_3$ |
|---|---|---|---|---|---|---|---|---|---|
| 3 | 0.734 | 0.722 | 5 | 0.239 | x | x | x | | |
| 3 | 0.775 | 0.765 | 5 | 0.220 | x | x | | x | |
| 3 | 0.753 | 0.742 | 5 | 0.230 | x | x | | | x |
| 4 | 0.803 | 0.793 | 6 | 0.206 | x | x | x | x | |
| 4 | 0.797 | 0.785 | 6 | 0.210 | x | x | x | | x |
| 4 | 0.793 | 0.781 | 6 | 0.212 | x | x | | x | x |
| 5 | 0.805 | 0.792 | 7 | 0.207 | x | x | x | x | x |

Regression Equation for Modified Mastics

$$\text{Mastic Jnr} = -0.431 + 0.764\ \text{ACJnr} + 0.564\ \text{CONC}_{0.05} + 0.292\ \text{CONC}_{0.15} + 0.007\ \text{CaO} \qquad \text{Eq. 5.3}$$

| Predictor | Estimate | Standard Error | P | VIF |
|---|---|---|---|---|
| Constant | -0.431 | 0.077 | <0.0001 | 0.000 |
| ACJnr | 0.764 | 0.056 | <0.0001 | 1.000 |
| $CONC_{0.5}$ | 0.564 | 0.055 | <0.0001 | 1.333 |
| $CONC_{0.15}$ | 0.292 | 0.055 | <0.0001 | 1.333 |
| CaO | 0.007 | 0.002 | <0.0001 | 1.000 |

The best model for mastic Jnr for modified asphalt (Eq. 5.3) following variables: AC Jnr, CaO and CONC (Table 5.8). The $R^2$ for thie model is 0.765 based on parameters. The CaO predictor coefficient of 0.007 suggests that if all other variables are held fixed each unit of increase in CaO increase modified mastic Jnr by 0.007. This is in line with the experimental findings that an increase in CaO decreases the rutting resistance. Lower resistance to rutting is given by higher value of Jnr.

Similar to the regression model for mastics based on CCP and unmodified binder, the modified regression model was selected using the best combination of the lowest RMSE, Mallows Cp and difference between $R^2$ and adjusted $R^2$. Model estimates, p-values and VIF are described for all variables used in the regression equation. It is important to notice that all VIF are lower than 10 and that all variables included in the model are statistically significant.

Figures 5.1 and 5.2 provide the plots for the residuals vs. fitted values. These plots aid on assessing the quality of the regression models to fit the experimental data. The residuals for both regression models are randomly distributed around the 0 line. This suggests that the linear relationship assumption was reasonable. The residuals roughly from a horizontal band around the 0 line, indicating that the variances of the error terms are equal.

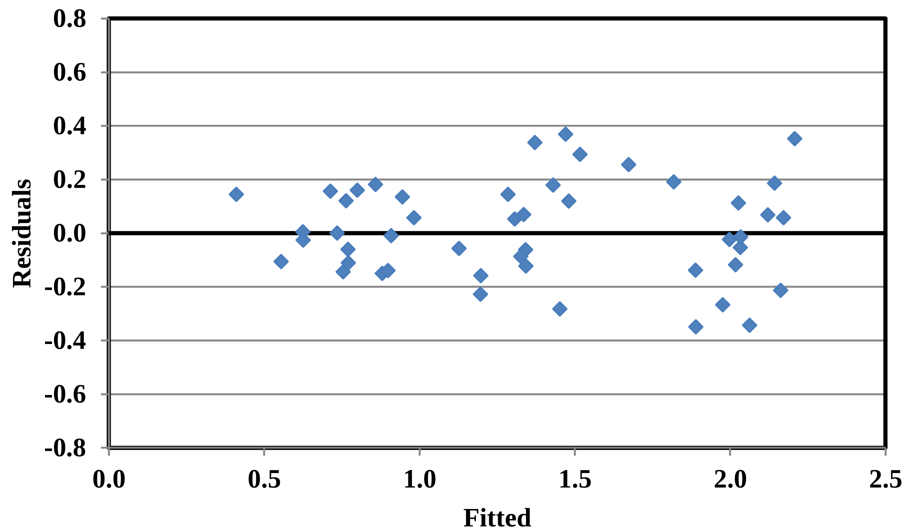


**Figure 5.1 Residuals for unmodified mastics Jnr regression**

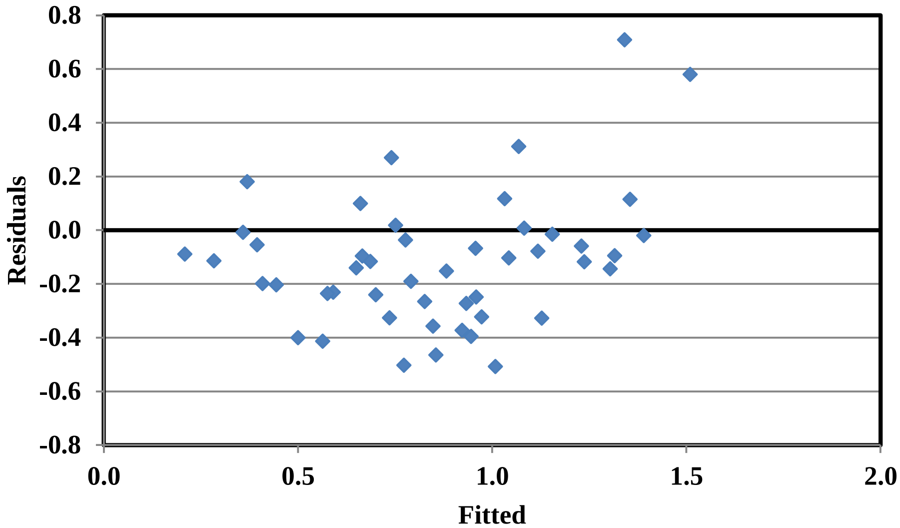


**Figure 5.2 Residuals for modified mastics Jnr regression**

It is recommended that mastics with CCPs are tested prior to application; however, the proposed develop regression models is to estimate the contribution of CCP and estimate the long-term response of HMA. For known characteristics, the Jnr at particular CCP concentration of mastics can be estimated.

# CHAPTER 6.

# FIELD AND MIXTURE APPROACH

We Energies, the main utility company in the state of Wisconsin constructed a pilot pavement project at their facility (Oak Creek, WI) with an asphalt mix with 10% (by weight) of WE05 Class C fly ash replacing the asphalt binder. In addition a control section with ordinary (control) HMA fly ash was constructed.

The Superpave® mix design methodology was used to design the E-1 asphalt mixes for the private road section at the We Energies coal power plant in Oak Creek, WI. The Superpave® mix design involved the selection of asphalt binder and aggregates materials that meet the Superpave® specification requirements, and then conducting the volumetric analysis of the specimens compacted with the Supepave® Gyratory Compactor (SGC). With control and precise testing conditions the gyratory compactor provides values of density for each gyration, simulating the field conditions. This is of great importance because the mechanical properties and the response of the asphalt mixes in the pavement applications are strongly dependent on the compaction degree achieved during the compaction process.

Two types of mixes were produced a binder course (top layer) mix with 12.5 mm nominal maximum size (NMAS) and a base course (bottom layer) mix of 19.0 mm nominal maximum size (NMAS). According to WisDOT Specification Standards 04-06 an E-1 Hot Mix Asphalt (HMA) mix was designed to sustain between $0.3 \leq 1x10^6$ ESALS and for the service life of 20 years.

The asphalt mix samples obtained at the project site as supplied by the asphalt mix producer were used to compact the top and base courses samples of Hot Mix Asphalt (HMA) and ASHphalt in the laboratory using the SGC. The SGC was used to determine the compaction process volumetrics and to provide the information about the compactability of both asphalt mixes. The volumetric analysis of the asphalt samples plays an important role since it provides the indication of the mixture's pavement service performance and; therefore, gives some indication of the mixture's probable pavement service life (Asphalt Institute, 2001).

During the field placing and compaction no operational changes were observed. Similar numbers of roller passes and patterns were used for both mixes. This is a clear indication that the field compaction effort did not exhibit any difference during the field compaction when ASHphalt mix section was compared with the control section.

## 6.1 LABORATORY MIXTURE COMPACTION

Superpave® mix methodology was used to design the Hot Mix Asphalt (HMA) and ASHphalt samples for the asphalt top and base layer; 12.5 mm and 19.0 mm NMAS, respectively. These samples were compacted to 60 gyrations which is the design number of gyrations ($N_{des}$). Table 6.1 presents the gradations of the ASHphalt and HMA mixes and the WisDOT limits based on their NMAS. The samples were compacted with the Superpave® Gyratory compactor at temperatures between 140 and 145°C.

**Table 6.1 Job Mix Formula used for pilot project and corresponding WisDOT limits**

| Sieve Sizes | | 12.5 mm | | 19.0 mm | |
|---|---|---|---|---|---|
| | | JMF | WisDOT Limit | JMF | WisDOT Limit |
| 1” | 25.0 mm | 100.0 | - | 100.0 | 100 |
| ¾” | 19.0 mm | 100.0 | 100 | 99.0 | 90-100 |
| ½” | 12.5 mm | 97.5 | 90-100 | 88.5 | 90 max |
| 3/8” | 9.5 mm | 86.9 | 90 max | 79.6 | - |
| #4 | 4.75 mm | 65.9 | - | 60.5 | - |
| #8 | 2.36 mm | 51.3 | 28-58 | 46.1 | 23-49 |
| #16 | 1.18 mm | 41.5 | - | 36.5 | - |
| #30 | 0.60 mm | 31.3 | - | 27.3 | - |
| #50 | 0.30 mm | 13.1 | - | 12.0 | - |
| #100 | 0.15 mm | 5.8 | - | 5.7 | - |
| #200 | 0.075 mm | 4.3 | 2.0-10 | 4.3 | 2.0-8.0 |
| FAA | | 42.4 | - | 42.8 | - |
| Gsb | | 2.656 | - | 2.658 | - |

Table 6.2 reports on the asphalt mix volumetric information obtained from the contractor. The specific gravity of asphalt binder (Gb) was assumed as 1.030. The bulk specific gravity of the aggregate mix (Gsb) and the effective specific gravity of the aggregate (Gse) together with the asphalt absorption (Pba) were calculated using the given volumetric information. Both asphalt mixes used 20% of fractioned reclaimed asphalt pavement (FRAP). This accounts for 0.9% of the total asphalt cement (Total Pb) for both asphalt mixes. Table 6.3 presents WisDOT 04-06 requirements for a12.5 mm and 19.0 mm NMAS mixes.

**Table 6.2 Asphalt mix volumetric data**

| Asphalt Mixes | 12.5 mm | 19.0 mm |
|---|---|---|
| Added Pb, % | 4.6 | 4.2 |
| Total Pb, % | 5.5 | 5.1 |
| Gsb | 2.658 | 2.658 |
| Gse | 2.724 | 2.724 |
| Gb | 1.030 | 1.030 |
| Pba | 0.939 | 0.939 |

**Table 6.3 The WisDOT mix requirements**

| Nominal Size | 12.5 mm | 19.0 mm |
|---|---|---|
| Min. VMA, % | 14 | 13 |
| Va @ Ndes, % | 4 | 4 |
| VFA, % | 70-76 | 65-78 |
| D/B ratio, % | 0.6-1.2 | 0.6-1.2 |

The ASHphalt and HMA mix volumetrics were measured in the laboratory using a CoreLok machine following AASHTO T331. The volumetrics measured were maximum theoretical density (Gmm) of loose asphalt mix and bulk density (Gmb) of compacted asphalt mix. The percent of aggregates (Ps), percent of asphalt binder (Pb) and dust to binder ratio (D/B ratio) were calculated for each mix from the contractor job mix formula design. With these parameters calculated the voids in the mineral aggregate (VMA), voids filled with asphalt (VFA), air voids (Va) and effective asphalt content (Pbe) were estimated and compared with WisDOT 04-06 standards requirements. Table 6.4 indicates the volumetric results for both asphalt mixes.

**Table 6.4 ASHphalt and HMA measured volumetric**

| Asphalt Mixes | 12.5 mm ASHPhalt | 12.5 mm HMA | 19.0 mm ASHPhalt | 19.0 mm HMA |
|---|---|---|---|---|
| %Gmm | 2.497 | 2.483 | 2.510 | 2.509 |
| %Gmb | 2.391 | 2.389 | 2.404 | 2.414 |
| Pb, % | 4.950 | 5.500 | 4.590 | 5.100 |
| Ps, % | 95.050 | 94.500 | 95.410 | 94.900 |
| Pbe, % | 4.058 | 4.613 | 3.694 | 4.209 |
| VMA, % | 14.498 | 15.064 | 13.830 | 13.707 |
| VA, % | 4.2 | 3.8 | 4.2 | 3.8 |
| VFA, % | 70.852 | 74.869 | 69.122 | 72.616 |
| D/B ratio, % | 1.17 | 0.93 | 1.30 | 1.02 |

The addition of fly ash increases the percentage of voids in the pavement filled with asphalt binder (Table 6.4). Even though ten percent of the asphalt binder was replaced in the mixture with Class C WE05 fly ash, there was only a 0.4% increase in the amount of air voids.

It was also observed that the 12.5 mm NMAS ASHphalt mix provides a slightly lower VMA value than the 12.5 mm mix. On the other hand, the 19.0 mm nominal size ASHphalt and HMA mix resulted in very similar VMA value. The VMA for all mixes are within the minimum requirements of WisDOT standards. The VMA limits are required to ensure the durability and sufficient particle coating. Good resistance to permanent deformation requires low voids in the mineral aggregate (VMA).

The compaction effort in terms of number of gyrations to achieve 92% Gmm (8% air voids) was compared for both mixes in terms of effort required to achieve the same level of compaction. The target 92% Gmm represents the density at the completion of construction of the asphalt layer. The gyrations are an indication of the bulk shear resistance of the asphalt mix. Both mixes were compacted to $N_{des}$ gyrations (Figure 6.1 and 6.2).

Based on the results on Figure 6.1 and 6.2 the ASHphalt mixes did not appear to impede the compaction process when compared to the control HMA mixes. The Construction Densification Index (CDI) is the area under the densification curve from 8 gyrations up to a density of 92%Gmm. The CDI represents work done during the construction period to achieve 8% air voids. The Traffic Densification Index (TDI) is the area under the densification curve from 92% Gmm density to 98% Gmm density. The TDI represents work needed to resist traffic loading during pavement service life.

Using numerical method based on Simpson's 1/3 rule the area for both indexes was estimated. The Simpson's 1/3 rule used a second-degree polynomial to more accurately estimate the area under a curve. Since all the asphalt mixes were compacted to $N_{des}$ gyrations, the 98% Gmm density was not reach and the TDI was estimated based on the maximal density reached (96% Gmm). The CDI and TDI calculated for investigated mixes did not differ much. The ASHphalt mixes resulted in a slightly lower CDI indicating easier compaction compared to the control HMA.

**Table 6.5 CDI and TDI results**

| | **12.5 mm Mix** | | **19.0 mm mix** | |
|---|---|---|---|---|
| **%Gmm x N** | **ASHphalt** | **HMA** | **ASHphalt** | **HMA** |
| **CDI** | 366.93 | 364.60 | 366.64 | 366.37 |
| **TDI** | 4535.74 | 4545.01 | 4535.73 | 4548.08 |

On the other hand, control HMA resulted in slightly higher TDI indicating some reduction to traffic resistance when compared to the ASHphalt mixes. These results clearly indicate that substituting 10% of the asphalt cement by fly ash is viable and sustainable option as it improves the compaction or resistance to traffic while reducing cost and impact to the environment.

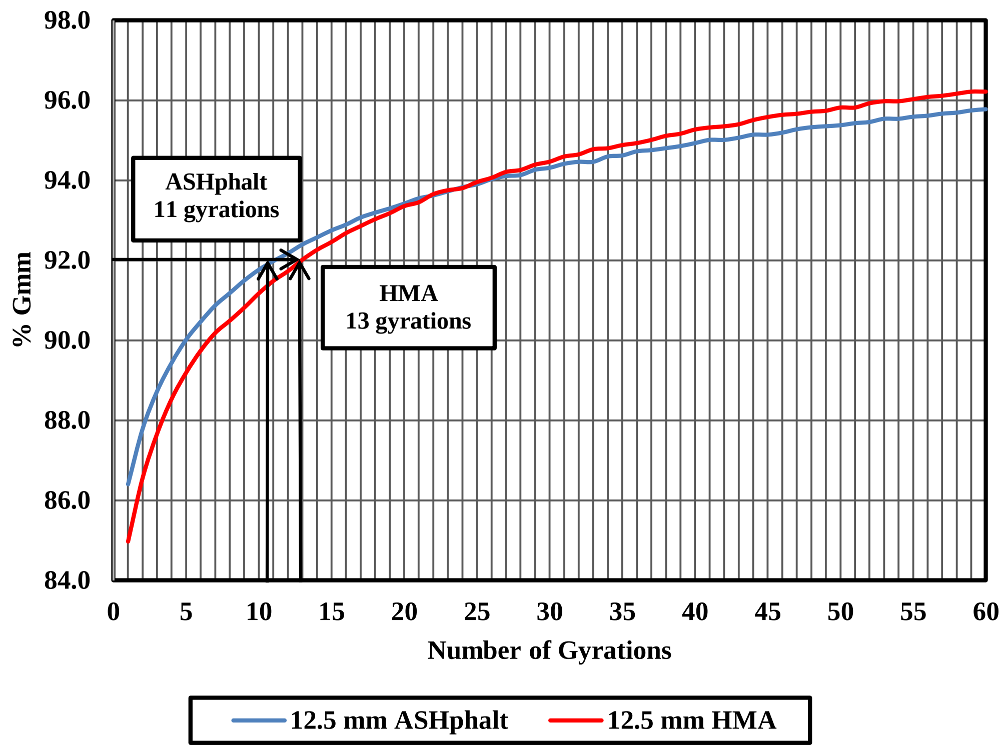


**Figure 6.1 Densification curves for 12.5 mm NMAS mixes**

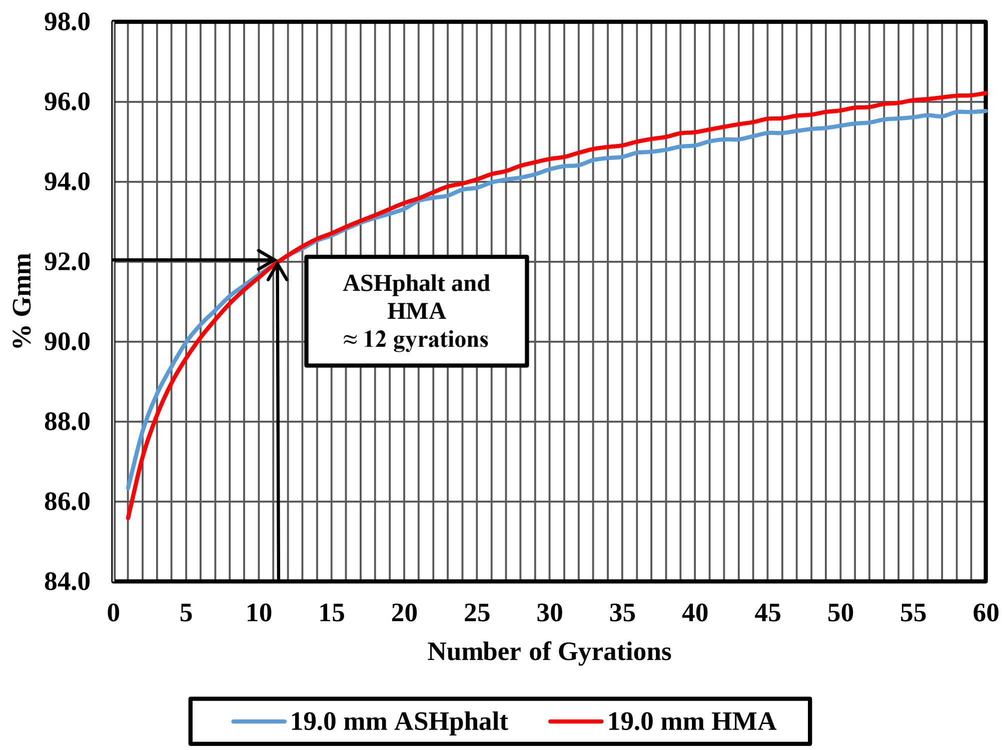


**Figure 6.2 Densification curves for 19.0 mm NMAS mixes**

Although the incorporation of fly ash into the mix facilitated compaction, special consideration needs to be taken to ensure that cracking and durability performance are not sacrificed because of potential reduction in an adequate asphalt film thickness (i.e., due to reduced covering of the aggregates due to the added surface area of the fly ash fine particles in). The stiffness at low temperatures and cracking resistance are good indicators of the mixes' ability to withstand these exposures.

## 6.2 ASHPHALT FIELD IMPLEMENTATION

Both pavement sections of the service road, ASPhalt and control HMA, were tested with the Falling Weight Deflectomenter (FWD). The non-destructive testing was conducted to determine the field pavement modulus using a backcalculation procedure. According to the 1993 AASHTO Guide for the Design of Pavement Structures, the FWD is used as a mean of evaluating the conditions of existing pavements. The impact load used in this study was approximately 40 kN. The pavement surface deflections were recorded by seven sensors located at 0, 1.0, 1.5, 2.0, 3.0, 4.0, and 5.0 ft from the center of the loading plate and FWD tests were performed at 100 ft intervals. The measured deflection data were used to back calculate the elastic modulus of the pavement layer as well as that of the support layers. According to FWD results, the average modulus for the ASHphalt and control HMA section for 2012 and 2014 are compared in Figure 6.3.

The 2012 testing results reveal that the modulus is for the ASHPhalt section surface layer (with 10% of binder is replaced by WE05 Class C fly ash) exhibits a modulus value of about 9% higher than the control section of pavement. For 2014 the ASHPhalt surface modulus increased by 19% over a course of two years. On the other hand, the modulus of the control HMA section dropped by 3%. These results are well correlated with compaction effort analysis and TDI predictions.

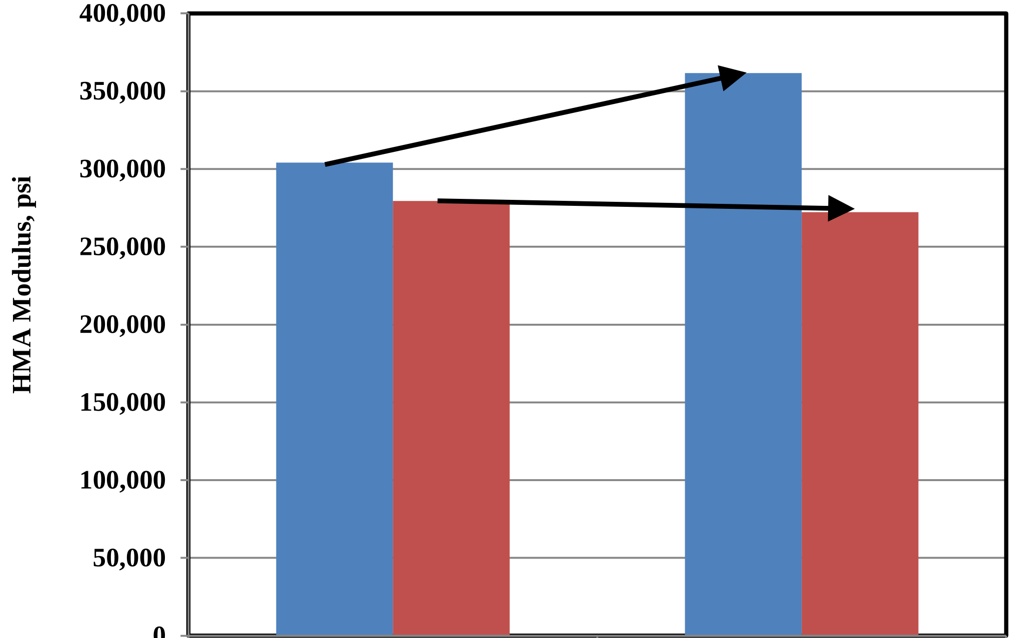


| | 2012 | 2014 |
|---|---|---|
| ASHPhalt | 304,090 | 361,624 |
| Control HMA | 279,469 | 272,280 |

**Figure 6.3 The elastic modulus of pavement based on a non-destructive FWD test**

The structural number represents the structural strength of a pavement required for a given combination of soil support, total traffic expected (ESALs), terminal serviceability and environment. The results for the structural strength as estimated from the FWD and layer thickness data are presented in Figure 6.4. It can be concluded that the ASHphalt section outperformed the control HMA section. The mechanical performance was improved inspite of a common expectation for the reduction of the structural strength of the pavement over time. Further study is needed to understand and explain such abnormal response observed for ASHphalt.

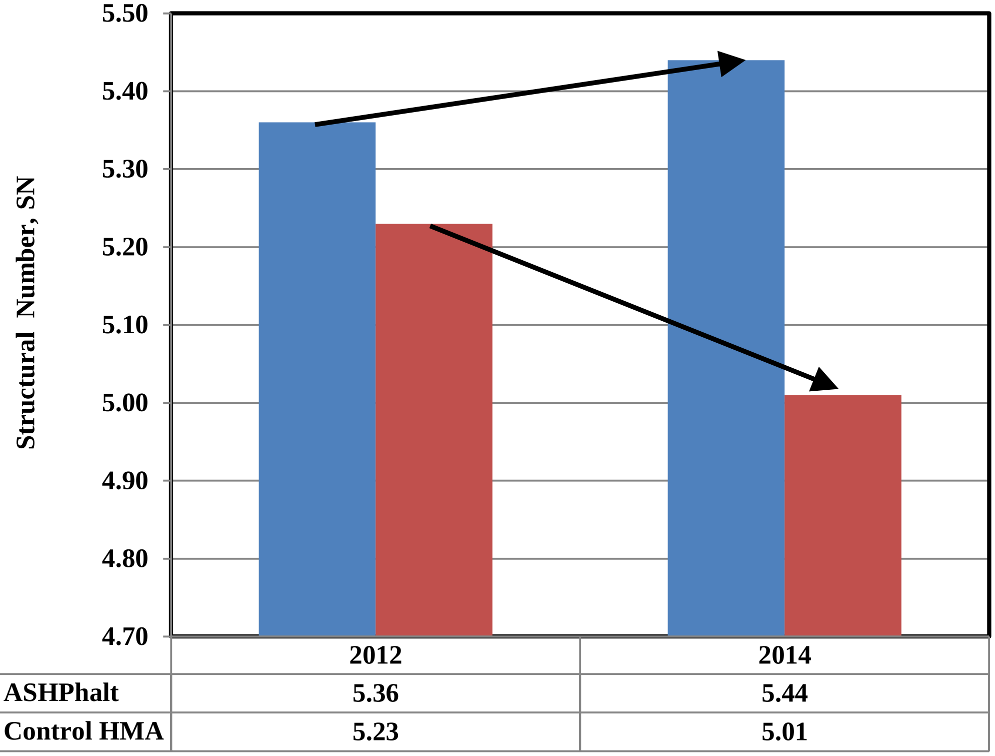


**Figure 6.4 Pavement structural number**

## 6.3 COST BENEFITS

The detailed rheological and performance results at the mastic level for investigated mixtures and field results presented in this chapter provide a good indication that CCPs are viable alternative materials providing enhanced properties in terms of the commonly accepted performance criteria used by the asphalt industry.

Table 6.6 and 6.7 present a cost and benefit analysis which compares the cost of the components needed to produce 1 ton of HMA to the cost of the components to produce 1 ton of ASHphalt. The analysis was based on estimated prices for the state of Wisconsin as of May 2015.

Substituting 10% of the asphalt cement in the HMA with Class C WE05 fly ash represents a reduction in cost of \$2.18/ton and \$2.00/ton for 12.5 mm and 19.0mm NMAS mixes, respectively. Incorporating 10% fly ash to substitute asphalt cement represents a 7 to 8% reduction of the total cost of the mixes.

This is a clear indication that utilizing selected by-products is also a cost-effective strategy as it aids in the reduction of asphalt cement used and also maintains the expected and improved performance.

**Table 6.6 Estimated Cost for 12.5 mm asphalt mix**

| **Components** | **Cost (\$/ton)** | **HMA JMF** | **HMA(\$/ton)** | **ASHphalt JMF** | **ASHphalt (\$/ton)** |
|---|---|---|---|---|---|
| **FRAP** | 6.00 | 19.1% | 1.15 | 19.1% | 1.15 |
| **7/8” Chip** | 8.00 | 0% | 0 | 0% | 0.00 |
| **5/8” Chip** | 8.00 | 15.3% | 1.22 | 15.3% | 1.22 |
| **3/8” Chip** | 8.00 | 11.5% | 0.92 | 11.5% | 0.92 |
| **Man. Sand** | 12.00 | 13.4% | 1.61 | 13.4% | 1.61 |
| **Natural Sand** | 5.00 | 36.3% | 1.82 | 36.3% | 1.82 |
| **AC (PG58-28)** | 500.00 | 4.4% | 21.99 | 4.0% | 19.79 |
| **Fly ash C** | 5.00 | - | - | 0.4% | 0.02 |
| **Total** | | 100% | **28.70** | 100% | **26.52** |

**Table 6.7 Estimated Cost for 19.0 mm asphalt mix**

| **Components** | **Cost (\$/ton)** | **HMA JMF** | **HMA(\$/ton)** | **ASHphalt JMF** | **ASHphalt (\$/ton)** |
|---|---|---|---|---|---|
| **FRAP** | 6.00 | 19.2% | 1.15 | 19.2% | 1.15 |
| **7/8” Chip** | 8.00 | 10.6% | 0.84 | 10.6% | 0.84 |
| **5/8” Chip** | 8.00 | 11.5% | 0.92 | 11.5% | 0.92 |
| **3/8” Chip** | 8.00 | 10.6% | 0.84 | 10.6% | 0.84 |
| **Man. Sand** | 12.00 | 15.4% | 1.84 | 15.4% | 1.84 |
| **Natural Sand** | 5.00 | 28.8% | 1.44 | 28.8% | 1.44 |
| **AC (PG58-28)** | 500.00 | 4.0% | 20.15 | 3.6% | 18.14 |
| **Fly ash C** | 5.00 | - | - | 0.4% | 0.02 |
| **Total** | | 100% | **27.20** | 100% | **25.20** |

# CHAPTER 7.

# CONCLUSIONS

1. The materials used in this research represent a wide range of CCPs with different physical properties and chemical compositions. These CCPs can be grouped as Class C and F fly ash materials as well as SDA products with high content of CaO and sulfites.
2. The addition of up to 15% by volume of CCPs results in a linear increase in complex modulus, G*. Further increase of CCP concentration leads to a significant increase of the complex modulus. For example, 15% addition of WE05 C, increases the G* value by 55.6% compared to the unfilled binder. Further addition of 10% of CCP (to 25% loading) increases the stiffness by an additional 68.6%. The research results also reveal that SDA materials are the most interactive (affecting the G*) with reference PG58-28 and polymer modified (PM) PG70-28 binders, while Class C fly ash mastics had the least increment of the G* (similar to plasticizing effect). It was noted that 25% and higher concentrations of ultra-fine CCPs with high content of calcium sulfite (e.g., DL16) is highly sensitive to polymer modification (e.g., binder PG70-28). This observation confirms that CCPs follow the standard theory of particulate materials inclusion in viscoelastic matrix. However, the impacts of some CCPs indicate that interaction between the asphalt binder and the particulates materials takes place.
3. The relative complex modulus (G*r) was used as an attempt to evaluate the interaction between the CCPs and the binders used. With addition of filler or CCP, the increase in mastic G*r is linear (designated as diluted region) until reaching a

critical volume concentration where the rate of increase becomes nonlinear and rapidly reaches an asymptotic linear trend (characterized as jammed packing state). It was observed that up to 15% CCP volume concentration the slope is small; however at concentrations ranging from 25 to 40% a more pronounced increase of the slope is observed indicating the achievement of jammed state characterized by particle-to-particle interactions. The addition of up to 40% of Class C fly ash resulted in lower G*r vs. corresponding values for reference limestone filler. Class F fly ash had a very similar behavior as limestone filler. All these materials provide potential increase in rutting resistance. Very high increase of the G*r observed for the SDA based mastics at dosages higher than 15% could indicate the materials that are potentially more difficult to mix and compact. The results demonstrate that the increase of complex modulus is not binder dependent.

4. The Superpave® binder specification requires the viscosity of unaged asphalt binder to be reported as an indication of constructability or workability. According to Bahia et al. (2011), the relative viscosity of mastics can reach the max value of 5 (vs. the viscosity limit for unfilled unaged asphalts of 3 Pa.s tested at 135 °C plant mixing temperature). Based on the investigation of 8 CCPs and reference filler materials mixed with 3 types of asphalt binders, a favorable performance was demonstrated by Class C fly ash and also SDA SF15. With exception of SDA DL16, other CCPs did not cause any detrimental effect on the workability as compared to the reference filler.
5. The Superpave® rutting factor $G^*/\sin\delta$ was calculated in order to demonstrate the rutting resistance of CCP-based mastics. The addition of CCPs increases the rutting

resistance compared to corresponding plain binder. At all tested concentrations the unaged mastics based on PG58-28 and PG64-28 had G*/sinδ results above the corresponding plain binders. These findings clearly indicate that the addition of CCPs (and reference filler) to plain asphalt binders increase the rutting resistance (as measured by G*/sinδ). The mastics based on PG70-28 PM binders also had an increase in rutting resistance with the exceptions of few SDA materials (DL16, WP03 and SF15) which provided softening effect corresponding to the extension of the asphalt binder. This is an important observation which must be investigated at the HMA level to prove the ability of SDA to replace the asphalt binder without any detrimental effects on performance.

6. To characterize the rutting resistance of polymer modified binders the Multiple Stress Creep Recovery (MSCR) test was proposed to characterize the deformation resistance and recovery influenced by the polymer modification (D'Angelo 2009). In this research the effect of CCPs on rutting resistance of mastics based on four binders was investigated in terms of the non-recoverable compliance or quantifying damage resistance ($J_{nr}$, AASHTO TP70-13) and percent of damage recovery. It was confirmed that all CCPs improve the rutting resistance of mastics based on plain and PM binders (as demonstrated by the decreasing values of the $J_{nr}$). The PM binder based with low dosage of Class C and F fly ash had an improved performance vs. reference filler. With an increase in concentration, the improvement effect of fly ash becomes comparable to that of the reference filler. The SDA materials consistently demonstrate high sensitivity in combinations with modified binders. The extent of its effect varies significantly depending on the dosage and binder type. Still, it is evident

that the general trend is that the increase in CCPs and filler concentration leads to the decrease in $J_{nr}$ value and, consequently, to the improvement of the rutting resistance as measured by the $J_{nr}$.

7. The percent recovery test was originally developed for modified binders to quantify the added elasticity as unmodified binders at high PG testing temperature have little or no recovery after the loading. In this research, the mastics based on four plain/unmodified and PM asphalt binders were evaluated. Although mastics based on plain binders and CCPs had improved values of recovery (by 100%+), such improvement cannot be considered as significant. For example, the percent recovery for DL16 (at 25% loading) based mastic increased from 1.44% for reference to 4.16%. This is still insufficient to cause any real change in the performance. For PM binders the recovery depends on the type of modification, and the integrity of the polymer. In case of Class C fly ash, there are minor changes in percent recovery; however, the SDA materials at concentrations below 25% had a severe reduction in the recovery when combined with PG64-28 and had only minor change when combined with PG70-28. When combined with the PM binder PG70-28, Class F fly ash had the most significant improvement in the percent recovery. The mechanism by which polymer and CCP modification interact is still under investigation, but it is envisioned that the CCPs can bond to the polymers so the effect is mainly observed in damage resistance rather than recovery. It was observed that, depending on the asphalt grade and concentration, some of the CCPs outperform the reference filler. Further investigation may be necessary to maximize the effect of the CCPs in terms of recovery.

8. The Superpave® binder specification defines a fatigue factor, G*sinδ, as surrogate to fatigue damage resistance of RTFO and PAV aged asphalt cements. The research results demonstrate that for unaged plain/unmodified binders, the stiffness of the mastics increase rapidly beyond the 5,000 kPa limit. The PG58-28 based mastics with WE08 C, LG14 F, and SF15 SDA CCPs at up to 15% dosage can meet the binder specifications. The PG64-28 based mastics with up to 5% CCP concentration continue to meet the binder specifications. All the mastics with PG70-28 meet the binder specifications. For PG58-28 (with the exception of mastics prepared with Class C fly ash WE05 at 5% and 15% dosage) the G*sinδ values are lower than obtained with the reference limestone filler. It is important to note that the reference filler had the most rapid rate of increase while the Class C fly ash had the least increase of the rate. This indicates that CCPs <u>mastics are less prone to fatigue damage in terms of G*sinδ when compared to the reference limestone filler.</u>
9. The aging index was used to characterize the increase in G* due to PAV aging vs. G* of unaged mastics. It was demonstrated that the addition of CCP as compared to reference limestone filler can retard the aging of mastics. For PG58-28 based mastics with SF15 SDA CCPs the aging index was improved vs. the reference fillers at all tested concentration levels. For PG64-28 based mastics with WE05 C and SF15 SDA CCPs the aging index was improved for all concentrations. For PG70-28 based mastics with DL16 SDA CCPs the aging index was also improved at all concentrations. At 15% and 25% concentrations all mastics demonstrate improved (lower) aging index than the reference filler (with few exceptions). The research results demonstrate that, with an addition of reference filler, the mastic is more

sensitive to aging. However, the CCPs, in general did not follow the same trend. For example, the aging index for SDA - polymer modified binder mastics did not change with an addition of CCP. Therefore, it can be concluded that the addition of the CCP leads to retardation of aging (as compared to the natural fillers). This conclusion must be further confirmed through an additional mixture testing.

10. Low temperature cracks develop in aged material when the stresses induced by freezing exceed the tensile strength of the asphalt mixture. To address the low temperature response the Superpave® binder specification defines the creep stiffness (St) and the m-value. It was demonstrated that at up to 5% of CCP loading, for mastics based on PG58-28 and PG70-28, the stiffness was within the 300 MPa Superpave® limit set for binders. The stiffness of the PG64-28 plain binder is right at the limit and, subsequently, any CCP or filler addition affected the mastics to exceed the Superpave® binder limit. Previous research demonstrated that the addition of WE05 can reduce the stiffness of the mastics based on PG58-28 and PG64-28 below the plain binder level, while in PG70-28 mastics, at up to 25% loading did not increase the stiffness. It was observed that at low temperature the addition of Class F fly ash did not demonstrate significant increase in stiffness, while the DL16 based mastics were characterized by an extreme increase in the stiffness.
11. It is evident that most mastics with CCP have a higher creep stiffness than those with the reference filler; however, as m-values indicate, some CCPs result in the mastics which are able to relax low temperatures stresses better than the reference filler. The m-value test is not designed to characterize the resistance of the mastics to thermal cracking, but it can be used to compare the effect of different fillers. For thermal

relaxation, Class C and Class F fly ash were able to maintain an acceptable level of relaxation (above the Superpave limit of 0.3) for materials at most concentrations. Again, Class C fly ash and, especially WE05, improve the relaxation modulus of the binders at 5% and maintain the same level of relaxation at higher concentrations. However, for the PG 64-28 binder, the unfilled binder itself did not meet the specification limits (indicating that must be graded as a PG64-22 binder). Yet, with the help of Class C WE05 fly ash, the binder low temperature limit was decreased from -22°C to -28°C.

12. The stiffening rate ($S_R$) was used to quantify the CCP and binder interaction and as a characteristic of the performance. In this research, a good correlation was observed between the stiffening rate and CCP characteristics (up to 15% concentration) for plain/unmodified asphalt binders. Based on the analysis of mastics with 15% CCP and unmodified asphalt binders (PG58-28 and PG64-28), the Rigden voids parameter strongly correlates with the stiffening rate. In addition to RV, the $Al_2O_3$, CaO, $SiO_2$, $SO_3$, SAF, LOI and $D_{10}$ parameters have a significant effect on the stiffening rate. An increase in $Al_2O_3$, $SiO_2$, SAF and $D_{10}$ results in a decrease of the stiffening rate which is an indication of plasticizing (softening) effect. On the other hand, higher CaO, $SO_3$ and LOI values result in an increase in the stiffening rate resulting in stiffer mastics. Different trends were observed in PG70-28 based mastics. For example, the Rigden voids parameter did not have any correlation for up to 15% of CCP addition. For mastics with 25% of CCP and higher, the parameters such as $Al_2O_3$, $Fe_2O_3$, $SiO_2$, $SO_3$ content and Rigden voids have the highest correlation with $S_R$. It can be concluded that at low concentrations (less than 15%), the CCPs act as physical inclusion causing

an overall increase in stiffness irrespective of the CCPs physical or chemical properties. As the concentration increases, the CCP composition and properties start to affect the stiffness. The Rigden Voids, $Al_2O_3$, CaO, $SiO_2$, $SO_3$, and LOI content are the primary indicators affecting the mastic performance. The mastic properties can be considered as a bridge between the filler properties and asphalt mixture performance indicators.

13. The multiple regression analysis for unmodified asphalts indicates that Rigden Voids is the main characteristics of CCP which has a significant influence on rutting behavior of unmodified mastics based binders. On the other hand, the regression analysis for mastics based on modified asphalt indicates that CaO content is the CCP parameter which has a significant influence on the rutting behavior. The $R^2_{adj}$ are 0.886 and 0.765 for corresponding regression models. This indicates that these CCPs characteristics are sufficient to adequately predict the Jnr of the mastics with CCPs.
14. The addition of CCPs into the asphalt mix did not impede the compaction process. When fly ash was used to replace the asphalt binder, no negative effects were observed in the compaction. Replacing 10% by weight of asphalt binder with Class C fly ash enable to maintain the same or higher level of low temperature performance. This translates into the cost sustainable practices important for the field application enabling the reduction of the cost of the final product (given that the asphalt binder is the most expensive component of the mixture).
15. The addition of fly ash to HMA, ASHphalts also provides a safe use of a by-product while reducing the dependence on petroleum products. Considering the results listed

above, it is clear that the use of CCPs can lead to improvement of long-term performance of asphalt pavements.

# REFERENCES


1. ACI Committee 226 3R-87. Fly Ash in Concrete. ACI Mater. J. 11, 381-409 (1987)
2. Adrian, D. W. and A. J. Giacomin. "The quasi-periodic nature of polyurethane melt in oscillatory shear". *Journal of Rheology*, Vol. 36, Issue 7, October 1992, pp. 1227-1243.
3. Alonso, J. L., Wesche, K. Characterization of Fly Ash. Fly Ash in Concrete, Properties and Performance, pp. 3-23, Rilem Report, E & FN Spon, New York (1992).
4. Ali, N., Chan, J.S., Simms, S., Bushman, R., and Bergan, A.T. 1996. Mechanistic evaluation of fly ash asphalt concrete mixtures. Journal of Materials in Civil Engineering, 8 (1): 19-25.
5. American Coal Ash Association (ACAA). Fly Ash Facts for Engineers. Federal Highway Administration. FHWA-IF-03-019. 2003
6. Anderson, D.A., J.P. Tarris and D. Brock, 1983. Dust collector fines and their influence on mixture design. J. Assoc. Asphalt Paving Technol., 51: 353-397.
7. Anderson, D. A., Goetz, W. H. Mechanical Behavior and Reinforcement of Mineral Filler-Asphalt Mixtures. Proceedings of the Association of Asphalt Paving Technologists. Vol. 42. 1973.
8. Asi, I., and Assa'ad, A. 2005. Effect of Jordanian oil shale fly ash on asphalt mixes. Journal of Materials in Civil Engineering, 17 (5): 553-559.
9. Asphalt Institute. (2003).Performance Graded Asphalt Binder Specification and Testing. Superpave Series No. 1 (SP-1). Asphalt Institute. Lexington, KY
10. Asphalt Institute. (2001). Superpave Mix Design. Superpave Series No. 2 (SP-02). Asphalt Institute. Lexington, KY
11. Bahia, H. U., Hanson, D. I., Zeng, M., Zhai, H., Khatri, M. A., and Anderson, R. M. 2001. NCHRP Report 459 Characterization of Modified Asphalt Binders in Superpave Mix Design. National Cooperative Highway Research Program, Transportation Research Board, National Research Council, Washington, D.C.
12. Bahia, H. U., Perdomo, D., and Turner, P. Applicability of Superpave Binder Testing Protocols to Modified Binders. Transportation Research Record 1586. pp. 16-21. 1997
13. Boduszynski, M. M., McKay, J. F., and Latham, D.R. Asphaltenes, Where are you? Association of Asphalt Paving Thechnology (AAPT). Louisville, Kentucky. 1980.
14. Brown, A. B., J. W. Sparks and O. Larsen. Rate of Change of Softening Point, Penetration and Ductility of Asphalt in Bituminous Pavement. Proceedings AAPT, Vol. 26, 1957.
15. Brown, E. R., Haddock, J. E., and Crawford, C. Investigation of Stone Matrix Asphalt Mortars. Transportation Research Record 1530. Transportation Research Board, National Research Council, Washington, DC. 1996. pp. 95-102.
16. Cabrera, J.G., and Zoorob, S. 1994. Design of low energy hot rolled asphalt. The Civil Engineering Materials Unit, Department of Civil Engineering, University of Leeds, United Kingdom.
17. Carpenter, C.A. 1952. A comparative study of fillers in asphaltic concrete. Public Roads, 27(5): 101-110.
18. Churchill, E.V., and Amirkhanian, S.N. 1999. Coal ash utilization in asphalt concrete mixtures. Journal of Materials in Civil Engineering, 11 (4): 295-301.

19. Diamond, S. Selection and Use of Fly Ash for Highway Concrete. Joint Highway Research Project, Purdue University, Indiana (1985).
20. Dukatz, E L. and Anderson, D. A. The Effect of Various Fillers on the Mechanical Behavior of Asphalt and Asphaltic Concrete. Proceedings of the Association of Asphalt Paving Technologists. Vol. 49. pp. 530. 1980.
21. Electric Power Research Institute (EPRI). Classification of Fly Ash for Use in Cement and Concrete. CS-5116, Project 2422-10. Palo Alto, California 94304, USA (1987).
22. Einstein A. 1911. Berichtigungzumeiner Arbeit: Eineneue Bestimmung der Molekül-dimensionen. Ann. Phys. 34:591–592.
23. Faheem, A. F., Hintz, C. Bahia, H.U. "Test Methods and Specification Criteria for Mineral Filler Used in HMA", NCHRP 9-45 Final Report. 2011.
24. Faheem, A.F. 2009. Conceptual phenomenological model for interaction of asphalt binders with mineral fillers (Doctoral dissertation, University of Wisconsin Madison, 2009).
25. Faheem, A.F., Bahia H.U. 2010. Modelling of Asphalt Mastic in Terms of Filler-Bitumen Interaction
26. Ferry, J.D. Viscoelastic Properties of Polymers. John Wiley & Sons, 1980.
27. Finn, F. N., K. Nair and J. M. Hilliard. Minimizing Premature Cracking in Asphaltic Concrete Pavement. TRB, NCRHP Report 195, 1978.
28. Galloway BM. A review of the use of mineral filler in asphalt-aggregate mixtures. Fly ash applications in 1980 conference; 1980.
29. Henning, N.E. 1974. Evaluation of lignite fly ash as a mineral filler in asphaltic concrete. Report No. Item 2 (73).Twin City Testing and Engineering Laboratory, St. Paul, Minnesota.
30. Heukelom, W., and Wija, P. W. O. Viscosity of Dispersions Governed by Concentration and Rate of Shear. Journal of Asphalt Paving Technologists. Vol 40. 1971.
31. Joshi, R. C. Experimental Production of Synthetic Fly Ash from Kaolinite. MS Thesis, Iowa State University (1970)
32. Joshi. R. C., Lam, D. T. Sources of Self-Hardening Properties of Fly Ashes. Materials Research Proceedings, Vol. 86, pp. 183-184. MRS. Pittsburg (1987).
33. Kandhal, P. S., L. D. Sandvig, W. C. Koehler and M. E. Wenger. Asphalt Viscosity-Related Properties of In-Service Pavements in Pennsylvania. ASTM, Special Technical Publication No. 532, 1973.
34. Kandhal, P. S., and M. E. Wenger. Asphalt Properties in Relation to Pavement Performance. TRB, Transportation Research Record 544, 1975.
35. Kandhal, P. S. Low-Temperature Ductility in Relation to Pavement Performance. ASTM, Special Technical Publication 628, 1977.
36. Kandhal, P. S. et al. Low-Temperature Properties of Paving Asphalt Cement. TRB, State-of-the-Art Report 7, 1988.
37. Kandhal, P. S., L. D. Sandvig and M. E. Wenger. Shear Susceptibility of Asphalts in Relation to Pavement Performance. Proccedings AAPT, Vol. 42, 1973.
38. Kandhal, P. S. Low Temperature Shrinkage Cracking of Pavements in Pennsylvania. Proceedings of the AAPT, Vol. 47, 1978.
39. Lakes, R. (2009). *Viscoelastic Materials*. New York, NY. Cambridge University Press, 1st edition.

40. Lee, Dah-Yinn. Asphalt Durability Correlation in Iowa. HRB, Highway Research Record 468, 1973.
41. McCarthy, G. J., Johansen, D. M., Steinwand, S. J. X-ray diffraction Analysis of Fly Ash. In: Barrett, C. S., et al. (eds.) Advances in X-ray Analysis, Vol. 31. Plenum Press, New York (1988).
42. Macosko, C. (1994). *Rheology. Principles, Measurements and Applications.* Wiley-VCH, Inc.
43. Mehta, P. K. Standard Specification for Mineral Admixtures- An Overview. ACI SP 91, 637-658 (1988).
44. Meyers, M. A. and Chawla, K. K. (2008). *Mechanical Behavior of Materials.* Cambridge University Press, 2nd edition.
45. Mogawer, W. S., and Stuart, K. D. Effects of Mineral Fillers on Properties of Stone Matrix Asphalt Mixtures. Transportation Research Record 1530. Transportation Research Board, National Research Council, Washington, DC. 1996. pp. 86-94.
46. Philpot, T. (2011). *Mechanics of Materials: An intergrated learning system*. John Wiley & Sons, Inc., 2nd edition.
47. Puzinauskas, V.P. 1983. Filler in asphalt mixtures. The Asphalt Institute, Research Report No. 69 (2).
48. Ramme, B. W. and Tharaniyil, M. P., Coal Combustion Products Utilization Handbook, Second Edition, We Energies, 2004, 288 pp.
49. Read, J. and D. Whiteoak. The Shell Bitumen Handbook. Shell UK Oil Products Limites, 2003.
50. Richardson, C. The Theory of the Perfect Sheet Asphalt Surface. Journal of Industrial Engineering and Chemistry. Pp 463-465, 1915.
51. Richardson, C. The Theory of the Perfect Sheet Asphalt Surface. Journal of Industrial Engineering and Chemistry. Pp 463-465, 1905. .
52. Richardson, C. 1905. The modern asphalt pavement. J. Wiley & sons, NY.
53. Rigden, P.J. The Use of Fillers in Bituminous Road Surfaings. A Study of Filler-Binder Systems in Relation to Filler Characteristics. Journal of the Society of Chemical Industry. September, 1947.
54. Roberts, F., Kandhal, P., Ray Brown, E. Lee, D., Kennedy, T. (1996). Hot Mix Asphalt Materials, Mixture Design and Construction. National Asphalt Pavement Association Research and Education Foundation. 2nd Edition.
55. Rosner, J.C., Chehovits, J.G., and Morris, G.R. 1982. Fly ash as a mineral filler and anti-strip agent for asphalt concrete. Challenge of change-6th International Ash Utilization Symposium Proceedings. United States Department of Energy, Morgantown.
56. Sankaran, K.S., and Rao, D.R. 1973. The influence of the quality of filler in asphaltic paving mixtures. Indian Roads Congress, 35: 141-151.
57. Shashidar, N., and Romero, P. Factors Affecting the Stiffening Potential of Mineral Fillers. Transportation Research Record 1638. Transportation Research Board, National Research Council, Washington, DC. 1998. pp. 94-100
58. Siddique, R., Iqbal Khan, M. (2011). *Supplementary Cementing Materials*. Springer-Verlag Berlin Heidelberg.
59. Sobolev, K., 2003, Recycling of Waste Glass in Eco-Cement. American Ceramic Society Bulletin, USA, 82(9): 9501-9507.

60. Sobolev, K., and Naik, T.R. 2005.Performance as a Factor for Sustainability of the Cement Industry. CANMET/ACI International Symposium on Sustainable Development of Cement and Concrete, Toronto, Canada, 295 - 312.
61. Sobolev, K., Flores, I., N. M. Wasiuddin (Wasi), "The Use of Fly Ash as Filler in Asphalt Cement: Phase I," Final Report, UWM-We Energies, 2011, 17 p.
62. Standard Terminology Relating Materials for Roads and Pavements. ASTM D8-13a. 2013
63. Standard Specification for Mineral Filler for Bituminous Paving Mixtures. ASTM D242/D 242M-09. 2009.
64. Standard Practice for Classification of Soils for Engineering Purposes (Unified Soil Classification Sytem). ASTM D2487-11. 2011.
65. Suheibani, A.R.S. 1986. The use of fly ash as an asphalt extender. PhD dissertation. University of Michigan, Ann Arbor.
66. Sybilski, D. 1996. Zero-Shear Viscosity of Bituminous Binder and Its Relation to Bituminous Mixture's Rutting Resistance, Transportation Research Record: Journal of the Transportation Research Board, 1535: 15-21.
67. Tadros, T. F. *Rheology of Dispersions: Principles and Applications*. WILEY-VCH Verlag GmbH & Co. KGaA, Weinheim. 2010.
68. Tapkın, S. 2008. Improved asphalt aggregate mix properties by portland cement modification. Can. J. Civ. Eng. 35: 27-40.
69. Tons, E. et al. 1983.Fly ash as an asphalt reducer in bituminous base courses. Report prepared by the University of Michigan, The Board of Water and Light. Consumer Power Co. and Detroit Edison Co. Detroit, Michigan.
70. Vallerga, B. A., C. L. Monismith and K. Granthem. A Study of Some Factors Influencing the Weathering of Paving Asphalts. Proceedings AAPT, Vol. 26, 1957.
71. Warden, W.B., Hudson, S.B., and Howell H.C. 1952.Evaluation of mineral filler in terms of practical pavement performance. Proceedings of the Association of Asphalt Paving Technologists. 27(52): 101-110
72. Wasiuddin, N.M., Selvamohan, S., Zaman, M.M. and Guegan, M.L.T. 2007.A Comparative Laboratory Study of Sasobit® and Aspha-Min® in Warm Mix Asphalt", Transportation Research Record, 1998: 82-88.
73. Winninford, R. S. The Rheology of Asphalt-Filler Systems as shown by the Microviscometer. American Society for Testing and Materials. STP309. pp. 109-120. 1961
74. Witczak, M. W., Kaloush, K., Pellinen, T., El-Basyouny, M., Von Quintus, H. Simple Performance Test for Superpave Mix Design. TRB, NCRHP Report 465, 2002.
75. Zimmer, F.V. 1970. Fly ash as bituminous filler. United States Department of Interior, Bureau of Mines. Washington, D.C.

# APPENDIX A

**Superpave®mix design for field project**

**REPORT OF SUPERPAVE VOLUMETRIC MIX DESIGN**
**(AASHTO MP-2, PP-28, T312 & ASTM D-4867)**

Issued Date: 6/8/2009
Amended Date: 6/16/2009

DESIGN NUMBER: 509809 JOB: 40023
PLANT: 40023 MIX TYPE: B-1 MIX TEMPERATURE: 145°C - 134°C
MIX SIZE: 19.0 mm Design ESAL Range (mil.): 0.3 to < 1

**Compactive Effort: (Gyrations)** Ni: 7 Nd: 60 Nm: 75

**Binder Data:** GRADE: PG 58-28 SOURCE: CRM Milwaukee Gb: 1.035 RAP Pb: 4.49

**AGGREGATE SOURCE DATA**

| AGG | AGGREGATE | SOURCE | TEST# | LOCATION |
|---|---|---|---|---|
| AGG #1 | FRAP | 40023 | 8-B-09 | |
| AGG #2 | 7/8" Chip | Prager | 41-A-09 | W1/2 S7 T4N R19E Racine Co. |
| AGG #3 | 5/8" Chip | Prager | 38-A-09 | W1/2 S7 T4N R19E Racine Co. |
| AGG #4 | 3/8" Chip | Prager | 39-A-09 | W1/2 S7 T4N R19E Racine Co. |
| AGG #5 | MFG'D Sand | Prager | 40-A-09 | W1/2 S7 T4N R19E Racine Co. |
| AGG #6 | Natural Sand | Bloomfield | 30-A-09 | SW1/4 S1 and SE1/4 S2 T1N R19E Walworth Co. |
| AGG #7 | Deg | Bloomfield | 1 | SW1/4 S1 and SE1/4 S2 T1N R19E Walworth Co. |

**AGGREGATE GRADATION**

| | | Agg #1 | Agg #2 | Agg #3 | Agg #4 | Agg #5 | Agg #6 | Agg #7 | JMF | SPECIFICATION MIN | SPECIFICATION MAX |
|---|---|---|---|---|---|---|---|---|---|---|---|
| % BLEND | | 20.0 | 11.0 | 12.0 | 11.0 | 16.0 | 29.7 | 0.3 | | | |
| 2 | 50.0 mm | 100.0 | 100.0 | 100.0 | 100.0 | 100.0 | 100.0 | 100.0 | 100.0 | 0.0 | 0.0 |
| 1-1/2 | 37.5 mm | 100.0 | 100.0 | 100.0 | 100.0 | 100.0 | 100.0 | 100.0 | 100.0 | 0.0 | 0.0 |
| 1 | 25.0 mm | 100.0 | 100.0 | 100.0 | 100.0 | 100.0 | 100.0 | 100.0 | 100.0 | 100.0 | 100.0 |
| 3/4 | 19.0 mm | 100.0 | 90.5 | 100.0 | 100.0 | 100.0 | 100.0 | 100.0 | 99.0 | 90.0 | 100.0 |
| 1/2 | 12.5 mm | 99.4 | 13.1 | 85.2 | 100.0 | 100.0 | 100.0 | 100.0 | 88.5 | 0.0 | 90.0 |
| 3/8 | 9.5 mm | 94.5 | 6.3 | 28.2 | 98.5 | 100.0 | 99.2 | 100.0 | 79.6 | 0.0 | 0.0 |
| #4 | 4.75 mm | 72.1 | 3.4 | 2.7 | 23.8 | 96.4 | 91.2 | 100.0 | 60.5 | 0.0 | 0.0 |
| #8 | 2.36 mm | 56.5 | 2.5 | 2.1 | 3.2 | 58.1 | 81.9 | 100.0 | 46.1 | 23.0 | 49.0 |
| #16 | 1.18 mm | 44.7 | 2.2 | 1.9 | 2.7 | 31.4 | 72.3 | 100.0 | 36.5 | 0.0 | 0.0 |
| #30 | 0.60 mm | 34.8 | 2.0 | 1.7 | 2.5 | 16.7 | 56.1 | 100.0 | 27.3 | 0.0 | 0.0 |
| #50 | 0.30 mm | 22.3 | 1.9 | 1.7 | 2.4 | 8.1 | 17.6 | 100.0 | 12.0 | 0.0 | 0.0 |
| #100 | 0.15 mm | 15.0 | 1.7 | 1.6 | 2.3 | 3.7 | 3.9 | 100.0 | 5.7 | 0.0 | 0.0 |
| #200 | 0.075 mm | 11.8 | 1.5 | 1.4 | 2.2 | 2.4 | 2.2 | 100.0 | 4.3 | 2.0 | 8.0 |
| | FAA | 42.7 | 0.0 | 0.0 | 0.0 | 47.2 | 40.5 | 0.0 | 42.8 | | |
| | Gsb | 2.655 | 2.673 | 2.668 | 2.642 | 2.664 | 2.654 | 2.654 | 2.658 | | |

**AGGREGATE DATA FOR BLENDED DESIGN JMF**

CRUSH 1F/2F: 97.3 / 94.7 Gsb: 2.658 Moist. Absorption: 1.5 L.A. WEAR: 0.0 (100) ELONGATED: 2.1 (5/1)
FAA: 42.8 Gsa: 2.764 Dust Proportion: 1.0 0.0 (500)
SE: 97 Gse: 2.724 Soundness: 0.0 Freeze-Thaw: 0.0

**VOLUMETRIC DATA**

| Point | Added Pb | Total Pb | Gmm | Gmb | Va | VMA | VFB | Unit Wt. | %Gmm Ni | %Gmm Nm | TSR |
|---|---|---|---|---|---|---|---|---|---|---|---|
| A | 3.6 | 4.5 | 2.538 | 2.395 | 5.6 | 13.9 | 59.7 | 2389 | | | |
| B | 4.1 | 5.0 | 2.519 | 2.413 | 4.2 | 13.8 | 69.6 | 2406 | | | |
| C | 4.6 | 5.5 | 2.500 | 2.430 | 2.8 | 13.6 | 79.4 | 2423 | | | |
| JMF | 4.2 | 5.1 | 2.515 | 2.414 | 4.0 | 13.8 | 71.0 | 2407 | 90.8 | 96.6 | 73.1 |
| | | Corr. Factor: | 0.000 | | | | | | | | TSR N = 16 |
| SPECIFICATION | | | - | | 4.0 | 13.0 | 65 - 78 | | 90.5 | 98.0 | |

Comments: WisDOT Aggregate Test Number:225-131-2009 WisDOT Verification Number 250-0130-2009
Eliminate Deg. Bloomfield Natural Sand = 30% Project ID 1030-23-70
A change in binder grade or source is recognized without the need for additional mix design testing.

Wisconsin Certified Hot Mix Asphalt Technician IIIS

THE TEST DATA SHOWN ON THIS REPORT PERTAIN ONLY TO THE MATERIAL SUBMITTED FOR DESIGN.
AASHTO MP2 MODIFIED TO MEET CUSTOMER REQUIREMENTS.

**REPORT OF SUPERPAVE VOLUMETRIC MIX DESIGN**
**(AASHTO MP-2, PP-28, T312 & ASTM D-4867)**

Issued Date: 5/26/2009
Amended Date: 6/4/2009

DESIGN NUMBER: 506809 JOB: 40023
PLANT: 40023 MIX TYPE: E-1 MIX TEMPERATURE: 145°C - 134°C
MIX SIZE: 12.5 mm Design ESAL Range (mil.): 0.3 to < 1

**Compactive Effort: (Gyrations)** Ni: 7 Nd: 60 Nm: 75

**Binder Data:** GRADE: PG 58-28 SOURCE: CRM Milwaukee Gb: 1.035 **RAP Pb:** 4.49

**AGGREGATE SOURCE DATA**

| AGG | AGGREGATE | SOURCE | TEST# | LOCATION |
|---|---|---|---|---|
| AGG #1 | FRAP | 40023 | 8-B-09 | |
| AGG #2 | 5/8" Chip | Prager | 38-A-09 | W1/2 S7 T4N R19E Racine Co. |
| AGG #3 | 3/8" Chip | Prager | 39-A-09 | W1/2 S7 T4N R19E Racine Co. |
| AGG #4 | MFG'D Sand | Prager | 40-A-09 | W1/2 S7 T4N R19E Racine Co. |
| AGG #5 | Natural Sand | Bloomfield | 30-A-09 | SW1/4 S1 and SE1/4 S2 T1N R19E Walworth Co. |
| AGG #6 | Deg | Bloomfield | 1 | SW1/4 S1 and SE1/4 S2 T1N R19E Walworth Co. |

**AGGREGATE GRADATION**

| | | Agg #1 | Agg #2 | Agg #3 | Agg #4 | Agg #5 | Agg #6 | JMF | SPECIFICATION MIN | SPECIFICATION MAX |
|---|---|---|---|---|---|---|---|---|---|---|
| % BLEND | | 20.0 | 16.0 | 12.0 | 14.0 | 37.7 | 0.3 | | | |
| 2 | 50.0 mm | 100.0 | 100.0 | 100.0 | 100.0 | 100.0 | 100.0 | 100.0 | 0.0 | 0.0 |
| 1-1/2 | 37.5 mm | 100.0 | 100.0 | 100.0 | 100.0 | 100.0 | 100.0 | 100.0 | 0.0 | 0.0 |
| 1 | 25.0 mm | 100.0 | 100.0 | 100.0 | 100.0 | 100.0 | 100.0 | 100.0 | 0.0 | 0.0 |
| 3/4 | 19.0 mm | 100.0 | 100.0 | 100.0 | 100.0 | 100.0 | 100.0 | 100.0 | 100.0 | 100.0 |
| 1/2 | 12.5 mm | 99.4 | 85.2 | 100.0 | 100.0 | 100.0 | 100.0 | 97.5 | 90.0 | 100.0 |
| 3/8 | 9.5 mm | 94.5 | 28.2 | 98.5 | 100.0 | 99.2 | 100.0 | 86.9 | 0.0 | 90.0 |
| #4 | 4.75 mm | 72.1 | 2.7 | 23.8 | 96.4 | 91.2 | 100.0 | 65.9 | 0.0 | 0.0 |
| #8 | 2.36 mm | 56.5 | 2.1 | 3.2 | 58.1 | 81.9 | 100.0 | 51.3 | 28.0 | 58.0 |
| #16 | 1.18 mm | 44.7 | 1.9 | 2.7 | 31.4 | 72.3 | 100.0 | 41.5 | 0.0 | 0.0 |
| #30 | 0.60 mm | 34.8 | 1.7 | 2.5 | 16.7 | 56.1 | 100.0 | 31.3 | 0.0 | 0.0 |
| #50 | 0.30 mm | 22.3 | 1.7 | 2.4 | 8.1 | 17.6 | 100.0 | 13.1 | 0.0 | 0.0 |
| #100 | 0.15 mm | 15.0 | 1.6 | 2.3 | 3.7 | 3.9 | 100.0 | 5.8 | 0.0 | 0.0 |
| #200 | 0.075 mm | 11.8 | 1.4 | 2.2 | 2.4 | 2.2 | 100.0 | 4.3 | 2.0 | 10.0 |
| | FAA | 42.7 | 0.0 | 0.0 | 47.2 | 40.5 | 0.0 | 42.4 | | |
| | Gsb | 2.655 | 2.668 | 2.642 | 2.664 | 2.654 | 2.654 | 2.656 | | |

**AGGREGATE DATA FOR BLENDED DESIGN JMF**

CRUSH 1F/2F: 95.9 / 93.3 Gsb: 2.656 Moist. Absorption: 1.4 L.A. WEAR: 0.0 (100) ELONGATED: 2.6 (5/1)
FAA: 42.4 Gsa: 2.759 Dust Proportion: 0.9 0.0 (500)
SE: 97 Gse: 2.713 Soundness: 0.0 Freeze-Thaw: 0.0

**VOLUMETRIC DATA**

| Point | Added Pb | Total Pb | Gmm | Gmb | Va | VMA | VFB | Unit Wt. | %Gmm Ni | %Gmm Nm | TSR |
|---|---|---|---|---|---|---|---|---|---|---|---|
| A | 4.0 | 4.9 | 2.513 | 2.365 | 5.9 | 15.3 | 61.4 | 2359 | | | |
| B | 4.5 | 5.4 | 2.495 | 2.385 | 4.4 | 15.1 | 70.9 | 2379 | | | |
| C | 5.0 | 5.9 | 2.476 | 2.404 | 2.9 | 14.8 | 80.4 | 2398 | | | |
| JMF | 4.6 | 5.5 | 2.491 | 2.391 | 4.0 | 14.9 | 73.2 | 2385 | 90.8 | 96.3 | 82.0 |
| | | Corr. Factor: | 0.000 | | | | | | | | TSR N = 16 |
| SPECIFICATION | | | | | 4.0 | 14.0 | 65 - 78 | | 90.5 | 98.0 | |

Comments: WisDOT Aggregate Test Number: 225-131-2009 WisDOT Verification Number - 250-0106-2009
Eliminate Deg. Bloomfield Natural Sand = 38% Project ID 1030-23-70
A change in binder grade or source is recognized without the need for additional mix design testing.

Wisconsin Certified Hot Mix Asphalt Technician IIIS

THE TEST DATA SHOWN ON THIS REPORT PERTAIN ONLY TO THE MATERIAL SUBMITTED FOR DESIGN.
AASHTO MP2 MODIFIED TO MEET CUSTOMER REQUIREMENTS.

# EMIL G. BAUTISTA

## EDUCATION

University of Wisconsin-Milwaukee
**Ph.D. Civil Engineering,** January 2011 – expected May 2015.

- Dissertation: "*Effect of Coal Combustion Products (CCPs) on Constructability, Damage and Aging Resistance of Asphalt Mastics and Asphalt Mixtures*"

University of Wisconsin-Madison
**M.S. Civil Engineering,** June 2009.

- Independent Study: "*Development of a Testing Procedure to Evaluate the Rheological Properties of Bitumen in Reclaimed Asphalt Pavement without Solvent Extraction and Recovery*"

Universidad Iberoamericana (UNIBE); Santo Domingo, Dominican Republic
**B.S. Civil Engineering,** August 2006.

- Graduated with Honors (Summa Cum Laude)
- Thesis: "*Analysis and Recommendations for the Storm Water Drainage Solution of the Low Points of Los Prados, El Quisqueya and Los Millones*"

## WORK EXPERIENCE

University of Wisconsin-Milwaukee, Civil & Environmental Engineering Department
**Research/Project Assistant**, January 2011 – Present

- Team leader for a Wisconsin Department of Transportation (WisDOT) study on the development of construction specification for base and subbase unbound granular materials construction of pavement structures.
- Interpreted and reviewed advanced laboratory and field characterization tests for geo-materials including Dynamic Cone Penetrometer (DCP), Light Weight Deflectometer (LWD), GeoGauge, Falling Weight Deflectometer (FWD).
- Provided guidance and feedback to engineers and researchers at UW-Milwaukee in the areas of geotechnical and pavement engineering, advanced laboratory test of geomaterials, characterization of unbound granular materials, experimental geomechanics, plasticity, advanced rheology, linear and non-linear viscoelasticity.
- Leader researcher of a team that field methods for pavement reconstruction using the Falling Weight Deflectometer (FWD).
- Provided technical support in the development of new test procedures and standards for transportation industry and departments of transportation (DOTs)
- Wrote and reviewed technical publications, standards, and reports for sponsor agencies and clients.

**Teaching Assistant**, January 2012 – May 2013

- Teach students the fundamentals of Soil Mechanics laboratory tests for:
  - Visual identification of soils, sieve analysis, liquid and plastic limits, engineering classification of soils, Proctor compaction, permeability, direct shear, unconfined compression, consolidation and triaxial tests.
- Help students develop fundamental knowledge in soil mechanics:
  - Classification of soils, seepage analysis, principle of effective stress, capillarity, stress distribution, one-dimensional consolidation and settlement, Mohr-Coulomb strength theory, total and effective stress strength parameters.

- Design and analysis of foundations (shallow and deep) and earth retaining structures.

COBAUSA, Santo Domingo, Dominican Republic
**Project Engineer**, January 2010 – December 2010

- Supervised construction work done in the field and provided support to construction personnel, including foremen and topography crews.
- Wrote daily reports to update project managers on a weekly basis.
- Created Gantt charts to show activities to oversee work completed within the timeframe of the project
- Developed bids for construction projects with high social impact in the Dominican Republic (e.g., schools).

TAVAREZ & ASSOCIATES ARCHITECTS, INC., Madison, WI
**Volunteer Intern/AutoCAD Operator,** July 2009-December 2009

- Preparation of construction documents using Autodesk-AutoCAD software in line with industry and government standards
- Materials and specifications research.
- Cost Estimating.
- Construction administration services.

University of Wisconsin-Madison, Dept. of Civil and Environmental Engineering
**Research Assistant**, September 2007 – May 2009

- Researched civil engineering materials, asphalt mixtures and pavements structures. Special focus in Reclaimed Asphalt Pavement (RAP) and Warm Mix Additives (WMA). Conduct literature reviews and collect and analyze data.
- Tested asphalt binder following the Superpave protocol. Worked with WMA and study their effect in the asphalt binder as well as the asphalt mixture.
- Worked in developing a system to determine low temperature properties of the aged bitumen in RAP.

COBAUSA, Santo Domingo, Dominican Republic
**Entry Level Civil Engineering**, September 2006 – August 2007

- Developed budgets, cost analysis and scheduled project programming for renovation of sports facilities such as baseball, softball and soccer stadiums.
- Worked in the development of construction documents and project planning.
- Prepared of construction documents using Autodesk-AutoCAD software.
- Researched materials and specifications. Estimated cost and provided administrative support services.

Universidad Iberoamericana (UNIBE), Santo Domingo, Dominican Republic, Civil Engineering Dept.
**Teaching Assistant**, January 2006 – August 2006

- Fluid Mechanics: Worked out solutions to applied problems on the static and dynamic behavior of liquids.
- Hydraulics: Analyzed pipe~~s~~ systems, managed the behavior of the different types of hydraulics systems and identified the general aspects of hydraulics channels.

## SIGNIFICANT CONTINUING EDUCATION AND CERTIFICATION

- "*Satellite Hazardous Waste Generator Annual Training*", University Safety & Assurances at University of Wisconsin-Milwaukee; September 29th, 2014

- "*Professor Training Certificate in Asphalt Technology*", National Center of Asphalt Technology (NCAT)**,** Auburn, Alabama, June 2014
- "*Chemical Hygiene Plan and Laboratory Safety Training*", University Safety & Assurances at University of Wisconsin-Milwaukee; July 25th, 2013
- "*Material and Design Inputs for New Pavement Design and for Pavement Rehabilitation with Asphalt Overlays for AASHTO ME Design software*"**,** Federal Highway Administration, training webinars. January-February 2013
- "*Construction Safety & Health*"**,** U. S. Department of Labor. Occupational Safety and Health Administration, May 2009.

## RESEARCH PROJECTS & INTERESTS

- **The Effective Use of Different Types of Fly Ash in Green Asphalt Pavements.** Sponsor: Energy Power Research Institute (EPRI) and We Energies. 2013-2016
- **Base Compaction Specification Feasibility Analysis.** Sponsor: Wisconsin Highway Research Program (WHRP). 2011-2013
- **Mechanistic-Empirical Pavement Analysis and Design.** Sponsor: National Center for Freight & Infrastructure Research & Education (C-Fire). 2011-2012
- **Resilient Modulus Testing of Steel Slag and Steel Slag-Aggregate Mixtures**. Sponsor: Bureau of Technical Services, Wisconsin Department of Transportation (WisDOT). 2011
- **Design System for HMA Containing a High Percentage of RAP Material.** Sponsor: FHWA Federal Highway Administration (ARC) 2007 – 2009
- **Warm Mix Additives and Mixtures.** Sponsor: Federal Highway Administration (ARC). 2007 - 2009

## FIELD INSTRUMENTATION SKILLS

Dynamic Cone Penetrometer (DCP), Light Weight Deflectometer (LWD), GeoGauge, Falling Weight Deflectometer (FWD), Sand Cone.

## LABORATORY INSTRUMENTATION SKILLS

Triaxial test (Resilient Modulus), Direct Shear tester, Consolidation test, Rotational Viscometer, Rolling Thin Film Oven, Pressure Aging Vessel, Dynamic Shear Rheometer, Bending Beam Rheometer, Superpave Gyratory Compactor, CoreLok.

## COMPUTER SKILLS

Windows – Operating System, MS Word, MS Excel, MS Powerpoint, MS Project, AASHTOWare Pavement, Ansys, Grapher, Surfer, Map Viewer, Auto Cad, MicroStation, Primavera, $MC^2$

## PRESENTATIONS, PUBLICATIONS AND REPORTS

- **Bautista, E. G.,** Faheem, A. F., Saha, R., Sobolev, K. **(2015).** Characterization of Damage and Aging Resistance of Asphalt Mastics with Coal Combustion By-Products. American Society of Civil Engineers (ASCE) International Airfield & Highway Pavements Conference, June 2015.

- **Bautista, E. G.** and Saha, R., 2014, Coal Combustion By-Products (CCP) in Hot Mix Asphalt (HMA). Mid-Continent Transportation Research Forum 2014, Wisconsin Transportation Center.

- Titi, H. H., Tabatabai, H., Faheem, A., Druckrey, A., Tutumluer, E., and **Bautista, E.** (2014). "Evaluation of Compacted Aggregate Base Course Layers," in press, Geocongress 2014, ASCE Geotechnical Special Publication, American Society of Civil Engineers.

- Titi, H., **Bautista, E. G.,** Horowitz, A. 2013. Mechanistic-Empirical Pavement Analysis and Design. National Center for Freight & Infrastructure Research & Education (C-FIRE). College of Engineering, Department of Civil and Environmental Engineering, University of Wisconsin-Madison. Paper No. 13-2

- Titi, H., **Bautista, E. G.**, Druckrey, A., Tabatabai, H., Faheem, A., Tutumluer, E. 2013. Evaluation of Aggregate Base Compaction for Density and Modulus Based Specification. Mid-Continent Transportation Research Symposium. Iowa State University. Iowa Department of Transportation.

- Titi, H., Tabatabai, H., **Bautista, E. G.**, Druckrey, A., Faheem, A., Tutumluer, E. 2012. Base Compaction Specification Feasibility Analysis. Wisconsin Department of Transportation (WisDOT). WisDOT ID no. 0092-11-02

- **Bautista, E. G.**, Mangiafico, S., Bahia, Hussain U., and Ma, Tao. Evaluation of Rheological properties of bitumen in RAP without extraction and recovery. Transportation Research Board, Poster Presentation, 2009.

- **Bautista, E. G.** and Mangiafico, S., 2008, Fundamental Investigation of the Effects of Recycle Asphalt Pavement on Asphalt Pavement Performance. Mid-Continent Transportation Research Forum 2008, Wisconsin Transportation Center.

- Bahia, Hussain U., Mangiafico, S., and **Bautista, E. G.** 2008, Rheological Propeties of Bitumen in RAP – How to account for it in Recycled Asphalt Mixtures. Recycling and Rehabilitation Conference, New Zealand, 2008.


## LANGUAGES

Spanish (Native Speaker) and English

## AWARDS AND HONORS

| | |
|---|---|
| Chancellor Awards – University of Wisconsin-Milwaukee | 2011 to 2015 |
| National Center of Asphalt Technology, Professor Training Scholarship ($2,000) | 2014 |

## OTHER ACTIVITIES

American Society of Civil Engineers (ASCE)
Wisconsin Green Building Alliance (WGBA)
American Society of Safety Engineers (ASSE)
Construction Club, UW-Madison
Transportation Research Board (TRB) Subcommittee AFP70(1) - Unbound Granular Materials